

# **Investigation of a Yellow Lake Pigment using 2D-LC and EC-SERS**

By: Maddison Margaret Eisnor

A Thesis Submitted to

Saint Mary's University, Halifax, Nova Scotia

In Partial Fulfilment of the Requirements for the Degree of

Bachelor of Science with Honours in Chemistry

April 2020, Halifax, Nova Scotia

Copyright Maddison Margaret Eisnor, 2020

Approved: Dr. Christa Brosseau  
Professor  
Chemistry Department

Approved: Dr. Jason Masuda  
Professor  
Chemistry Department  
Chair

Date: April 27<sup>th</sup>, 2020

## **Certification**

Investigation of a Yellow Lake Pigment using 2D-LC and EC-SERS

By: Maddison Margaret Eisnor

Copyright Maddison Margaret Eisnor, 2020

I hereby certify that this thesis was completed by Maddison Margaret Eisnor in partial fulfillment of the requirements of the Degree of Bachelor of Science with Honours in Chemistry at Saint Mary's University and I certify that this is truly the original work carried out by Maddison Margaret Eisnor.

Thesis Supervisor

Dr. Christa L. Brosseau

---

Chairperson of the Chemistry Department

Dr. Jason Masuda

---

Date: April, 2020

**Abstract**

## Investigation a of Yellow Lake Pigment using 2D-LC and EC-SERS

The identification of natural organic pigments is fundamental for the conservation, preservation, and historical interpretation of artwork. Natural pigments, derived from plant and insect sources, can experience fading and degradation over time due to light, air, and humidity exposure. As such, these naturally-derived pigments are referred to as *fugitive* pigments. Although these pigments are derived from simple sources, it can be a significant challenge to characterize these pigments by a single method since they are found in complex matrices and are comprised of many components varying in their chemical structure and properties. Many spectroscopic techniques have been used successfully for the identification of fugitive pigments, such as Raman and infrared spectroscopy. Although these techniques are quite useful, they have their disadvantages. Raman spectroscopy is inherently weak, with only one in a million photons undergoing inelastic scattering. In addition, molecules which are also fluorescent, such as many natural organic pigments, will be difficult to detect using Raman spectroscopy due to the competing fluorescence. An enhanced variant of Raman spectroscopy, called surface-enhanced Raman spectroscopy or SERS, has shown much promise in this area over the past 15 years, with many natural organic pigments being identified in precious artworks as a result. However, a significant limitation of SERS is the ability to identify organic pigments present in a complex mixture and this limitation is due to the fact that SERS by itself offers no separation capabilities. While coupling of separation techniques such as thin layer chromatography and liquid chromatography have been attempted and have been successful, even for artist colourants, the combination of multidimensional chromatography and SERS has not yet been attempted and is the focus of this thesis work.<sup>1,2</sup>

Multidimensional liquid chromatography (2D-LC) is appropriate for addressing the increasing demand for decoding complex samples and has recently been found to be useful for the separation of artist colourants.<sup>3</sup> However, it remains challenging to identify the components in such complex mixtures in a rapid and confirmatory way. Consequently, this thesis work has explored a 2D-LC-EC-SERS method, wherein electrochemical SERS (EC-SERS) is used as the offline detection modality for multidimensional chromatography. This thesis work hypothesizes that 2D-LC-EC-SERS can be used for the identification of components in pigment samples, with a future goal of elucidation of the pigment degradation pathways for yellow lake pigments in particular.

## **Acknowledgements**

First and foremost, I want to thank my research supervisor, Dr. Christa Brosseau, for your guidance and support, and for allowing me to have an amazing opportunity working in your

research lab. Continuously throughout my undergraduate degree, you have inspired me with your knowledge and dominance in your field. Additionally, you opened my eyes to how applicable and relevant analytical chemistry is in solving the world's most challenging problems. I would also like to thank Melanie Davidson for being my mentor and for training me on how to operate the 2D-LC. Your patience and great personality were much appreciated. I want to thank past and current Brosseau lab group members: Gaius St. Marie, Shruti Bindsri, Stephanie Amrieh, Dalal Alhatab and Najwan Albarghouthi. I want to extend my appreciation to Kaleigh McLeod and Carolyn Farling. You were a massive help in keeping me sane during this time in my life and were always there for me, especially lifting me up when I was down, thanks to you both. Patricia Granados, thank you for all your help with operating and mastering the 2D-LC and countless other instruments at SMU. As well as Alyssa Doue for being so helpful and always positive. Thank you, Dr. Xiang Yang, for helping me obtain SEM images and EDX results. And thank you, Dr. Kristin Wustholz and Shelley Svoboda for introducing me to this project and providing pigment samples. I want to acknowledge the chemistry faculty for providing me with my incomparable education in chemistry and continuously being inspired.

Finally, I want to say an enormous thank you to my friends and family, especially my Mom and Dad. For providing me their unceasing support and the opportunity to attend university through their hard work and sacrifices they have made, which allowed me to follow my dreams.

## **Table of Contents**

## **Page #**

Abstract

**iii**

Acknowledgements

**v**

List of Abbreviations

**x**

List of Figures

**xi**

List of Tables	xix
<b>Chapter 1: Introduction</b>	<b>1</b>
1.1 Research Goal	1
1.2 Introduction	3
1.3 Literature Review	8
1.3.1 Yellow Lake Pigments	8
1.3.2 Analysis of Dyes and Pigments	12
1.3.3 Analysis of Pigments with Raman Spectroscopy	13
1.3.4 Analysis of Dyes and Pigments with Surface-Enhanced Raman Spectroscopy	14
1.3.5 Analysis of Dyes and Pigments with Chromatography	17
1.3.6 Analysis of Dyes and Pigments with Surface-Enhanced Raman Spectroscopy coupled with Chromatography	19
1.3.7 Analysis of Dyes with Multidimensional Chromatography	21
1.4 Theory	23
1.4.1 Liquid Chromatography	23
1.4.2 Multidimensional Liquid Chromatography	28
1.4.3 Raman Spectroscopy	34
1.4.4 Surface-Enhanced Raman Spectroscopy	36
1.4.5 Electrochemistry	38
1.4.6 Electrochemical Surface-Enhanced Raman Spectroscopy	41
<b>Chapter 2: Experimental</b>	<b>43</b>
2.1 Reagents and Materials	43
2.2 Methods	43
2.2.1 Preparation of Polyphenol Standards	43
i. Individual Polyphenol Standards	43
ii. Polyphenol Standards Mixture	44

2.2.2	Yellow Lake Pigment Extraction	45
2.2.3	Liquid Chromatography	45
i.	First Dimension Parameters	45
ii.	Second Dimension Parameters	46
iii.	Second Dimension with Fraction Collection Parameters	47
2.2.4	Electrochemical Surface Enhanced Raman Spectroscopy	48
i.	Silver Nanoparticle (AgNP) Synthesis	48
ii.	Preparation of EC-SERS Substrates	49
iii.	EC-SERS Analysis	49
<b>Chapter 3: Results and Discussion</b>		<b>51</b>
3.1	2D-LC Studies	51
3.1.1	Reseda Lake and Buckthorn Berries Yellow Lake Reference  Pigment	51
3.1.2	Polyphenol Standards and Polyphenol Standard Mixture	52
3.1.3	Reseda Lake/Buckthorn Berries Pigment Heart Cuts	60
3.1.4	Comparison of Yellow Lake Pigments	62
3.1.5	Sunlight Effect on Reseda Lake/Buckthorn Berries Pigment	66
3.1.6	Reseda Lake/Buckthorn Berries Pigment Heart Cuts Used for  EC-SERS Analysis	67
3.2	EC-SERS Studies	72
3.2.1	Polyphenol Standards	72
3.2.2	Polyphenol Standards Mixture	75
3.2.3	Polyphenol Standards Mixture Fractions	79
3.2.4	Reseda Lake and Buckthorn Berries Pigment Fractions	82
3.2.5	<sup>2</sup> D Mobile Phase Eluate (95:5% (v/v) 0.1% Formic Acid in Acetonitrile / 0.1% Formic Acid in Water)	85

3.2.6 Identification of <sup>2</sup> D Mobile Phase Eluate	86
3.3 SEM-EDX Analysis on Reseda Lake and Buckthorn Berries Reference Pigment	92
3.4 QTOF MS Analysis Results of 11.59 minute peak	96
<b>Chapter 4: Conclusions</b>	<b>99</b>
<b>Chapter 5: Future Work</b>	<b>101</b>
<b>Chapter 6: References</b>	<b>102</b>
<b>Appendix</b>	<b>107</b>

### List of Abbreviations

1D	one-dimension
<sup>1</sup> D	first dimension
2D	two-dimension
<sup>2</sup> D	second dimension
2D-LC	two-dimensional liquid chromatography
2D-LC-SERS	two-dimensional liquid chromatography with SERS detection
2D-LC-EC-SERS	two-dimensional liquid chromatography with electrochemical surface-enhanced Raman spectroscopy
AgNP	silver nanoparticles
CE	counter electrode

DAD	diode array detection
EC-SERS	electrochemical surface-enhanced Raman spectroscopy
EDX	energy dispersive x-ray spectroscopy
GC	gas spectrometry
HPLC	high performance liquid chromatography
HPLC-MS	high performance liquid chromatography with MS detection
HPLC-SERS	high performance liquid chromatography with SERS detection
IHP	inner Helmholtz plane
IR	infrared spectroscopy
LC	liquid chromatography
LC×LC	comprehensive multidimensional liquid chromatography
LC-LC	heart-cutting multidimensional liquid chromatography
LSP	localized surface plasmons
LSPR	localised surface plasmon resonance
mLC-LC	multiple heart-cutting multidimensional liquid chromatography
MS	mass spectrometry
NP	normal phase
NMR	nuclear magnetic resonance
OCP	open circuit potential
OHP	outer Helmholtz plane
PSP	propagating surface plasmons
QTOF	quadrupole time-of-flight
RE	reference electrode
RP	reverse phase
SEM	scanning electron microscopy
SEM-EDX	scanning electron microscopy - energy-dispersive X-ray spectroscopy
SERS	surface-enhanced Raman spectroscopy
SPE	screen-printed electrode
TLC	thin layer chromatography
UHPLC	ultra-high-performance liquid chromatography
UV-vis	ultra-violet visible spectroscopy
WE	working electrode

## List of Figures

Figure	Figure Caption	Page #
1.3.1.1	Schematic representation of alizarin dyestuff, aluminum mordant and madder lake pigment.	9
1.3.1.2	Chemical structures of polyphenol compounds present in Reseda lake pigment; luteolin and apigenin.	10
1.3.1.3	Chemical structures of polyphenol compounds present in Stil de Grain lake pigment; emodin, rhamnetin, quercetin and kaempferol.	11

1.4.1.1	Simple chromatogram depicting retention time, $t_R$ , and peak width, $w$ .	24
1.4.1.2	A van Deemter plot for the determination of optimum chromatographic flow rate ( $u$ ).	27
1.4.2.1	Schematic diagram of the comprehensive (LCxLC) and heart-cutting (LC-LC) modes in 2D-LC (© <a href="http://www.theanalyticalscientist.com">www.theanalyticalscientist.com</a> 2014. Reproduced with Permission, Courtesy of <a href="http://www.theanalyticalscientist.com">www.theanalyticalscientist.com</a> .)	30
1.4.2.2	Configurations of an 8-port/2-position valve needed for LC-LC separation (© Agilent Technologies, Inc. 2015. Reproduced with Permission, Courtesy of Agilent Technologies, Inc.).	31
1.4.2.3	Schematic diagram exhibiting various levels of orthogonality (© 2019 Elsevier B.V. All rights reserved. Reproduced with Permission, Courtesy of Elsevier B.V.)	33
1.4.3.1	Diagram showing the different light scattering modes: Rayleigh, Stokes, and anti-Stokes scattering (adapted from Turrell et al.).	35
1.4.4.1	Schematic illustration of localized surface plasmon resonance (LSPR) of free electrons in the metal nanosphere are driven into collective oscillation due to strong interactions with incident light (adapted from Rycenga et al).	37
1.4.5.1	Schematic depiction of the electrical double layer (Grahame model) (adapted from reference <sup>53</sup> ).	40
3.1.1.1	<sup>1</sup> D chromatogram of the Reseda lake/buckthorn berry pigment (5:95% (v/v) formic acid: methanol) at 264 nm. Retention times are stated above each main peak.	52
3.1.2.1	Chemical structures polyphenols: luteolin, kaempferol, rhamnetin, quercetin, apigenin, emodin, caffeic acid, and chlorogenic acid.	53
3.1.2.2	<sup>1</sup> D chromatograms for 25 ppm (5:95% (v/v) formic acid/methanol) solutions of chlorogenic acid, caffeic acid, quercetin and luteolin at 327 nm with retention times stated above each main peak.	54
3.1.2.3	<sup>1</sup> D chromatogram for 25 ppm (5:95% (v/v) formic acid/methanol) mixture of chlorogenic acid, caffeic acid, quercetin and luteolin at 327 nm with retention times stated above each main peak.	55
3.1.2.4	<sup>1</sup> D chromatograms for 25 ppm (5:95% (v/v) formic acid/methanol) solutions of apigenin and emodin at 363 nm and 292nm with retention times stated above each main peak.	56

<b>3.1.2.5</b>	<sup>1</sup> D chromatograms for 2000 ppm and 500 ppm (5:95% (v/v) formic acid/methanol) solutions of kaempferol and rhamnetin at 363 nm with retention times stated above each main peak.	<b>56</b>
<b>3.1.2.6</b>	<sup>1</sup> D chromatogram (5:95% (v/v) formic acid/methanol) mixture of chlorogenic acid, caffeic acid, quercetin, luteolin, kaempferol, rhamnetin, apigenin and emodin (31 ppm each) at 363 nm with retention times and names of compounds stated above each main peak.	<b>57</b>
<b>3.1.2.7</b>	Relabelled <sup>1</sup> D chromatogram of the Reseda Lake/buckthorn berry pigment (5:95% (v/v) formic acid/methanol) at 264 nm with retention times and polyphenol component stated above each main peak.	<b>59</b>
<b>3.1.3.1</b>	<sup>2</sup> D chromatogram 1.11 minute peak heart cut of the yellow lake pigment (5:95% v/v, formic acid/methanol) chromatogram at 292 nm with retention times stated above each main peak.	<b>61</b>
<b>3.1.3.2</b>	<sup>2</sup> D chromatogram of 1.35 minute peak heart cut of the yellow lake pigment (5:95% (v/v) formic acid: methanol) chromatogram at 292 nm with retention times stated above each main peak.	<b>61</b>
<b>3.1.3.3</b>	<sup>2</sup> D chromatogram of 11.66 minute peak heart cut of the yellow lake pigment (5:95% (v/v) formic acid/methanol) chromatogram at 292 nm with retention times stated above each main peak.	<b>62</b>
<b>3.1.4.1</b>	<sup>1</sup> D chromatogram of Reseda lake pigment (5:95% (v/v) formic acid/methanol) at 327 nm (A) and a picture of the pigment in 5:95% (v/v) formic acid/methanol.	<b>64</b>
<b>3.1.4.2</b>	<sup>1</sup> D chromatogram of buckthorn berry pigment (5:95% (v/v) formic acid/methanol) at 327 nm (A) and a picture of the pigment in 5:95% v/v formic acid: methanol.	<b>64</b>
<b>3.1.4.3</b>	<sup>1</sup> D chromatogram overlays of the different yellow lake pigments (5:95% (v/v) formic acid/methanol) at 264 nm (A) and 327 nm (B).	<b>65</b>
<b>3.1.5.1</b>	Pictures of before (left) and after (right) the yellow lake sample in 5:95% (v/v) formic acid/methanol was exposed to sunlight for 1 week.	<b>66</b>
<b>3.1.5.2</b>	Overlay of chromatograms of yellow lake sample before and after having sun exposure for 1 week at 327 nm.	<b>67</b>
<b>3.1.6.1</b>	<sup>1</sup> D chromatogram of the Reseda Lake/buckthorn berry pigment (5:95% (v/v) formic acid/methanol) at 264 nm. Retention times are stated above each main peak.	<b>68</b>

<b>3.1.6.2</b>	<sup>2</sup> D chromatogram of the cut 2 of Reseda Lake/buckthorn berry pigment (5:95% (v/v) formic acid/methanol) at 327 nm. Retention times are stated above each main peak.	<b>69</b>
<b>3.1.6.3</b>	<sup>2</sup> D chromatogram of the cut 3 of Reseda Lake/buckthorn berry pigment (5:95% (v/v) formic acid/methanol) at 327 nm. Retention times are stated above each main peak.	<b>69</b>
<b>3.1.6.4</b>	<sup>2</sup> D chromatogram of the cut 6 of Reseda Lake/buckthorn berry pigment (5:95% v/v, formic acid: methanol) at 327 nm. Retention times are stated above each main peak.	<b>70</b>
<b>3.1.6.5</b>	<sup>2</sup> D chromatogram of the cut 7 of Reseda Lake/buckthorn berry pigment (5:95% (v/v) formic acid/methanol) at 327 nm. Retention times are stated above each main peak.	<b>70</b>
<b>3.1.6.6</b>	<sup>2</sup> D chromatogram of the 11.59 minute peak of Reseda Lake/buckthorn berry pigment (5:95% (v/v) formic acid/methanol) at 327 nm. Retention times are stated above each main peak.	<b>71</b>
<b>3.2.1.1</b>	EC-SERS analysis of 2000 ppm caffeic acid on the surface of AgNP coated screen-printed electrode (Cathodic, 0.1V stepwise progression from 0V to -1.0V and Anodic, 0.1V step-wise progression from 0V to -1.0V) on the surface of AgNP coated screen-printed electrode using an excitation wavelength of 780 nm with a laser power of 80 mW and acquisition time of 30 seconds.	<b>73</b>
<b>3.2.2.1</b>	Comparison of EC-SERS spectra of mixture of chlorogenic acid, caffeic acid, quercetin, luteolin, kaempferol, rhamnetin, apigenin and emodin (31 ppm each) on the surface of AgNP coated screen-printed electrode using an excitation wavelength of 780 nm with a laser power of 80 mW and acquisition time of 30 seconds.	<b>76</b>
<b>3.2.2.2</b>	Comparison of EC-SERS spectra of eight polyphenol compounds in a mixture (8 Flav Mix), 2000 ppm quercetin standard and 500 ppm rhamnetin standard at -0.1V during the cathodic progression on the surface of AgNP coated screen-printed electrode using an excitation wavelength of 780 nm with a laser power of 80 mW and acquisition time of 30 seconds.	<b>77</b>
<b>3.2.2.3</b>	Comparison of EC-SERS spectra of eight polyphenol compounds in a mixture (8 flavonoid mixture) standard and 500 ppm rhamnetin standard at -0.1V during the cathodic progression on the surface of AgNP coated screen-printed electrode using an excitation wavelength of 780 nm with a laser power of 80 mW and acquisition time of 30 seconds.	<b>78</b>

<b>3.2.2.4</b>	Comparison of EC-SERS spectra of eight polyphenol compounds in a mixture (8 Flav Mix) and 2000 ppm quercetin standard at OCP during the anodic progression on the surface of AgNP coated screen-printed electrode using an excitation wavelength of 780 nm with a laser power of 80 mW and acquisition time of 30 seconds.	<b>79</b>
<b>3.2.3.1</b>	Comparison of EC-SERS spectra of caffeic acid from eight polyphenols in a mixture (A) and comparison with 2000 ppm caffeic acid standard EC-SERS spectra (B) with the in air spectrum 2D-LC fraction of caffeic acid from 8 polyphenol mixture on the surface of AgNP coated screen-printed electrode using an excitation wavelength of 780 nm with a laser power of 80 mW and acquisition time of 30 seconds,	<b>81</b>
<b>3.2.3.2</b>	Comparison of in air (A) and -1.0V (B) EC-SERS spectra of 8 polyphenol mix 2D-LC fractions and the <sup>2</sup> D mobile phase on the surface of AgNP coated screen-printed electrode using an excitation wavelength of 780 nm with a laser power of 80 mW and acquisition time of 30 seconds.	<b>82</b>
<b>3.2.4.1</b>	Comparison of EC-SERS spectra of chlorogenic acid fraction of Reseda lake/buckthorn berry pigment (A) and with 2D-LC fraction of 2000 ppm chlorogenic acid standard (B) on the surface of AgNP coated screen-printed electrode using an excitation wavelength of 780 nm with a laser power of 80 mW and acquisition time of 30 seconds.	<b>83</b>
<b>3.2.4.2</b>	Comparison between EC-SERS spectra of 2D mobile phase and chlorogenic acid fraction from Reseda lake/buckthorn berry pigment on the surface of AgNP coated screen-printed electrode using an excitation wavelength of 780 nm with a laser power of 80 mW and acquisition time of 30 seconds.	<b>84</b>
<b>3.2.4.3</b>	Comparison of EC-SERS spectra of 11.59 minute peak fraction of Reseda lake/buckthorn berry pigment (A) and with <sup>2</sup> D mobile phase (B) on the surface of AgNP coated screen-printed electrode using an excitation wavelength of 780 nm with a laser power of 80 mW and acquisition time of 30 seconds.	<b>85</b>
<b>3.2.5.1</b>	Comparison of EC-SERS spectra of the <sup>2</sup> D mobile phase (95:5% (v/v) 0.1% formic acid in acetonitrile/0.1% formic acid in water) on the surface of AgNP coated screen-printed electrode using an excitation wavelength of 780 nm with a laser power of 80 mW and acquisition time of 30 seconds.	<b>86</b>
<b>3.2.6.1</b>	Comparison of cathodic EC-SERS spectra (A) and comparison of anodic EC-SERS spectra (B) of prepared solution of 95:5% (v/v) 0.1% formic acid in acetonitrile/ 0.1% formic acid in water on the surface of AgNP coated screen-printed electrode using an excitation wavelength of 780 nm with a laser power of 80 mW and acquisition time of 30 seconds.	<b>87</b>

<b>3.2.6.2</b>	Comparison of cathodic EC-SERS spectra (A) and comparison of anodic EC-SERS spectra (B) of prepared solution of 0.1% formic acid in acetonitrile on the surface of AgNP coated screen-printed electrode using an excitation wavelength of 780 nm with a laser power of 80 mW and acquisition time of 30 seconds.	<b>88</b>
<b>3.2.6.3</b>	Comparison of cathodic EC-SERS spectra (A) and comparison of anodic EC-SERS spectra (B) of formic acid solution on the surface of AgNP coated screen-printed electrode using an excitation wavelength of 780 nm with a laser power of 80 mW and acquisition time of 30 seconds.	<b>89</b>
<b>3.2.6.4</b>	Comparison between EC-SERS spectra of <sup>2</sup> D mobile phase eluate and various prepared solutions of the <sup>2</sup> D mobile phase on the surface of AgNP coated screen-printed electrode using an excitation wavelength of 780 nm with a laser power of 80 mW and acquisition time of 30 seconds.	<b>91</b>
<b>3.3.1</b>	SEM image showing the particles present in Reseda lake/buckthorn berry pigment extract solution under 50 μm magnification (voltage: 20 keV, Det: SE, Tescan MIRA3 LMU Field Emission SEM)	<b>93</b>
<b>3.3.2</b>	EDX spectrum of Reseda lake/buckthorn berry pigment extract solution present in Figure 3.3.1 (voltage: 20 keV, Det: SE, Tescan MIRA3 LMU Field Emission SEM)	<b>93</b>
<b>3.3.3</b>	SEM image of Reseda lake/buckthorn berry pigment under 20 μm magnification (voltage: 20 keV, Det: SE, Tescan MIRA3 LMU Field Emission SEM)	<b>94</b>
<b>3.3.4</b>	EDX spectrum of Reseda lake/buckthorn berry pigment in Figure 3.3.3. (voltage: 20 keV, Det: SE, Tescan MIRA3 LMU Field Emission SEM)	<b>95</b>
<b>3.4.1</b>	Negative mode of <sup>2</sup> D mobile phase (95/5 % (v/v) 0.1% formic acid in acetonitrile/0.1% formic acid in water (A) and Reseda Lake/buckthorn berry pigment (B).	<b>96</b>
<b>3.4.2</b>	Positive mode of <sup>2</sup> D mobile phase (95/5 % (v/v) 0.1% formic acid in acetonitrile/0.1% formic acid in water (A) and Reseda Lake/buckthorn berry pigment (B).	<b>98</b>
<b>A1</b>	Comparison of EC-SERS spectra 250 ppm apigenin on the surface of AgNP coated screen-printed electrode using an excitation wavelength of 780 nm with a laser power of 80 mW and acquisition time of 30 seconds.	<b>107</b>
<b>A2</b>	Comparison of EC-SERS spectra of 2000 ppm chlorogenic acid on the surface of AgNP coated screen-printed electrode using an excitation wavelength of 780 nm with a laser power of 80 mW and acquisition time of 30 seconds.	<b>107</b>

<b>A3</b>	Comparison of EC-SERS spectra of 250 ppm emodin on the surface of AgNP coated screen-printed electrode using an excitation wavelength of 780 nm with a laser power of 80 mW and acquisition time of 30 seconds.	<b>108</b>
<b>A4</b>	Comparison of EC-SERS spectra of 2000 ppm kaempferol on the surface of AgNP coated screen-printed electrode using an excitation wavelength of 780 nm with a laser power of 80 mW and acquisition time of 30 seconds.	<b>108</b>
<b>A5</b>	Comparison of EC-SERS spectra of 2000 ppm luteolin on the surface of AgNP coated screen-printed electrode using an excitation wavelength of 780 nm with a laser power of 80 mW and acquisition time of 30 seconds.	<b>109</b>
<b>A6</b>	Comparison of EC-SERS spectra of 2000 ppm quercetin on the surface of AgNP coated screen-printed electrode using an excitation wavelength of 780 nm with a laser power of 80 mW and acquisition time of 30 seconds.	<b>109</b>
<b>A7</b>	Comparison of EC-SERS spectra of 500 ppm rhamnetin on the surface of AgNP coated screen-printed electrode using an excitation wavelength of 780 nm with a laser power of 80 mW and acquisition time of 30 seconds.	<b>110</b>
<b>A8</b>	Comparison of EC-SERS spectra of apigenin 2D-LC fraction from 8 polyphenol mix (A) and comparison with 250 ppm apigenin standard EC-SERS spectrum with 0.0V anodic spectrum of apigenin 2D-LC fraction from 8 polyphenol mix (B) on the surface of AgNP coated screen-printed electrode using an excitation wavelength of 780 nm with a laser power of 80 mW and acquisition time of 30 seconds.	<b>110</b>
<b>A9</b>	Comparison of EC-SERS spectra of chlorogenic acid 2D-LC fraction from 8 polyphenol mix (A) and comparison with 2000 ppm chlorogenic acid standard EC-SERS spectrum with in air spectrum of chlorogenic acid 2D-LC fraction from 8 polyphenol mix (B) on the surface of AgNP coated screen-printed electrode using an excitation wavelength of 780 nm with a laser power of 80 mW and acquisition time of 30 seconds.	<b>111</b>
<b>A10</b>	Comparison of EC-SERS spectra of quercetin 2D-LC fraction from 8 polyphenol mix (A) and comparison with 2000 ppm quercetin standard EC-SERS spectrum with OCP cathodic spectrum of quercetin 2D-LC fraction from 8 polyphenol mix (B) on the surface of AgNP coated screen-printed electrode using an excitation wavelength of 780 nm with a laser power of 80 mW and acquisition time of 30 seconds.	<b>111</b>

- A11** Comparison of EC-SERS spectra of luteolin 2D-LC fraction from 8 polyphenol mix (A) and comparison with 2000 ppm luteolin standard EC-SERS spectrum with OCP cathodic spectrum of luteolin 2D-LC fraction from 8 polyphenol mix (B) on the surface of AgNP coated screen-printed electrode using an excitation wavelength of 780 nm with a laser power of 80 mW and acquisition time of 30 seconds. **112**
- A12** Comparison of EC-SERS spectra of rhamnetin 2D-LC fraction from 8 polyphenol mix (A) and comparison with 500 ppm rhamnetin standard EC-SERS spectra with -1.0V spectrum of rhamnetin 2D-LC fraction from 8 polyphenol mix on the surface of AgNP coated screen-printed electrode using an excitation wavelength of 780 nm with a laser power of 80 mW and acquisition time of 30 seconds. **112**
- A13** Comparison of EC-SERS spectra of emodin 2D-LC fraction from 8 polyphenol mix (A) and comparison with 250 ppm emodin standard EC-SERS spectrum with -1.0V spectrum of emodin 2D-LC fraction from 8 polyphenol mix (B) on the surface of AgNP coated screen-printed electrode using an excitation wavelength of 780 nm with a laser power of 80 mW and acquisition time of 30 seconds. **113**
- A14** Comparison of EC-SERS spectra of caffeic acid fraction of Reseda lake/buckthorn berry pigment (A) and with 2D-LC fraction of 2000 ppm caffeic acid standard (B) on the surface of AgNP coated screen-printed electrode using an excitation wavelength of 780 nm with a laser power of 80 mW and acquisition time of 30 seconds. **113**
- A15** Comparison between EC-SERS spectra of <sup>2</sup>D mobile phase and caffeic acid fraction from Reseda lake/buckthorn berry pigment at -1.0V on the surface of AgNP coated screen-printed electrode using an excitation wavelength of 780 nm with a laser power of 80 mW and acquisition time of 30 seconds. **114**
- A16** Comparison of EC-SERS spectra of kaempferol fraction of Reseda lake/buckthorn berry pigment (A) and with 2D-LC fraction of 2000 ppm kaempferol standard (B) on the surface of AgNP coated screen-printed electrode using an excitation wavelength of 780 nm with a laser power of 80 mW and acquisition time of 30 seconds. **114**
- A17** Comparison between EC-SERS spectra of <sup>2</sup>D mobile phase and kaempferol fraction from Reseda lake/buckthorn berry pigment at -1.0V on the surface of AgNP coated screen-printed electrode using an excitation wavelength of 780 nm with a laser power of 80 mW and acquisition time of 30 seconds. **115**

<b>A18</b>	Comparison of EC-SERS spectra of apigenin fraction of Reseda lake/buckthorn berry pigment (A) and with 2D-LC fraction of 250 ppm apigenin standard (B) on the surface of AgNP coated screen-printed electrode using an excitation wavelength of 780 nm with a laser power of 80 mW and acquisition time of 30 seconds.	<b>115</b>
<b>A19</b>	Comparison between EC-SERS spectra of <sup>2</sup> D mobile phase and apigenin fraction from Reseda lake/buckthorn berry pigment at -1.0V on the surface of AgNP coated screen-printed electrode using an excitation wavelength of 780 nm with a laser power of 80 mW and acquisition time of 30 seconds.	<b>116</b>

### List of Tables

<b>Table</b>	<b>Table Caption</b>	<b>Page #</b>
<b>2.2.1.1</b>	Individual polyphenol standard concentrations.	<b>44</b>
<b>2.2.3.1</b>	1D-LC parameters for the separation of polyphenol standards and yellow lake pigments.	<b>46</b>

<b>2.2.3.2</b>	2D-LC parameters for the separation of polyphenol standards and yellow lake pigments.	<b>47</b>
<b>2.2.3.3</b>	2D-LC with fraction collection parameters for the separation of polyphenol standards and yellow lake pigments.	<b>48</b>
<b>3.1.2.1</b>	Comparison of retention times of eight individual polyphenol standards analyzed separately and in a mixture.	<b>58</b>
<b>3.1.2.2</b>	Comparison of retention times of eight individual polyphenol standards, the polyphenol mixture and components in Reseda lake/buckthorn berry pigment with comparable retention times.	<b>59</b>
<b>3.2.1.1</b>	Voltages that provide the best EC-SERS signal for each polyphenol standard	<b>75</b>
<b>3.2.6.1</b>	Peak Assignments of Formic Acid. <sup>54</sup>	<b>89</b>

## **Chapter 1: Introduction**

### **1.1 Research Goal**

The purpose of this thesis is to detect and identify the many components found in yellow lake pigments. Two-dimensional liquid chromatography (2D-LC) coupled with electrochemical surface-enhanced Raman spectroscopy (EC-SERS) is explored in this thesis as a means towards this goal as an offline detection modality for this process. The identification of organic pigments in paintings is known to be one of the most challenging tasks in art conservation due to the complex mixture of colourants, mordants, and fillers, as well as the potential presence of degradation products that are produced over time.<sup>3,4</sup> For natural organic pigments in particular, degradation can occur due to exposure to light, pollutants, oxidation and humidity present in the artworks environment.<sup>3,5</sup> An understanding of which pigments are present, as well as their potential extent of degradation is very important to both the conservation treatments of an art object, as well as informing future display conditions.<sup>3,6,7</sup> For example, an art object found to contain many natural organic pigments which can readily fade (called fugitive pigments) may be only shown in the future under low light conditions, or a decision may be made to no longer show the object in a gallery setting. An ideal analytical method for identifying these pigments must be exceptionally sensitive, selective, minimally invasive (ideally non-invasive), and applicable to a wide range of pigments.<sup>8,9</sup> Two promising candidates that embody these characteristics include high-performance liquid chromatography (HPLC) and surface-enhanced Raman spectroscopy (SERS). HPLC has shown promise in separating and identifying the various components in complex paint samples.<sup>10-13</sup> However, it is not uncommon that HPLC separation for these complex mixtures can be poorly

resolved.<sup>1</sup> SERS has shown increasing usefulness as an analytical tool for the identification of pigments, particularly in light of the excellent sensitivity offered by this technique. However significant limitations remain, particularly related to the fact that some molecules have larger Raman scattering profiles than others. Therefore, consequently are detected preferentially, causing SERS analysis of complex mixtures challenging without an initial separation step.<sup>2,13-16</sup>

Multidimensional liquid chromatography (2D-LC) and electrochemical-SERS (EC-SERS) are advanced analytical techniques that can solve these limitations. 2D-LC has a much higher separation power than conventional HPLC, allowing for the potential separation of hundreds of components.<sup>3,17-19</sup> EC-SERS has recently been shown to offer both an increase in the sensitivity and selectivity of SERS, in some cases allowing for the detection of a species that could not be readily detected using SERS alone.<sup>20-21</sup> It is anticipated that by varying the electric potential applied to the substrate by using EC-SERS, a superior detection of the various components in yellow lake pigments will result. The main question this thesis project aims to address is if it is possible to use a 2D-LC-EC-SERS method to significantly enhance the separation *and* detection of the components in a yellow lake pigment sample. This investigation will begin by preparing various polyphenol standards such as apigenin, emodin, luteolin, etc., which are known to comprise the dye components of yellow lake pigments. The retention times gathered from the 2D-LC analysis and the EC-SERS signals of these standards (collected as fractions) will first be assessed as a proof-of-concept validation of the technique. Next, the retention times and EC-SERS spectra will be compared to the yellow lake pigment sample, in an effort to identify the various components in the yellow lake. If the goal of identifying the many

components in the yellow lake pigment sample is achieved, future work will consist of identifying the degradation products produced over time upon exposure to light and elucidating the pigment degradation pathways for yellow lake pigments in general.

## 1.2 Introduction

Since antiquity, organic dyes extracted from biological sources such as insects and plants have been used to create pigments and used as part of an artist's palette to create art.<sup>4</sup> Efficient dye detection is critical to conservation, preservation and historical interpretation of many works of art.<sup>6,7,22</sup> However these colourants often exist in complicated matrices and are not always easy to identify, particularly in the minute samples taken for analysis from precious artworks.<sup>2,4-7,9,14-15,22</sup> For example, these dyes may exist in association with metals, called mordants, which can complicate analysis.<sup>6,10</sup> In addition, if the colourant is insoluble and suspended in a medium (termed a pigment) the analysis can be further complicated by the medium.<sup>4,7</sup> A common form of pigment used since antiquity is called a lake pigment. A lake pigment consists of a dye molecule and an inorganic precipitating agent (called the mordant) such as aluminum or copper, which causes the dye to precipitate out as a pigment.<sup>6,7,10</sup> The nature of the metal can change the overall colour of the pigment and reduce how quickly the dye fades over time.<sup>6,7,10</sup> In addition, formation of the lake pigment produces a pigment which is more easily retained on fabric, for example, and has been key to successful textile dyeing since antiquity.<sup>4,6,7</sup> Common examples of lake pigments include the red lake pigments (madder lake, carmine lake) and the yellow lake pigments (Reseda lake, Stil de Grain).<sup>7</sup> These pigments are very complex, because, in addition to the many dyestuffs used to produce the colour, they also contain binders, fillers and degradation products, all of which make the analysis of the dyestuff itself a challenge.<sup>4,10</sup>

Clearly, fast and accurate detection of dyestuffs has some consequences such as not being able to obtain an art sample in some cases, or if possible to obtain one, it is very minuscule. In addition, not being able to fully identify all the dyestuffs present in the pigment can be a challenge since some dyestuffs are quite similar in structure. Therefore, this identification process must be carried out efficiently and in an effective and reliable manner to achieve a full characterization of the pigment under investigation.

Methods currently in place for dye and pigment analysis include spectroscopy (UV-Vis, infrared, NMR, Raman), microscopy (scanning electron and scanning-probe microscopy), and chromatography (liquid, gas and ion chromatography).<sup>8</sup> While most of these techniques are sensitive, selective and sometimes conclusive, there are limitations which include a requirement for a significant amount of sample, relatively high cost, and in some cases an inability to properly analyze complex mixtures.<sup>9,10</sup> A minimally destructive, highly characteristic, sensitive, selective, rapid, and broadly applicable analysis technique is necessary to detect and identify the various compounds present in these colourants. At present, a truly perfect analytical method that meets all of these requirements does not exist for the analysis of cultural heritage objects.

Raman spectroscopy is a technique based on the inelastic scattering of monochromatic light as a result of the incident light interacting with molecular vibrations. Raman spectroscopy provides valuable molecular fingerprints; however, it is an inherently weak technique due to the very low proportion ( $\sim 1$  in  $10^6$ ) of Raman scattered photons.<sup>22</sup> In addition, interfering fluorescence by the sample can occlude the much weaker Raman scattering.<sup>7</sup> To overcome these issues, surface enhanced Raman spectroscopy (SERS) involves incident light interacting with a noble metal surface which supports the surface

plasmons, which are the electromagnetic waves coupled to the collective oscillation of free electrons in the metal that causes a significant enhancement of normal Raman signal.<sup>23-25</sup> Surface plasmons can be classified as one of two types: localized surface plasmons (LSP), or propagating surface plasmons (PSP). LSPs are described in metals that are nanoscale in all dimensions, such as a nanosphere.<sup>24-26</sup> Contrarily, PSPs are described in metals that are nanoscale in one or two dimensions, such as a nanofilm or a nanowire, respectively.<sup>24,25</sup> SERS has steadily gained exposure as a candidate for dyestuff detection in dyes and pigments. SERS so far has been successful in identifying the organic and highly fluorescent dye present in the artwork, however, not typically for colourants containing one or more dye component.<sup>2</sup> In addition, it has been shown that it has been difficult to be able to identify the many chromophores present in a pigment mixture with SERS as one chromophore is often preferentially adsorbed to the surface of the SERS substrate (and thus more readily detected) while the other components are not.<sup>27</sup> In addition, some chromophores have larger Raman scattering profiles than others and are preferentially detected for this reason.<sup>27</sup>

Currently, the most widely used technique for the separation and detection of dyestuffs present in various dyes and pigments is high performance liquid chromatography (HPLC).<sup>14</sup> Although liquid chromatography is powerful and highly sensitive, it begins to reach the end of its separation capacity for highly complex samples such as natural extracts, metabolites and proteins that contain many components that are similar in structure.<sup>17-19</sup> Multidimensional liquid chromatography (2D-LC) is an emerging technique that addresses this issue due to the enhanced peak capacity allowing adequate separation of highly complex samples, which would be very advantageous in the analysis of various colourants.<sup>3</sup>

For example, 2D-LC was recently used to study the nature and approximate concentrations of dye degradation products in order to determine the condition of 17<sup>th</sup> and 19<sup>th</sup> century historical objects.<sup>3</sup>

SERS has recently been applied as a detection modality for chromatographic techniques such as thin-layer chromatography (TLC) and HPLC due to its excellent sensitivity and ease of application in dye and pigment analysis.<sup>1</sup> SERS is potentially an attractive alternative compared to other expensive and complicated detector modalities such as mass spectrometry because it renders a highly specific, molecular-level identification of chromophores from minimal sampling.<sup>7,9</sup> A significant disadvantage for TLC-SERS is the interaction of the compounds with the silica gel TLC substrate and this interaction can cause adsorption-induced spectral distortions of SERS spectra.<sup>1</sup> Therefore causing a significant decrease of the signal resolution and spectral quality in certain circumstances.<sup>1</sup> SERS coupled with these chromatographic techniques have other limitations such as there are many chemically similar compounds present in a dye or pigment, that would elute at the same time or have the same retention factor, known as coelution. Therefore, coeluted components will not be able to be individually identified afterwards with SERS.<sup>1</sup> Consequently, HPLC coupled with SERS requires a way to overcome this limitation in order to acquire more information about the dye and pigment under investigation.

This thesis seeks to explore the combination of two-dimensional liquid chromatography (2D-LC) with electrochemical-surface enhanced Raman spectroscopy (EC-SERS) as an offline detection modality. These combined techniques allow for a coupling of the powerful separation power of multidimensional chromatography with the

robust molecular fingerprinting capability of SERS. The addition of the electrochemical component to SERS (EC-SERS) provides an additional level of sensitivity and selectivity to the combination of LC and SERS. 2D-LC has been shown to be a promising tool for the separation of very complex samples with many components similar in structure and has recently

been found to be useful for the separation of artist colourants.<sup>3</sup> However, after a sample is within a 2D-LC system, the sample is significantly diluted and subsequently an ultrasensitive technique is needed for additional investigation. EC-SERS combines both electrochemistry and SERS by adding an electrical potential to the substrate in the presence of an electrolyte. The EC-SERS technique has been shown to improve the SERS spectrum of various molecules at different voltages, and this advantage could be very valuable in colourant analysis since it could allow other dyestuffs to adsorb to the surface of the substrate and produce a signal. In this thesis work, 2D-LC-EC-SERS will be explored for the first time for separation and identification of yellow lake pigments.

## 1.3 Literature Review

### 1.3.1 Yellow Lake Pigments

Natural dyes have been used since antiquity to colour objects such as textiles, sculptures and paintings.<sup>6</sup> However, identifying the dyestuff (colouring matter) present in a dye or pigment can be problematic as it is generally a minor component within a complex matrix.<sup>7</sup> The identification of colourants used in art is relevant to art historians and conservators for many reasons. For example, characterizing the artist's palette can allow one to gain knowledge and understanding of their practice.<sup>22</sup> Comparisons can then be made between other painters by tracing pigment use through history and geographical locations, which could be very useful to discover trade routes or technological evolution.<sup>22</sup> The choice of the particular pigment for colour and its distribution throughout the painting could also be related to social motivations of the artist such as the cost of the pigment.<sup>22</sup> Lastly not let the colourants used in an artwork to avoid fading over time by factors present in the artworks environment by establishing conservation treatments of these colourants.

Colourants can be divided into dyes and pigments, which are sources of colour in art; however, they have different properties. Dyes are made by dissolving the colouring matter, known as the dyestuff, in a liquid, which is then absorbed into the material to which they are applied to such as textile fibers.<sup>10</sup> One main property of dyes is that they are usually water-soluble and tend to fade quicker than pigments.<sup>6,7,10</sup> Pigments, on the other hand, are typically insoluble colourants as they consist of extremely fine particles of ground colourant suspended in a liquid medium such as an oil which forms a paint film that actually bonds to the surface to which it is applied.<sup>10</sup>

Lake pigments are technically classified as inorganic pigments and are formed by incorporating an organic dye molecule onto an inorganic substrate such as a metal (aluminum or calcium) which is called the mordant.<sup>6,10,14,28</sup> Lake pigments can then be fixed onto a textile such as silk or wool by using the mordant.<sup>6,10,14,28</sup> A common red lake pigment is madder lake containing alizarin as one of the primary dye components. Figure 1.3.1.1 is a schematic representation of alizarin dyestuff, aluminum mordant, and madder lake pigment.<sup>29</sup>

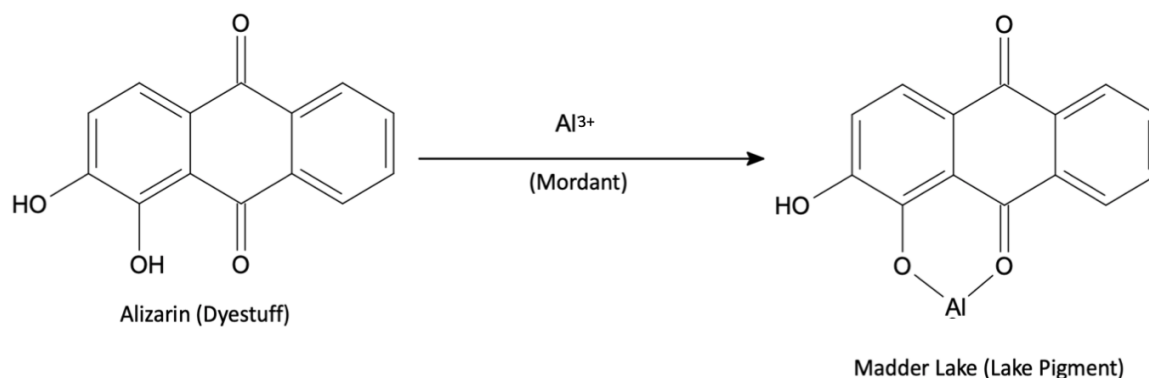
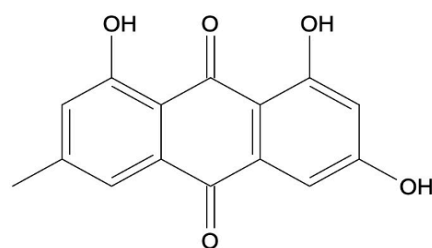


**Figure 1.3.1.1:** Schematic representation of alizarin dyestuff, aluminum mordant and madder lake pigment.

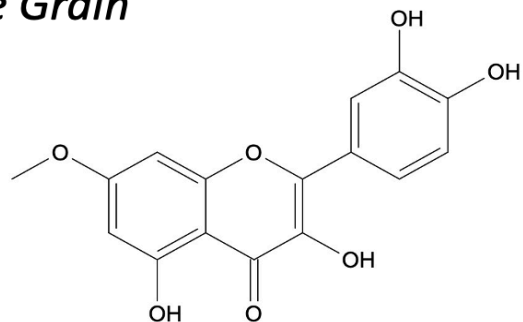
Two known yellow lake pigments are Reseda Lake and Stil de Grain. The yellow dyestuffs used to create these lake pigments were extracted from plant sources: weld (*Reseda luteola*) and unripened buckthorn berries (*Rhamnus cathartica*), respectively. These yellow lake pigments are an important part of an artist's palette because they are often used in optical mixtures with other pigments such as blue pigments (indigo or Prussian blue) to produce green pigments.<sup>30</sup> Chromophores which are present in dyestuffs are responsible for the colour in pigments.<sup>Error! Bookmark not defined.</sup> The chromophores that give the yellow colour in these lake pigments can be classified as curcuminoids, flavones, flavonols and anthraquinones, which are collectively known as polyphenol compounds.



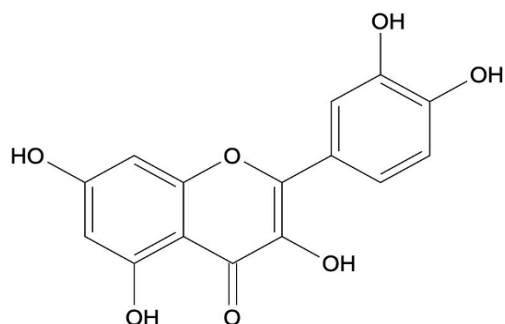
## *Stil de Grain*



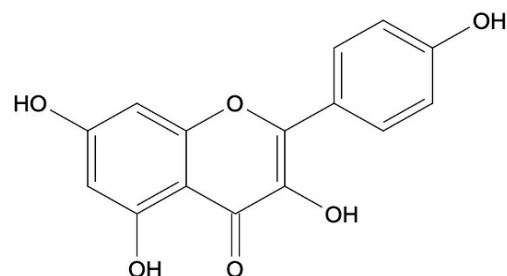
**Emodin**



**Rhamnetin**



**Quercetin**



**Kaempferol**

**Figure 1.3.1.3:** Chemical structures of polyphenol compounds present in Stil de Grain lake pigment; emodin, rhamnetin, quercetin and kaempferol.

As mentioned above, the identification of these pigments in artworks can be a significant analytical challenge. Complexation of dyestuffs with metal salts to produce lake pigments, as well as undesired interactions with other matrix components such as the textile, binding media, fillers and extenders further complicate the analysis.<sup>4</sup> Furthermore, the colouring components are particularly sensitive to light, air and humidity, so exposure frequently results in degradation of the dyestuff and produces by-products in the pigment or dye.<sup>3</sup> When these natural yellow dyes are present in an optical mixture, for example a green, as the yellow fades, the blue pigment remains, causing green components in paintings, such as grass and foliage, to take on an unnatural blue appearance. These are just

some of the issues that typically complicate the pigment identification process in minute samples taken from art historical objects.

### **1.3.2 Analysis of Dyes and Pigments**

Dye and pigment analysis are crucial for the conservation, preservation and historical interpretation of works of art. However, some of the major constraints of pigment and dye analysis include the complex nature of the sample and the limitation that sampling from a piece of art is often extremely limited or not allowed.<sup>4,6</sup> Thus, an ideal analytical technique to use for the identification of lake pigments has to be minimally destructive, highly characteristic, sensitive, selective, rapid, and applicable to a broad range of organic pigments. Many analytical techniques have been used for this purpose, such as many forms of spectroscopy (UV-Vis, infrared, NMR, Raman), microscopy (scanning electron and scanning-probe microscopy), and chromatography (liquid, gas and ion chromatography), all of which have their advantages and disadvantages.<sup>8</sup> For example, UV-Vis spectroscopy is not selective and gives limited information especially when the colourant is embedded within a complex matrix.<sup>10</sup> NMR is an excellent tool, but it is insufficient for very small amounts of sample and is unsuitable for analysis of trace amounts of colourant.<sup>10</sup> Gas chromatography has not been widely used in analyzing dyes because of the relatively high molar mass and polarity of analytes.<sup>8</sup> A derivatization of the target analyte(s) is therefore a necessary requirement for GC-MS. Since the amount of dyestuff present in the dye or pigment is typically very low due to the high tinting power of these colourants, non-invasive and ultrasensitive methods of analysis are preferred.<sup>6</sup> The next few sections will touch on some of the techniques used for pigment identification on art or textiles relevant to this thesis research.

### 1.3.3 Analysis of Pigments with Raman Spectroscopy

Raman spectroscopy is an established technique in pigment identification because it is known to be reliable, sensitive, rapid, and non-invasive.<sup>31,32,33</sup> Bell et al. successfully used this spectroscopic method to obtain and record 56 common pigments used in artworks prior to 1850.<sup>31</sup> Although some dyes are suitable for Raman spectroscopy, their Raman spectroscopic identification in art objects is often difficult for many reasons. For one, the power of laser excitation must be low enough to avoid decomposition or modification of the dye since they are readily photodegraded.<sup>6</sup> The amount of dye actually present in the work of art is small; consequently, the amount of sample is quite minimal and therefore often provides a weak spectral intensity.<sup>6,14</sup> Also, natural dyes are mostly mixtures of several compounds which complicates their analysis. Lastly, strong inherent fluorescence is often a significant background interference, obscuring the much weaker Raman scattering.<sup>6</sup> The result is a very weak Raman signal (if visible at all) superimposed on a very broad fluorescence background; this interference is generally more significant as the excitation wavelength for the Raman scattering process decreases, as the more energetic wavelengths are most capable of exciting strong fluorescence.<sup>32</sup> It was recently highlighted by Marucci et al. that Raman spectroscopy is not always able to fully characterize some pigments, especially natural organic dyes and pigments because fluorescence is typically produced.<sup>32</sup> However, Burgio et al. was able to use Fourier-transform Raman (FT-Raman) microscopy to identify 60 pigments and related materials because FT-Raman typically uses infrared excitation at 1064 nm, therefore greatly reducing the interfering fluorescence.<sup>33</sup> In conclusion, with the results conveyed by Bell et al. and Marucci et al. but additionally due to poor sensitivity, selectivity and large amount sample sizes (if not possible to do in situ)

and the inability to conclusively identify many natural organic pigments, this emphasizes the need to turn to other techniques for further investigation in this field of research.<sup>30,31,32</sup>

### **1.3.4 Analysis of Dyes and Pigments with Surface-Enhanced Raman Spectroscopy**

SERS has emerged over the past few decades as a promising technique for pigment analysis in art because it enhances the Raman signal produced and also quenches any fluorescence, due to the presence of a noble metal substrate.<sup>4,7,16,30</sup> The enhancement of Raman signal is demonstrated in the SERS spectra of a dye molecule which provides a unique molecular fingerprint of that molecule. In addition, SERS is extremely useful for the ultrasensitive detection of organic chromophores. Dyes, particularly the natural organic dyes, have chromophores with large  $\pi$ -electron systems and/or atoms carrying lone electron pairs, allowing for enhanced interaction with the metal SERS substrate.<sup>14</sup> SERS involves incident light interacting with a nanostructured noble metal surface and the molecule of interest that has adsorbed to that metal surface through electrostatic interaction, all of which produces an enhancement of Raman signal for the molecule. SERS has been recognized to be a reliable and effective method for the analysis of various lake pigments such as carmine lake, madder lake and Reseda lake in textiles, paintings and other cultural heritage objects.<sup>2,7,9,15</sup>

Detection of chromophores in dyes or pigments using SERS is dependent on several factors including the optical and structural properties of the substrate, the affinity of the analyte to the metal surface, surface coverage and the extent of the Raman enhancement.<sup>33</sup> However, there are various chromophores present in dyes and pigments that have various resonance wavelengths and chemical properties.<sup>33</sup> Therefore, successful identification of

all chromophores is quite challenging with only a microscopic sample. Jurasekova et al. reported through their investigation of weld-dyed wool and silk textiles that certain flavonoids such as luteolin dominate the SERS spectra even when present in a mixture containing other molecules such as apigenin. The reason behind this is that the Raman cross section of luteolin is larger than that of apigenin, and as such it is the predominant species contributing to the SERS signal for the mixture.<sup>4</sup> Error! Bookmark not defined.

A significant challenge when investigating lake pigments in particular is that since the dye molecules are coordinated to an ion such as calcium or aluminum, they cannot adsorb readily onto the metal SERS substrate, thus precluding the SERS enhancement from occurring.<sup>4</sup> Consequently, several *ad-hoc* sample pre-treatments have been developed prior to SERS analysis.<sup>4,6,7</sup> These sample pre-treatments are necessary in order to increase the sensitivity and decrease the ambiguous identification of chromophores present in the pigment by extracting the dyestuff(s) from the mordant.<sup>4,30</sup> SERS experiments on lake pigments initially relied on extractions in strong acids or alkali.<sup>4</sup> Pozzi et al. reported that sulfuric and hydrochloric acids have recently been used for the SERS analysis of yellow dyes and lake pigments in oil paint, with successful results.<sup>4,7</sup> Mayhew et al. demonstrated a simple extractionless hydrolysis step using 1:3 hydrochloric acid/methanol at room temperature that was effective in producing high-quality SERS spectra of buckthorn berries, stil de grain and Reseda lake.<sup>7</sup> Since very few SERS studies on yellow lake pigments are currently available, their work, to their knowledge, represented the first successful detection of Reseda lake using SERS.<sup>7,9</sup>

In spite of providing a high yield of extracted dye, such acids and some hydrolysis methods have been shown to interfere with the dye analysis because these acids cause

disruption of the matrix.<sup>4,34</sup> Consequently, this leads to the formation of degradation products and can cause decomposition of the dye, which can in turn inhibit the interaction between the dye and the metal nanostructure of the substrate.<sup>4,34</sup> Thus, valuable information is lost that could lead to the identification of a particular dyestuff. Gentler extraction procedures involving weaker acids such as formic acid have been established to avoid these issues.<sup>4,7,9</sup> In addition, *in-situ*, non-extractive hydrolysis methodologies have been used, although these are not as common in the literature. These types of methods do not severely degrade the analyte, but still facilitate dye detection and identification in most cases. Leona et al. developed an *in-situ*, non-extractive hydrolysis method involving a pre-treatment of the sample with hydrofluoric acid vapours in a closed chamber.<sup>14</sup> SERS spectra were reproducibly obtained for a number of lake pigments, including madder lake, with the use of this extraction method.<sup>14</sup>

Furthermore, non-extractive, non-hydrolysis methodologies have been used for the identification of chromophores in various artworks using only microscopic quantities of art sample, and this is possible when these samples are combined with colloidal silver to provide a SERS active component of the sample.<sup>15</sup> As a result, this method has provided valuable information on the dyes identified in the minute samples and avoids possible risks of dye degradation during extraction and hydrolysis.<sup>Error! Bookmark not defined.</sup> Jurasekova et al. were the first to use *in-situ* non-extractive and non-hydrolysis SERS, adding silver nanoparticles onto the fiber directly to produce a SERS signal for a reference fiber dyed with luteolin and apigenin.<sup>Error! Bookmark not defined.</sup> Brosseau et al. also used this type of method to successfully investigate reference materials and both synthetic and natural dyes present in various media including pastel samples once belonging to Mary Cassatt.<sup>9</sup> In

another article, Brosseau et al. analyzed three distinct red/purpled grain types obtained from a Winslow Homer watercolour painting that had experienced fading of its pigments.<sup>15</sup> Information gleaned from this study, including identification of the remaining dyestuffs, allowed for the digital reconstruction of the artwork, helping to inform the original intention of the piece.

All of these works highlight the usefulness and versatility of SERS for art conservation studies, since the pigment could be readily identified. However, often when analysing dyes and pigments just one of the many components in the sample gives a dominant SERS response, while the other chromophores are not detected. In addition, certain chromophores, such as the anthraquinone-based red dyes (alizarin, cochineal) tend to be easier to detect than others, including the natural yellows.<sup>7,9</sup> Hence, a separation technique prior to the SERS analysis is essential to obtain comprehensive identification of all components in an art sample.

### **1.3.5 Analysis of Dyes and Pigments with Chromatography**

The most used technique in dye and pigment analysis is high-performance liquid chromatography (HPLC). This technique has demonstrated the most consistent results in this field by identifying a large number of natural organic colourants used in art.<sup>6,8,9</sup> HPLC is sufficient in separating and subsequently identifying the many dyestuffs that are very closely related in dyes and pigments.<sup>11</sup> The combination of high separation power of HPLC coupled with complete online spectral characterization represents an important and indispensable advantage. For the most part, HPLC techniques are most commonly coupled with a diode-array detector (DAD). For example, Wouters et al. used HPLC-DAD to identify and quantify each dyestuff present in five red dyes present in dyed wool samples.<sup>11</sup>

Various studies have been done on the yellow dyes produced from weld and buckthorn berries plants with HPLC analysis. Cristea et al. used HPLC-DAD for qualitative and quantitative determination of flavonoid content in the weld plant, which is used to create the Reseda lake pigment.<sup>12</sup> The authors were able to effectively identify the presence of luteolin and its corresponding glycosidic compounds, which are all very similar in structure.<sup>12</sup> As well, Deveoglu et al. investigated the many components present in weld, buckthorn and bastard hemp plants and identified these components in yellow dyed wool through the use of reverse-phase HPLC-DAD.<sup>13</sup>

Perry et al. used HPLC coupled with electrospray ionization mass spectrometry (ESI-MS) to identify the flavonoids present in various yellow lake pigments that were incorporated in a large range of media and paintings.<sup>35</sup> The authors also analyzed raw plant materials of weld and buckthorn berries for comparison with the lake pigments. Coupling a MS detector to HPLC is the most common because of the greater sensitivity, selectivity, and the rich structural information on the many components MS provides compared to DAD. ESI is a type of MS, and therefore provides these advantages.<sup>35</sup> These authors were successful in identifying various flavonoids such as apigenin, luteolin, kaempferol, quercetin and rhamnetin through their analysis using HPLC-ESI-MS.<sup>35</sup>

The natural dyestuff components present in dyes and pigments are usually separated using reverse phase chromatography.<sup>8</sup> The mobile phases used in HPLC in earlier years were water and methanol; however, acetonitrile is increasingly popular because it has lower absorbance, in the 200 to 275 nm range, a lower UV cut-off, and lower back pressure due to lower viscosity compared to methanol.<sup>8</sup> Typically, a gradient elution is used in this type of analysis.<sup>8</sup> Most separations have been completed using

columns packed with three or five  $\mu\text{m}$  particles, and using an octadecyl silyl ( $\text{C}_{18}$ ) stationary phase.<sup>8</sup>

Although chromatographic methods are highly selective and sensitive, disadvantages of this technique include the destructive nature and the requirement for a significant amount of sample from a previous art object. For example, a typical analysis requires the removal of approximately 1 mg of sample or 0.5 to 5 mm of dyed fiber.<sup>8,9</sup> As mentioned before, such a large amount of sample is not always available from an artwork, which makes this technique limited for the analysis of colourants.

### **1.3.6 Analysis of Dyes and Pigments with Surface-Enhanced Raman Spectroscopy coupled with Chromatography**

It is known that SERS can be beneficial over other vibrational techniques, since it provides highly specific and molecular level identification of extremely small samples.<sup>2</sup> In addition, SERS has been successfully applied several times for identification of organic and highly fluorescence dyes. SERS satisfies many of the characteristics of an ideal analytical technique for detecting and identifying colourants in artworks. Nevertheless, the main limitation of SERS is encountered during an analysis of a dye that is complex, which is often the case of natural dyes, since it has more than one chromophore), or textiles dyed with a combination of colourants to obtain a particular colour. In such cases, complex spectra are obtained or, alternatively, just one component gives a dominant SERS response while the other chromophores are not detected.<sup>1</sup> A few papers have focused in the identification of dyestuffs in a mixture.<sup>2</sup> For these reasons, coupling SERS with chromatography for analysis of dyes could be of great interest, since HPLC has the ability to identify the widest spectrum of colourants, if provided with enough sample.

Recently, Brosseau et al. developed and tested two ad-hoc SERS methodologies to successfully detect dye components in reference dyes and samples from art.<sup>2</sup> Thin layer chromatography (TLC) has been used before as a separation technique in dye analysis; however, Brosseau et al. were the first to couple TLC with SERS to separate and identify lac dye and carmine in red and pink dyed fibers in works of art.<sup>2</sup> As well, *in situ* on-the-fiber extractionless, non-hydrolysis SERS was used to give excellent SERS spectra of the colourant, with very minimal preparation.<sup>2</sup> Additionally, Campanella et al. successfully used TLC-SERS to separate and then identify daylight fluorescent pigments (DFPS) in both reference samples and an artwork.<sup>36</sup> In this work, the authors mentioned that using TLC first to separate the individual components was mandatory considering the high complexity of these pigments. Subsequently, fast and reliable identification via SERS was completed through the use of silver nanoparticles applied directly on top of the separated components on the silica paper.<sup>36</sup> Therefore, the applicability of this technique, by separating and then identifying the many components used in dyes and pigments, is promising for art conservation, as it can also significantly reduce the amount of material and sophisticated equipment needed compared to HPLC.

TLC-SERS can be quite effective in separating and then detecting more than one chromophore present in a dye mixture. However, the sample could be much more complex with many more components, hence the time of separating and analysis could be longer.<sup>1</sup> Other limitations of TLC-SERS are the co-elution of chemically similar compounds and the interaction of the compounds with the silica gel TLC substrate, which can cause adsorption-induced spectral distortions of SERS spectra, resulting in a significant decrease of the signal resolution and spectral quality in some cases.<sup>1</sup> Hence, an HPLC-DAD-SERS

system could be beneficial in providing a very detailed characterization of colourants of interest and reduce analysis time.<sup>1</sup> Zaffino et al. developed a HPLC-PDA-SERS system and were the first to use their system to analyse various chromophores, a reference dye and an extract from a pink thread of an Italian carpet. In the literature, analysis of purine bases and illicit drugs were among the few analytes that have used a HPLC-SERS system.<sup>1</sup> The use of this hyphenated technique can offer, besides an effective separation of dyes in mixture, valuable vibrational information for each constituent to be used for identification purposes. Only a few analyses can be performed on the scarce amount of art sample, especially if micro-destructive techniques are employed. HPLC-PDA-SERS can overcome this issue, by allowing one to obtain a valuable characterization, integrating chromatographic (HPLC), electronic (UV-Vis detection), and vibrational (SERS detection) information in just one analysis.<sup>1</sup>

### **1.3.7 Analysis of Dyes with Multidimensional Chromatography**

Conventional one-dimensional (1D) LC-MS has indeed proved to be a very useful tool for identifying various colourants in works of art. However, given the complexity of the samples obtained from art historical objects, multidimensional chromatography offers a new and exciting realm of scientific exploration for this area. Pirok et al. studied the nature and approximate concentrations of dye degradation products in order to determine the condition of various cultural heritage products, so resulting development is made in conservation of these artworks.<sup>3</sup> Some dyes alone can contain 40 degradation products at varying concentrations; thus, a 1D-LC may not have the separation power needed for this purpose.<sup>3</sup> A technique with much higher separation power is needed such as multidimensional chromatography (2D-LC). Pirok et al. used this technique to investigate

extracts from 17<sup>th</sup> and 19<sup>th</sup> century historical objects and, due to the extra dimension present in this system, many of the components have been separated, but not all have been identified.<sup>3</sup> 2D-LC is particularly useful for this field of research since real art samples are complex mixtures. However, this technique has not been utilized for this purpose much. One of the disadvantages of this chromatographic technique is severe dilution of the sample after being analyzed in both dimensions. Therefore, an ultrasensitive technique, such as SERS, is needed as the offline detection modality to further identify and characterize these colourants used in art.<sup>3</sup>

## 1.4 Theory

### 1.4.1 Liquid Chromatography

High-performance liquid chromatography (HPLC) is a powerful separation technique, capable of resolving mixtures with large amounts of similar analytes.<sup>37</sup> HPLC is used in many fields such as medicine, pharmaceuticals, forensics, and microbiology.<sup>38-43</sup> Liquid chromatographic separations involve the sample being distributed within the two phases present in this process. These two phases are called the stationary and mobile phases. The former is often found fixed in place inside a column and is composed of organic solid with varying polarity, while the latter is a liquid that transports the sample through the column and the chromatographic system. During the separation, a chromatogram is produced that directly provides both qualitative and quantitative information regarding each component of the sample. A chromatogram is a plot of some function of solute concentration (absorbance, voltage, etc.). Each component in the mixture is indicated by a retention time, the time at which a solute reaches and is detected by the detector. Both the peak area and peak height are proportional to the amount of the corresponding component.<sup>Error! Bookmark not defined.</sup> The goal of chromatography is to completely separate all components in a sample in the shortest time possible.<sup>43</sup> To obtain this goal, several parameters within the separation should be optimized, such as the composition of the mobile and/or stationary phases, the flow rate and the nature of the stationary phase. Many parameters obtained from a chromatograph can be quite useful in expressing the quality of the separation and quantifying the separated components. Figure 1.4.1.1 depicts a simple chromatograph where the sample is injected onto the column at zero seconds, and any non-retained species is eluted as the  $t_0$  retention time which can be used to determine the flow rate of the mobile

phase. Species A and B have different retention times,  $t_R(A)$  and  $t_R(B)$ , since they individually interact with the stationary phase differently. The species that has a higher affinity for the stationary phase will elute later (species B in this example). The width of each peak can be defined as the intersection of the tangents on each side of the peak with the baseline. Error! Bookmark not defined.

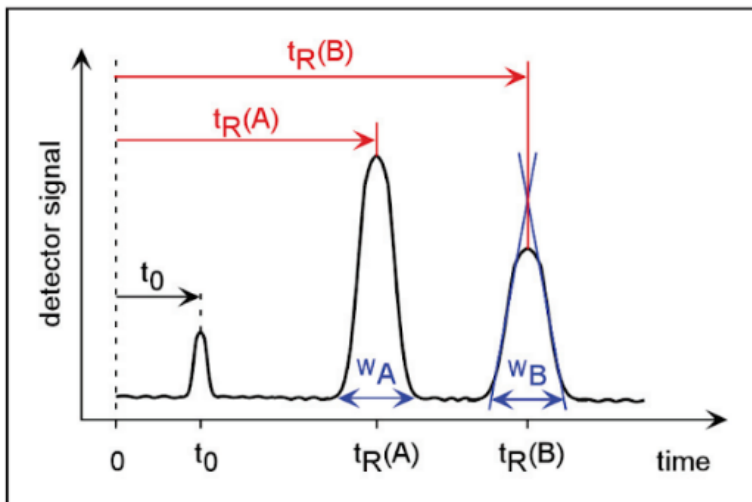


**Figure 1.4.1.1:** Simple chromatogram depicting retention time,  $t_R$ , and peak width,  $w$ .

The most important parameter in chromatography is to obtain great resolution in minimum amount of time. A resolution of 1.5 or greater between two peaks will ensure that the sample components are well separated to a degree at which the area or height of each peak may be accurately measured.<sup>44,45</sup> Resolution can be found by equation 1 below, where  $t_R$  represents the retention times of species A and B and  $w$  represents the peak widths of species A and B.

$$R = \frac{2(t_R(B) - t_R(A))}{(w_B + w_A)} \quad (1)$$

There are three parameters in chromatography that impact the resolution obtained during a chromatographic separation: retention factor ( $k$ ), selectivity factor ( $\alpha$ ) and

efficiency.<sup>44,45</sup> These three parameters that influence resolution is defined by the equation 2 shown below.

$$R = \frac{\sqrt{N}}{4} \times \frac{\alpha-1}{\alpha} \times \frac{k}{1+k} \quad (2)$$

The retention factor,  $k$ , is a parameter which can be used to measure the rate of the analyte migrating through a column.<sup>44</sup> The retention factor is a ratio of retention time of the analyte on the column to the retention time of the non-retained compound. The non-retained compound has no affinity for the stationary phase and elutes with the solvent at a time of  $t_0$ , which is known as the 'dead time'.<sup>44</sup> A high  $k$  value indicates that the sample is highly retained and has spent a significant amount of time interacting with the stationary phase.<sup>44,45</sup> If  $k$  is much smaller than 1, the analyte moves too quickly, and the elution time is too short to determine an exact retention time.<sup>Error! Bookmark not defined.</sup> Retention factors should be kept between 1 and 10 for good separations. The retention factor can be defined by equation 3.<sup>44,45</sup>

$$k = \frac{t_R - t_0}{t_0} \quad (3)$$

Selectivity factor is the ratio of retention factors of two peaks and its ability to distinguish between two components.<sup>44,45</sup> High  $\alpha$  values indicate good separation; however, this parameter is not directly indicative of the resolution. When the  $\alpha$  value is equal to one, it means that two species are co-eluting. Selectivity factor is defined by equation 4 below.

$$\alpha = \frac{k'_B}{k'_A} = \frac{t_{R(B)} - t_0}{t_{R(A)} - t_0} \quad (4)$$

There are two related terms that are widely used as quantitative measures of chromatographic column efficiency, such as plate height (H) or plate count of number of theoretical plates (N).<sup>45</sup> These two terms contribute to plate theory and are related by the equation 5 below,

$$N = \frac{H}{L} \quad (5)$$

where  $L$  is the length of the column packing.<sup>45</sup> The larger the number of plates (N), and the smaller the plate height (H), the better the efficiency of the chromatographic columns will be.<sup>45</sup> The number of theoretical plates can be determined by equation 6,

$$N = 16\left(\frac{t_R}{W}\right)^2 \quad (6)$$

where  $W$  is the width of the peak at its base (in units of time).<sup>45</sup> Plate theory is able to describe the efficiency of a column but fails to describe the shapes and breadths of the peaks based on how the analyte migrates through the column.<sup>45</sup>

A more realistic description of the processes occurring inside a column takes into account the time for the analyte to equilibrate between the stationary and mobile phases.<sup>45</sup> However, plate theory assumes the equilibrium is assumed to be established between both the mobile and stationary phases with the analyte from the beginning.<sup>45</sup> The resulting band shape of a chromatographic peak is therefore affected by the rate of elution.<sup>45</sup> Hence, rate theory takes into account not just the elution pattern of the peaks but also the shape and breadths of them.<sup>45</sup> A common phenomenon that occurs in chromatography is band broadening of the peaks.<sup>45</sup> Band broadening reflects the loss of column efficiency. The slower the rate of mass-transfer processes occurring while a solute migrates through the

column, the broader the peak.<sup>45</sup> The three parameters that influence band broadening are highlighted in the van Deemter equation (equation 7) that determines plate height.<sup>44,45</sup>

$$H = A + \frac{B}{u} + C \cdot u \quad (7)$$

The first term, A, represents the Eddy diffusion or multi-path term which describes the influence of column packing on band broadening, and this term is independent of flow rate. Analyte molecules will take different paths through the stationary phase at random if the packing is not uniform throughout the column. Consequently, this will cause broadening of the peak since there are different paths of different lengths. The second term, B/u, the longitudinal diffusion term, describes analyte movement from an area of high concentration to an area of low concentration.<sup>45</sup> The B/u term is inversely proportional to the flow rate (u).<sup>45</sup> The third term, C·u, the non-equilibrium mass transfer term, describes the resistance to mass transfer between the stationary phase and mobile phase, and is directly proportional to flow rate.<sup>45</sup> The optimum flow rate for a chromatographic separation can thus be determined by plotting H (plate height) as a function of u, as seen in Figure 1.4.1.2.

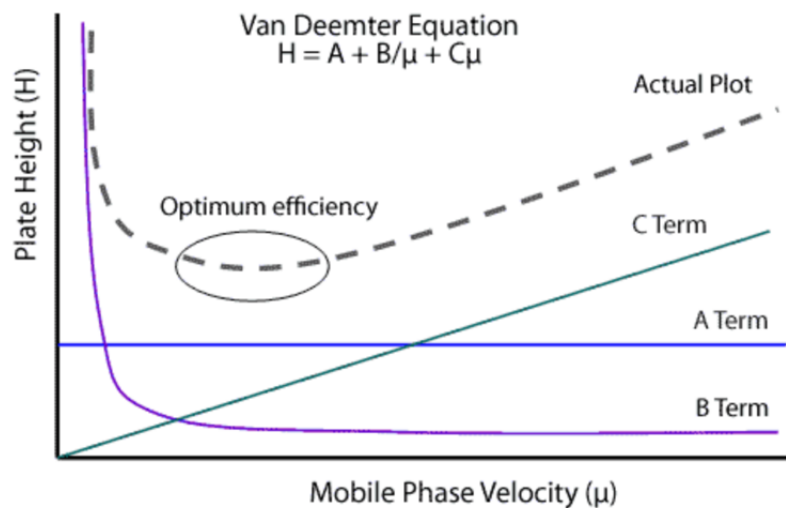


**Figure 1.4.1.2:** A van Deemter plot for the determination of optimum chromatographic flow rate ( $u$ ).

One of the limitations of HPLC is that it is, in some cases, unable to quickly separate mixtures of interest, and this generally arises from two distinct types of situations.<sup>46</sup> The first situation is mixtures that are too complex to be rapidly separated, for example, thousands of metabolites in biological samples, and consequently overtake the ability of the LC to separate the mixture into distinct components.<sup>17</sup> The second situation is mixtures that contain several species of interest that are very difficult to resolve because they are enantiomers and structural isomers.<sup>17</sup> These issues are very relevant for this thesis work involving polyphenol compounds that are very similar in structure, and which are derived from natural or complex samples, such as a painting sample. A potential solution to these complex situations is to move the separation into two dimensions, which drastically improves the separation power of liquid chromatography.

## 1.4.2 Multidimensional Liquid Chromatography

The increasing need to decode complex samples has created a demand for better separation power. The addition of an extra dimension of separation to a 1D-LC system,

which is known as multidimensional liquid chromatography, was one of the ways to answer this demand.<sup>17</sup> The primary limitations arise for 1D-LC for either intensely complex samples or samples that contain one or more pairs of compounds that are difficult to resolve.<sup>17</sup> As a rule of thumb, one dimensional LC offers a high probability for success for separating samples containing 10-20 compounds in 1 or 2 hours.<sup>19</sup> Complex samples include naturally occurring mixtures such as biological cells, blood, urine, environmental samples and synthetic polymers, especially copolymers.<sup>19</sup> These samples are too complex to be effectively separated in one dimension, and co-elution and peak overlap often occur as a result. Compounds difficult to resolve arise from being enantiomers or chemically similar in structure such that they would be challenging to separate from each other.<sup>19</sup> Therefore, multidimensional chromatography is a beneficial analytical technique in these cases.

To further separate the sample in the second dimension, there are two primary modes to choose from: comprehensive and heart cutting. In comprehensive two-dimensional liquid chromatography (LCxLC), a continuous stream of effluent from the <sup>1</sup>D column is transferred to the <sup>2</sup>D column.<sup>19</sup> In the latter heart cutting mode (LC-LC), only carefully selected portions (the hearts) of the <sup>1</sup>D peaks are transferred to the <sup>2</sup>D column for further separation.<sup>19</sup> Between these two modes, there are several subcategories that have been established, such as selective two-dimensional chromatography (sLCxLC) and multiple heart-cutting 2D-LC (mLC-LC). In principle, mLC-LC is simply an extension of LC-LC since single fractions from several <sup>1</sup>D peaks are transferred one at a time to the second dimension, often stored in a sample loop prior to <sup>2</sup>D analysis.<sup>19</sup> mLC-LC increases the scope of applicability of the heart cutting approach, as more analytes can be targeted for

further separation in a single chromatogram. The heart cutting mode is usually less complicated, and operating costs are lower compared to comprehensive 2D-LC. In addition, if the multiple heart cuts are stored, there is no significant limitation in the second dimension run time. The comprehensive mode typically takes longer than 1D-LC separations, with analysis times being 30 minutes to several hours.<sup>18</sup> Figure 1.4.2.1 is a schematic diagram of the comprehensive and heart-cutting modes in 2D-LC.

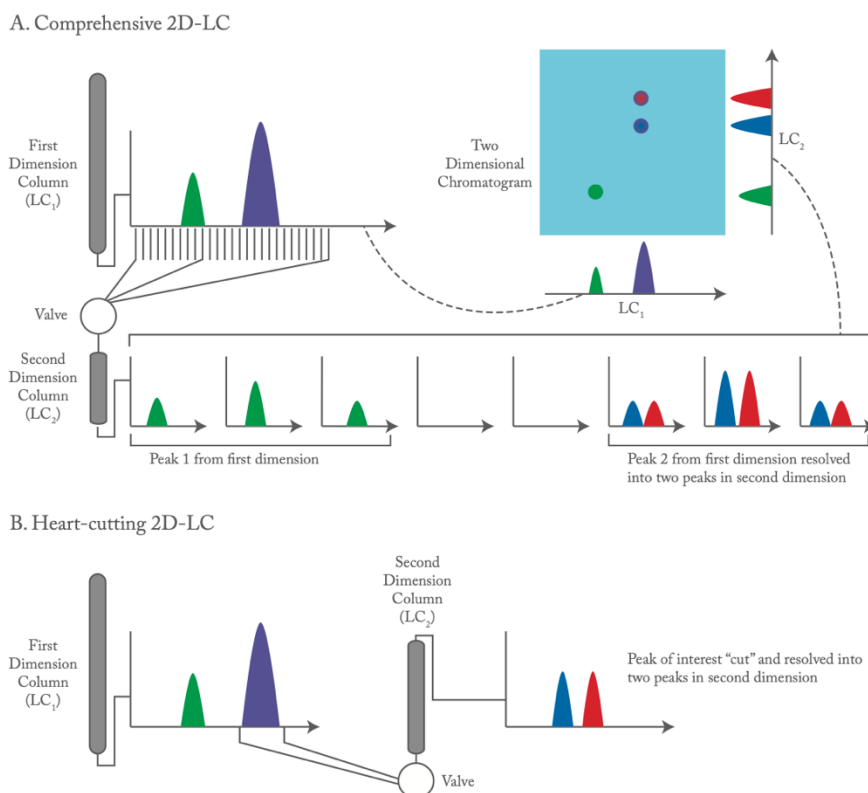


**Figure 1.4.2.1:** Schematic diagram of the comprehensive (LCxLC) and heart-cutting (LC-LC) modes in 2D-LC (© [www.theanalyticalscientist.com](http://www.theanalyticalscientist.com) 2014. Reproduced with Permission, Courtesy of [www.theanalyticalscientist.com](http://www.theanalyticalscientist.com)).

The heart of the multidimensional separation is the <sup>2</sup>D switching valve. In 2D-LC, the desired effluent(s) from the first dimension is/are captured and briefly stored in a sample loop within the <sup>2</sup>D switching valve. These cuts are then transferred to the <sup>2</sup>D column for

additional separation. A schematic of the valve and the switching positions for LC-LC are shown in Figure 1.4.2.2. In the top half of Figure 1.4.2.2, the blue line indicates the tubing is connecting the <sup>1</sup>D column to the waste. The red line is the tubing connecting the <sup>2</sup>D pump to the valve and then onto the <sup>2</sup>D column. Ports 4 and 5 show that there is a sample loop that temporarily contains the <sup>1</sup>D effluent until being transferred to the <sup>2</sup>D-column. In contrast, the second image on the bottom shows the valve position has moved to allow for the <sup>1</sup>D effluent to be transferred to the <sup>2</sup>D column. The instrument used for this thesis work is equipped with two decks, each containing 5 sample loops. One loop in each deck is kept open for continuous flow and not used to store cuts. Therefore, the 2D-LC is able to store eight <sup>1</sup>D cuts at any given time.

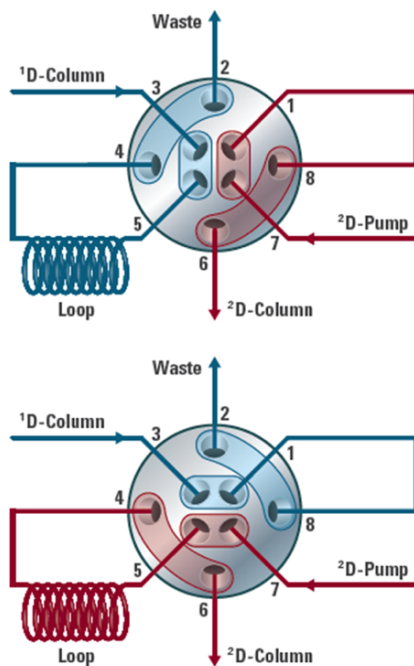


**Figure 1.4.2.2:** Configurations of an 8-port/2-position valve needed for LC-LC separation (© Agilent Technologies, Inc. 2015. Reproduced with Permission, Courtesy of Agilent Technologies, Inc.).

The real power of multidimensional chromatography is that incorporation of a second dimension of separation greatly increases the peak capacity without significantly

increasing analysis time.<sup>19</sup> Peak capacity is the most common metric used to define the limitations of 1D-LC in separating very complex samples with hundreds of components. Peak capacity is a theoretical construct that estimates the maximum number of peaks that can be separated at a specific resolution in the separation window. Peak capacity is taken as the time difference between the first eluting peak and the last eluting peak.<sup>17,19</sup> It is most convenient to choose peak capacity ( $n_c$ ) as the measure of resolving power. 2D-LC can achieve peak capacities of several thousand. For example, 10 000 is within a reasonable reach, while the maximum peak capacity achieved by 1D-LC is a few hundred depending on the analysis.<sup>17,18</sup> The enhancement of peak capacity is the main advantage of 2D-LC compared to 1D-LC. The product rule is to measure the resolving power of each of the two dimensions. The formula is expressed below (1).

$$n_{c,tot} = {}^1n_c + {}^2n_c \quad (1)$$

The total peak capacity obtained for a 2D-LC system ( $n_{c,tot}$ ) is the product of the peak capacity achieved in the first ( ${}^1n_c$ ) and second ( ${}^2n_c$ ) dimension.

Another essential concept in 2D-LC is the orthogonality between the two dimensions. For ideal multidimensional separations, the column's selectivities in both dimensions have to be completely independent from each another. Having two uncorrelated columns will provide the best chance of great separation in the <sup>2</sup>D. An example of that would be using either normal phase (NP) or reverse phase (RP) separation in the 1D, followed by whichever is not used in the second dimension. Figure 1.4.2.3 exhibits various levels of orthogonality.<sup>47</sup> Plot A demonstrates the best orthogonality, since the components are completely separated. While there is a small amount of orthogonality in plot F, it has

the lowest amount of this metric compared to the other plots, and this suggests that any co-eluting peaks in the  $^1D$  would also co-elute in the  $^2D$ , thus making the  $^2D$  separation redundant.<sup>47</sup> Plots B-E demonstrate various ways of how orthogonality is affected in a 2D-LC separation.<sup>47</sup> Plot B showcases excessive interactions between the analytes and the stationary phase, which is not desirable, while Plot C has low interaction between the analytes and the stationary phase in the column of the second dimension.<sup>47</sup> Plots D and E display poor choice of the first-dimension column, therefore affecting the orthogonality.<sup>47</sup>

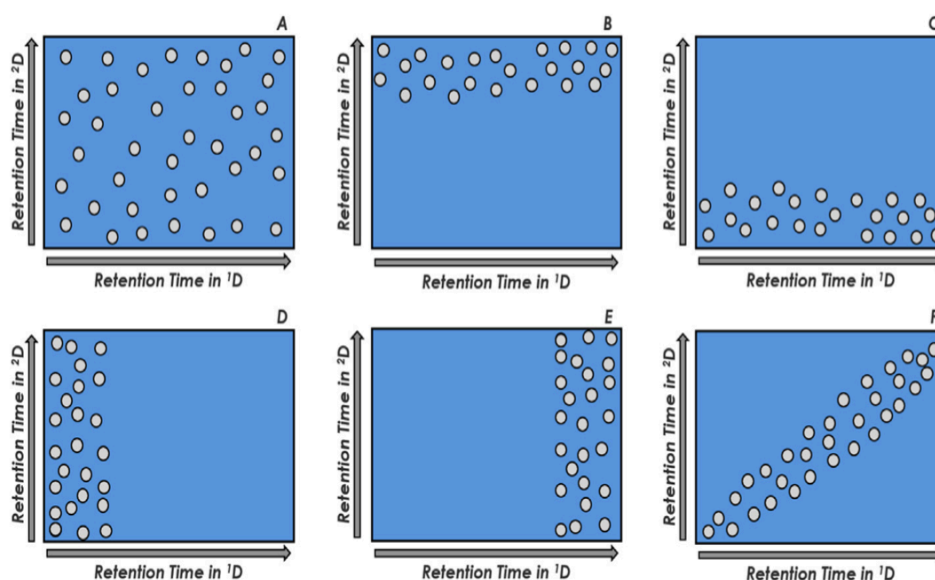


**Figure 1.4.2.3:** Schematic diagram exhibiting various levels of orthogonality (© 2019 Elsevier B.V. All rights reserved. Reproduced with Permission, Courtesy of Elsevier B.V.)

Although the separation power is significantly increased for 2D-LC, it is not always the best technique for every separation. Since 2D-LC uses multiple dimensions, the instrumentation and processing become much more complicated and thus expensive. It is also time-consuming and requires additional training and expertise. A sample should not be chosen for multidimensional separation if it can be adequately separated in a reasonable time using single dimension chromatography. Another disadvantage is that the successive dilution that occurs within the sample during the two separations may result in decreased

sensitivity of detection, and compatibility issues may arise.<sup>18</sup> In conclusion, the wider adoption of 2D-LC for routine analyses will require more effective and increasingly orthogonal separation modes that allow the greater use of the available 2D separation space.<sup>18</sup>

### 1.4.3 Raman Spectroscopy

Spectroscopy is based on the interaction between matter and electromagnetic radiation and is valuable for providing chemical and structural information on the samples of interest. Raman scattering, the phenomenon behind Raman spectroscopy, was first introduced in 1928 by Sir Chandrasekhara Venkata Raman.<sup>48</sup> Interaction of incident radiation with molecules of the sample by an intense monochromatic laser beam, typically in the UV-visible region, causes scattering of the incident light.<sup>48</sup> The scattered light includes both elastic scattering (Rayleigh scattering) and inelastic scattering (Raman scattering). Rayleigh scattering comprises most of the scattered light. In contrast, Raman scattering, is inherently very weak ( $\sim 10^{-5}$  of the incident beam) and scatters at a different frequency as the incident light and the energy difference (Raman shift) is what provides the vibrational fingerprint of the molecule of interest.<sup>48</sup>

The energy of Raman scattered light is either higher or lower frequency than that of the incident light depending upon the vibrational state of the molecule under investigation. When the frequency of the scattering light is lower than the frequency of the incident light, this process is referred to as Stokes Raman scattering.<sup>49</sup> In contrast, when the frequency of

the scattered light is higher than the incident light, this process is referred to as anti-Stokes scattering.<sup>49</sup> Figure 1.4.3.1 is a simplified schematic diagram that illustrates these concepts. Stokes lines are more intense than anti-Stokes lines because very few molecules exist in the excited state as compared to the ground state before irradiation, and due to Stokes lines being more intense, these lines are what is measured in conventional Raman spectroscopy.

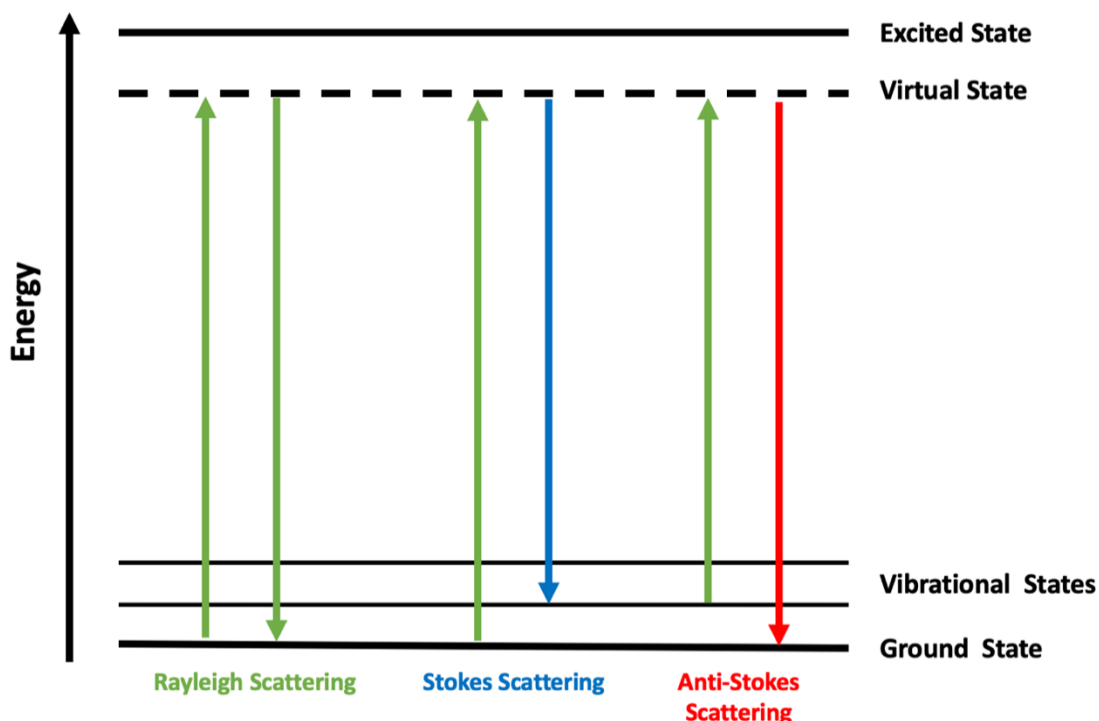


**Figure 1.4.3.1:** Diagram showing the different light scattering modes: Rayleigh, Stokes, and anti-Stokes scattering. (adapted Turrell et al.).

An essential requirement to obtain a Raman spectrum is a change in polarizability of a molecule during molecular vibration, which is probed by incident radiation.<sup>49</sup> Raman spectroscopy is a useful and widely applicable technique since it offers a molecular fingerprint of the sample of interest, requires no sample prep, is portable and is non-destructive.<sup>50</sup> However, as Raman spectroscopy, as mentioned above, is inherently weak, approximately only one photon out of a million undergoes inelastic scattering and fluorescence might interfere with the signal as such samples might not be detectable.

#### 1.4.4 Surface-Enhanced Raman Spectroscopy

Surface-enhanced Raman spectroscopy (SERS) was developed to overcome the inherent weakness of signal of Raman spectroscopy. To improve the signal produced from Raman spectroscopy, SERS involves measuring Raman scattering from an analyte adsorbed on a roughened surface of a noble-metal substrate such as silver, gold or copper.<sup>23</sup> The roughened surfaces are prepared through chemical roughening, metallic coating, or deposition of colloidal metallic nanoparticles on to a surface. A laser wavelength compatible with the chosen SERS metal is then used for excitation. In 1977, Jeanmaire and Van Duyne showcased that the degree of the Raman scattering signal can be significantly enhanced by this concept.<sup>50</sup>

The enhancement of the signal can be credited to two mechanisms: electromagnetic (EM) and chemical (CM) enhancement.<sup>23</sup> The first arises due to SERS using the localized surface plasmon resonance (LSPR) of either silver, gold or copper.<sup>26</sup> A strong electromagnetic field is then generated when the LSPR is excited by incident light, which depends on the excitation wavelength used.<sup>26</sup> Figure 1.4.4.1 demonstrates the LSPR created by the interaction of incident light and the free electrons of a metal nanosphere. When this occurs, the sample is subjected to the electromagnetic field and, consequently, the magnitude of the induced dipole of the molecule within the sample increases, causing the

intensity of the inelastic scattering to increase immensely.<sup>50</sup> The enhancement of scattering in this process is known as surface-enhanced Raman scattering, which emphasizes the crucial role the noble-metal substrate plays in this process.<sup>50</sup>

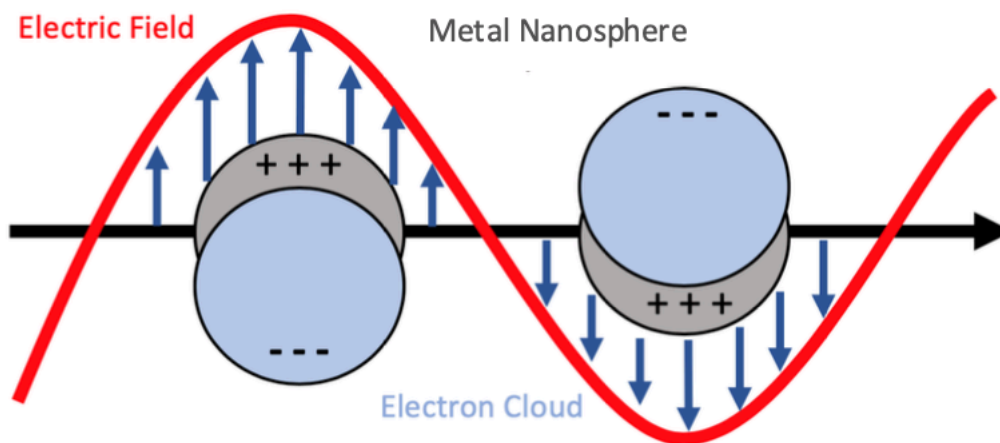


**Figure 1.4.4.1:** Schematic illustration of localized surface plasmon resonance (LSPR) of free electrons in the metal nanosphere that are driven into collective oscillation due to strong interactions with incident light (adapted Rycenga et al.).

Chemical enhancement mostly involves charge-transfer mechanisms between the molecule and the nanoparticle, where the excitation wavelength is compatible with the metal-molecule charge-transfer electronic states.<sup>26</sup> The CM enhancement is site-specific and analyte dependent; therefore, the molecule has to be directly adsorbed to the metal surface in order to experience this enhancement.<sup>50</sup> The EM enhancement includes several processes, such as the surface plasmon resonance, lightning-rod effect and coupling effect of the particle aggregate. These combined effects result in a giant SERS enhancement enabling unparalleled sensitivity, even down to the single-molecule level in some cases.<sup>51</sup> The electromagnetic mechanism is the dominant contributor of the SERS process providing an increase by  $10^5 - 10^8$  of signal, and the chemical mechanism only contributes an increase of  $10-10^3$ .<sup>23,26,51</sup> The total SERS enhancement from both electromagnetic and chemical

enhancement mechanisms may approach magnitudes of  $\sim 10^{10}$  -  $10^{11}$  for highly optimized systems.<sup>26</sup>

The critical part of performing a SERS experiment is the choice of the noble-metal substrate. Gold and silver are most often used because they are air stable, while copper is more reactive and cannot easily form stable nanostructures.<sup>26</sup> However, gold and silver are becoming rare metals, whereas copper is more earth abundant. The most important material in plasmonics is silver and this metal has many advantages over other metals such as gold, copper and aluminum. Silver is known to support surface plasmons in most of the UV-Vis-NIR spectrum comprising 300 to 1200 nm.<sup>23</sup>

SERS is a very sensitive and powerful technique with the detection of a single molecule having been reported.<sup>Error! Bookmark not defined.</sup> Another advantage of SERS is it quenches fluorescence that often occurs in normal Raman spectroscopy during the analysis of dyes. SERS sensing can be done very rapidly and is non-destructive. For these reasons, SERS has gained significant attention for the detection of many components in art, particularly dyes and pigments.

#### **1.4.5 Electrochemistry**

Electrochemistry is the study of electricity and how it relates to chemical reactions. Electricity can be generated by movements of electrons from one element to another (i.e. electron charge transfer processes that occur at a surface such as an electrode). Electrochemistry is widely used in batteries, fuel cells, environmental monitoring, industrial quality control and biomedical analysis.<sup>52</sup>

Electrochemical processes take place at the electrode-solution interface. The difference between various electroanalytical techniques depends on the type of electrical

signal used for the quantitation. Potentiometric and potentiostatic are the two principal types of electroanalytical measurements. These require at least two electrodes (otherwise known as conductors), and a contacting sample solution (otherwise known as electrolyte), which make up the electrochemical cell. The electrode surface is thus the link between an ionic and electronic conductor. Electrochemical cells can be classified as electrolytic, in which they are driven by an external source of electrical energy through non-spontaneous redox reactions, or Galvanic, in which they are spontaneously functioning by converting chemical potential energy into electrical energy through redox reactions.<sup>52</sup>

Potentiostatic techniques study the charge transfer process at the interface of the electrode and the solution.<sup>52</sup> The electrode potential is being used to derive an electron-transfer reaction and the resulting current is then measured.<sup>52</sup> Potentiostatic techniques measure chemical species that are electroactive meaning they can be made to reduce or oxidize, and this technique is advantageous because it is highly sensitive and selective, portable and cost-effective.<sup>52</sup> When electrodes are governed under potentiostatic control, there is additional influence of the charge held at the electrode. The surface develops a charge which then attracts ions of opposite charge to the surface that forms the electrical double layer. Figure 1.4.5.1 demonstrates the electrical double layer as described by the Grahame Model.<sup>53</sup> These interactions between the ions in solution and the electrode surface are electrostatic as a result of the fact that the electrode holds a charge density that arises from either an excess or deficiency of electrons at the electrode surface.<sup>53</sup> In order for the interface to remain neutral, the charge held on the electrode is balanced by the redistribution of ions close to the electrode surface.<sup>53</sup> The two layers that make up the electrical double layer are compact and diffuse layers. The compact layer contains an additional two layers,

termed inner and outer Helmholtz planes. The layer closest to the surface is the inner Helmholtz plane (IHP) and contains specifically adsorbed ions in order to maintain a neutral interface. The outer Helmholtz plane (OHP) is imaginary, passing through the non-specifically and solvated ions. The diffuse layer is a gradient of charge accumulation extending from the outer Helmholtz plane to the bulk solution.

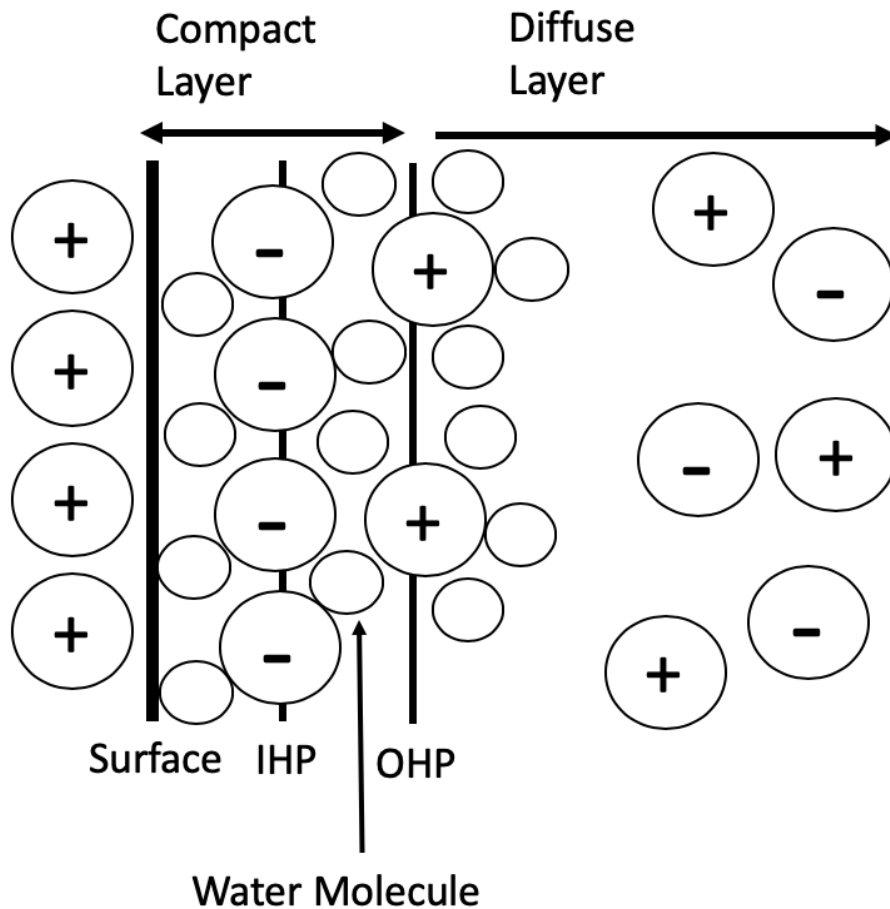


**Figure 1.4.5.1:** Schematic depiction of the electrical double layer (Grahame model) (adapted from<sup>53</sup>).

Electrochemical cells contain three electrodes such as the working (WE), reference (RE) and counter electrode (CE) when used in experiments where the electrode potential is controlled. The WE is where the electrochemical process occurs. The RE maintains at constant potential and is independent of solution properties. The most common reference

electrode is the silver-silver chloride (Ag/AgCl). The CE allows one to measure the potential of the working electrode while passing current. When choosing an electrolyte three factors have to be considered: solubility of the analyte, electrical conductivity and electrochemical stability. Electrolytes are within the concentration range of 0.1-1.0 M in potential-controlled experiments and are meant to maintain high ionic strength, decrease resistance of the solution and eliminate electromigration effects. Oxygen has to be purged out of the electrolyte by an inert gas to avoid interference with the electrochemical measurements.

#### **1.4.6 Electrochemical Surface-Enhanced Raman Spectroscopy**

Since SERS involves using noble metal substrates, it is natural to pair up this technique with electrochemistry. The electrochemical surface-enhanced Raman scattering (EC-SERS or electrochemical SERS) system measures the Raman spectrum of the studied analyte that has adsorbed to the surface of nanostructured electrodes, which is immersed in an electrolyte solution. It monitors changes as a result of applied voltage or current. Applying an electric potential to the surface of a SERS substrate *in situ* has been shown to increase the peak intensity of the analyte under investigation, consequently improving upon the already high sensitivity of SERS.

As previously mentioned, the dominating contributor to the SERS signal is the electromagnetic enhancement mechanism.<sup>23,26,51</sup> However, in this spectroelectrochemical technique, the chemical enhancement mechanism plays a much more crucial role than in SERS.<sup>51</sup> The chemical enhancement is contributed from several processes such as chemisorption interaction, the photon-driven charge transfer between adsorbate and substrate, and the coupling effect between the electron-hole pair and adsorbed molecules

between the molecule and the metal surface. However, these processes result in the relative weak enhancement; they determine the frequency shift and relative intensity of the spectral bands, which is essential for the EC-SERS characterization of chemical species.

Figure 1.4.6.1 demonstrates that when incident light makes contact with a nanostructured electrode surface, the SERS phenomenon occurs, in which a strong electric field is created in the electrical double layer region. There are two kinds of electric fields co-existing in the electrochemical system, such as the alternating EM-field and static electrochemical (EC) field. The EC-field could be quite substantial, influencing the interaction (or bonding) between metal and the adsorbate (i.e. complete adsorption or desorption), the molecular orientation of the analyte and the structure of the double layer, which may, in turn, cause the redistribution of the surface localized electric field.

EC-SERS has many advantages, including being sensitive and selective, simple, cost-effective, and portable.<sup>20,21</sup> Another advantage is SERS is dependent on the size and shape of the nanoparticles of the substrate and on the distance between the nanoparticles and the analyte. Therefore, when coupling SERS with electrochemistry, the distance between the nanoparticles of the substrate and the analyte is not as large, thus improving the SERS signal, since the interaction between these two components is improved. Lastly, by adjusting the potential of the electrode, different components of a complex analyte can adhere to the surface of the electrode, making this technique particularly useful in a comprehensive identification of yellow lake pigments.

## **Chapter 2: Experimental**

### **2.1 Reagents and Materials**

Yellow lake pigment was purchased from Kremer Pigments (New York, USA). Chromatographic analytical standards of luteolin (95%), quercetin dehydrate (96%), caffeic acid (98%), chlorogenic acid (96%), emodin (96%), apigenin (95%), rhamnetin (98%), and kaempferol (96%) were purchased from Toronto Research Chemicals (TRC) Canada (Toronto, Ontario). All chemicals were used without further purification and all solutions were prepared using formic acid/methanol (5:95%). Formic acid was purchased from Anachemia (Montreal, QC) and Fisher Scientific (Ottawa, Ontario). Acetonitrile (99.8%) and methanol (99.9%) was purchased from Fisher Scientific (Ottawa, Ontario). All glassware was placed in an acid bath composed of neat H<sub>2</sub>SO<sub>4</sub> overnight and was then thoroughly rinsed with Millipore water prior to use. AgNO<sub>3</sub> (99.9999%), NaBH<sub>4</sub> (≥96%), NaF (99%), and KCl (≥99%) were all purchased from Sigma Aldrich (St, Louis, MO, USA). Citric acid (>99%) was purchased from Alfa Aesar (Tewksbury, MA, USA) and sodium citrate from ACP (Montreal, Quebec). Screen printed electrodes (SPEs) (15 x 61 x 0.36mm) used as substrates for EC-SERS were purchased from Pine Research Instrumentation (Durham, NC, USA). Argon (99.999%) was purchased from Praxair Canada Inc. (Ontario, Canada).

### **2.2 Methods**

#### **2.2.1 Preparation of Polyphenol Standards**

### **i. Individual Polyphenol Standards**

The concentrations of the individual polyphenol standards were different depending on the polyphenol standard, because the masses of certain standards were limited. The concentrations of each polyphenol standard are listed in Table 2.2.1.1. The weighed mass of the polyphenol compound was then mixed with a 5:95% (v/v) formic acid/methanol to obtain a solution. Each standard solution was filtered using a 0.45  $\mu\text{m}$  PTFE syringe filter were put into a vial for LC analysis.

**Table 2.2.1.1:** Individual polyphenol standard concentrations.

<b>Polyphenol Standard</b>	<b>Concentration (ppm)</b>
<b>Caffeic Acid</b>	2000
<b>Chlorogenic Acid</b>	2000
<b>Luteolin</b>	2000
<b>Quercetin</b>	2000
<b>Apigenin</b>	250
<b>Emodin</b>	250
<b>Kaempferol</b>	2000
<b>Rhamnetin</b>	500

### **ii. Polyphenol Standards Mixture**

250 ppm solutions of each polyphenol standard were prepared in 5:95% (v/v) formic acid/methanol solution. 250  $\mu\text{L}$  of each standard was put into one vial to obtain a final

concentration of 31 ppm of each standard. The mixed standard was then filtered using a 0.45  $\mu\text{m}$  PTFE syringe filter into a vial for LC analysis.

### **2.2.2 Yellow Lake Pigment Extraction**

10 to 20 mg of the reference yellow lake pigment was weighed into an Eppendorf tube. 400  $\mu\text{L}$  of 5:95% (v/v) formic acid/methanol solution was added to the tube. The tube was then heated at 40°C for 30 minutes in a water bath. After cooling to room temperature, the extracted yellow solution was filtered using a 0.45  $\mu\text{m}$  PTFE syringe filter into a vial for LC analysis.

### **2.2.3 Liquid Chromatography**

#### **i. First Dimension Parameters**

Single dimension liquid chromatographic analysis was carried out on an Agilent 1290 Infinity II series UHPLC system (Agilent Technologies, Santa Clara, CA). The parameters of the first dimension are outlined in Table 2.2.3.1.

**Table 2.2.3.1:** 1D-LC parameters for the separation of polyphenol standards and yellow lake pigments.

<b>First Dimension Column</b>	Agilent ZORBAX SB-C18 (2.1 x 100 mm x 1.8)
<b>Injection Amount</b>	1.5 $\mu$ L
<b>Solvent A</b>	0.1% Formic Acid in Water
<b>Solvent B</b>	0.1% Formic Acid in Methanol
<b>Flow Rate</b>	0.2 mL/min
<b>Gradient</b>	50% B at 0 min 55% B at 3 min 80% B at 10 min 95% B at 11 min
<b>Column Temperature</b>	30°C
<b>Runtime</b>	20 minutes
<b>Post Runtime</b>	10 minutes
<b>Wavelengths</b>	204 nm, 249 nm, 264 nm, 292 nm, 327nm, 363 nm

## ii. Second Dimension Parameters

Multidimensional liquid chromatographic analysis was carried out on the same system. The first dimension separation was exactly as outlined above in Table 2.2.3.1.

The parameters of the second dimension are outlined in Table 2.2.3.2. Peaks of interest from the first dimension were further investigated in the second dimension by heart-cut mode. The threshold was chosen based on the intensity of peaks in the first dimension.

**Table 2.2.3.2:** 2D-LC parameters for the separation of polyphenol standards and yellow lake pigments.

<b>Mode</b>	Heart-Cut mode
<b>First Dimension Column</b>	Agilent ZORBAX Bonus-RP, 2.18 x 50 mm, 1.8 $\mu$ m
<b>Injection Amount</b>	1.5 $\mu$ L
<b>Solvent A</b>	0.1% Formic Acid in Water
<b>Solvent B</b>	0.1% Formic Acid in Acetonitrile
<b>Flow Rate</b>	1.0 mL/min
<b>Gradient</b>	50% B at 0 min 95% B at 1.4 min
<b>Column Temperature</b>	30°C
<b>Runtime</b>	20 minutes
<b>Post Runtime</b>	10 minutes
<b>Wavelengths</b>	204 nm, 249 nm, 264 nm, 292 nm, 327nm, 363 nm

### iii. Second Dimension with Fraction Collection Parameters

Multidimensional liquid chromatographic analysis was carried out on the same system. The first dimension separation was exactly as outlined above in Table 2.2.3.1 The parameters of the second dimension with fraction collection are stated in table 2.2.3.3.

Peaks of interest in the second dimension were collected as fractions. The threshold was chosen based on the intensity of peaks in the second dimension. Fractions were collected into an Agilent 96-well plate and then were put in vials for spectroscopic studies.

**Table 2.2.3.3:** 2D-LC with fraction collection parameters for the separation of polyphenol standards and yellow lake pigments.

<b>Mode</b>	Heart-Cut mode
<b>First Dimension Column</b>	Agilent ZORBAX Bonus-RP, 2.18 x 50 mm, 1.8 $\mu$ m
<b>Injection Amount</b>	1.5 $\mu$ L
<b>Solvent A</b>	0.1% Formic Acid in Water
<b>Solvent B</b>	0.1% Formic Acid in Acetonitrile
<b>Flow Rate</b>	1.0 mL/min
<b>Gradient</b>	50% B at 0 min 95% B at 1.4 min
<b>Runtime</b>	20 minutes
<b>Post Runtime</b>	10 minutes
<b>Column Temperature</b>	30°C
<b>Wavelengths</b>	204 nm, 249 nm, 264 nm, 292 nm, 327nm, 363 nm

## 2.2.4 Electrochemical Surface Enhanced Raman Spectroscopy

### i. Silver Nanoparticle (AgNP) Synthesis

1.0 mL of silver nitrate solution (0.1 M), 3.4 mL of aqueous sodium citrate (5%), and 0.6 mL of citric acid (0.17 M) were added into a 250 mL three-neck flat-bottom flask

with 95.0 mL of water. 0.2 mL of freshly prepared sodium borohydride solution (0.1 mM) was then added into the above mixture at room temperature under magnetic stirring. The mixture was allowed to stand at room temperature for 1 min and then brought to boil under reflux within 20 minutes under magnetic stirring. After boiling for 1 hour, the dark murky green solution was allowed to cool to room temperature. Two 715  $\mu\text{L}$  aliquots of colloidal suspension were added to Eppendorf tubes, which were then centrifuged at 8 000 rpm for 20 minutes (Labnet PRISM microcentrifuge, Edison, NJ, USA). The supernatant was then removed and discarded, and the remaining paste put into one Eppendorf tube and centrifuged again. The final paste was adjusted to a concentration of 0.4 M with water.

### **ii. Preparation of EC-SERS Substrate Preparation**

Screen printed electrodes were modified with nanoparticles for use in EC-SERS detection. Three layers of the AgNP paste were drop coated onto the working electrode surface of a carbon screen printed electrode in 5  $\mu\text{L}$  aliquots, drying fully between layers. Using three layers of the AgNP paste was found to be the optimal amount to ensure uniform surface coverage. The electrodes were then immersed in 0.5 M KCl for 30 minutes to remove citrate, rinsed with ultrapure water and dried prior to application. 5.0  $\mu\text{L}$  of the analyte solution (phenol standards, yellow lake pigment solution, or fractions) was then deposited onto the modified electrode surface and allowed to air dry prior to spectroscopic studies.

### **iii. EC-SERS Analysis**

A Pine Research Instrumentation portable USB Wavenow potentiostat/galvanostat (Durham, NC, U.S.A.) was used for conducting electrochemical measurements with the

electrochemical software, Aftermath Data Organizer (version 1.2.4361), also produced by Pine Research Instrumentation. Modified SPEs were placed in the electrochemical cell, which was a standard glass vial. The in air spectrum could then be collected and this spectrum is an important reference as it represents the SERS signal. The open circuit potential (OCP) spectrum could then be collected when the 0.1 M NaF supporting electrolyte (purged with argon for 30 minutes prior to use) was added to the electrochemical cell containing the SPE. The system was first stepped in the cathodic direction (0.0 V to -1.0 V) and then the anodic direction (-1.0 V to 0.0V), both in increments of 0.1V. At each applied potential a SERS spectrum was collected. All potentials are reported versus Ag/AgCl reference electrode.

## **Chapter 3: Results and Discussion**

### **3.1 2D-LC Studies**

#### **3.1.1 Reseda Lake and Buckthorn Berries Yellow Lake Reference Pigment**

As explained previously, Reseda Lake is a type of yellow lake pigment. Buckthorn berry is used to make another yellow lake pigment, Stil de grain. The pigment under investigation in this thesis is a mixture of Reseda lake and buckthorn berries. This pigment was chosen for analysis because originally Dr. Kristen Wustholz from the College of William & Mary was interested in using the 2D-LC to observe its power in separating possibly more components in a Reseda lake art sample than a conventional LC system. The purpose of that work was to help inform the conservation treatment of the colours of a colonial portrait of Mary Purdie, part of the Colonial Williamsburg Foundation Collection. Figure 3.1.1.1 is a chromatogram of Reseda Lake/ buckthorn berries mixtures, demonstrating the complexity of this pigment sample since many different components are present and not well resolved. For example, the peaks between 8.16 and 8.35 minutes and between 11.43 and 11.66 minutes are not completely resolved. The resolution of these peaks is below 1.5, which is the optimum resolution to attain complete separation. In particular, it is of interest in this thesis work to identify the peak appearing with a retention time of 11.66 minutes, as it is the component with the highest intensity, implicating it is present in the highest concentration in this pigment. In addition, as will be described later,

it is likely that this component is responsible for the bulk of the pigment degradation behaviour.

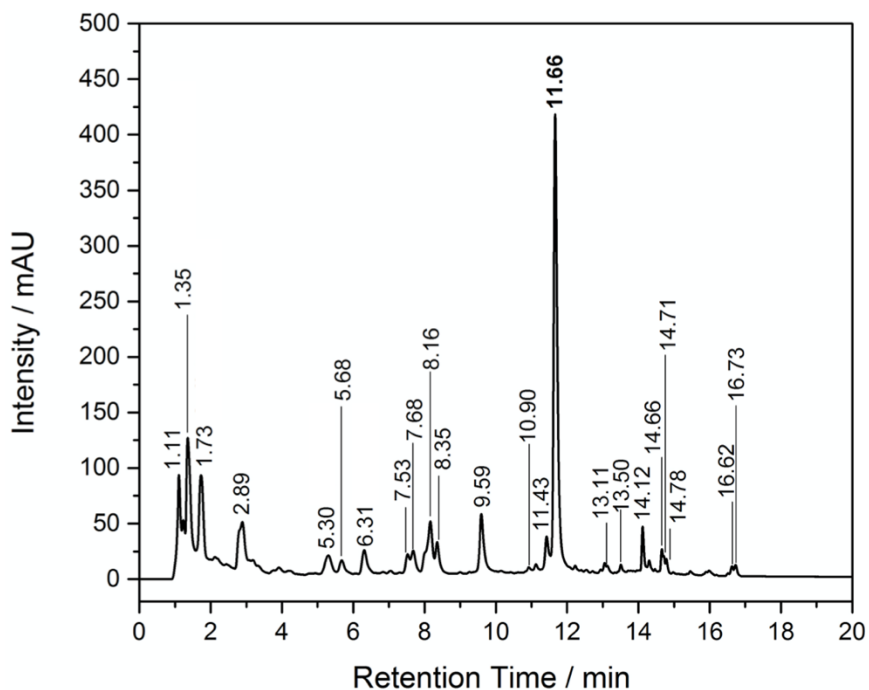


**Figure 3.1.1.1:** <sup>1</sup>D chromatogram of the Reseda lake/buckthorn berry pigment (5:95% (v/v) formic acid: methanol) at 264 nm. Retention times are stated above each main peak.

### 3.1.2 Polyphenol Standards and Polyphenol Standard Mixture

As shown by Figure 3.1.1.1, the Reseda lake/buckthorn berry pigment is complex. Therefore, it was vital to first establish reference 1D-LC chromatograms of various polyphenol compounds that are known to be found in these yellow lake pigments, in order to identify these components in the yellow lake pigment through retention time comparisons. The chemical structures of each polyphenol compound used in this thesis work are shown in Figure 3.1.2.1.

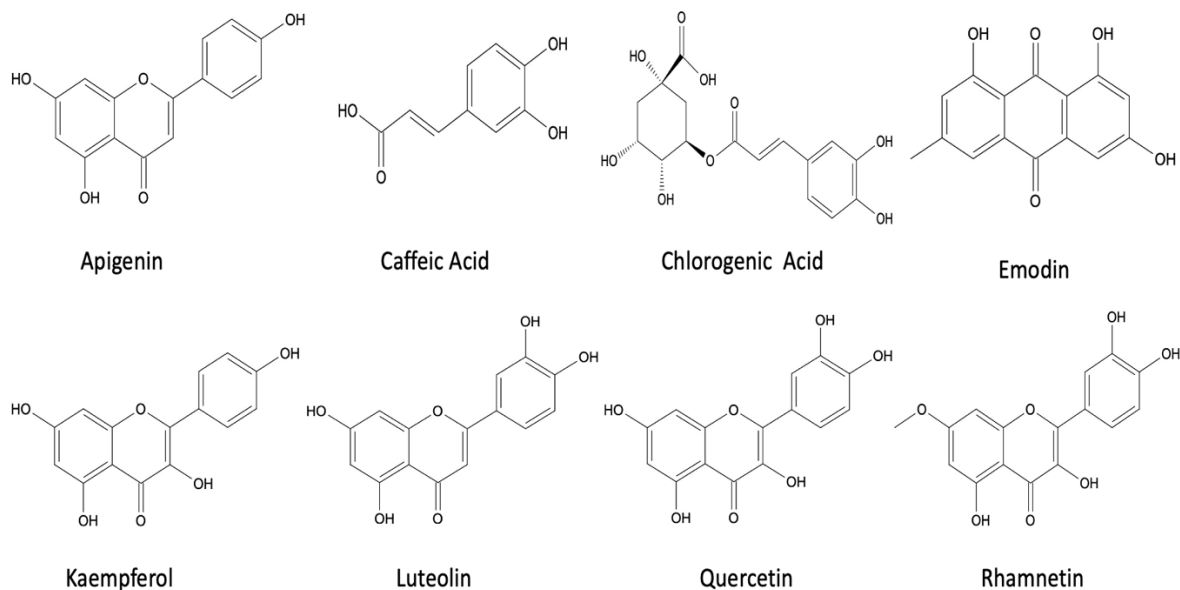


**Figure 3.1.2.1:** Chemical structures polyphenols: luteolin, kaempferol, rhamnetin, quercetin, apigenin, emodin, caffeic acid, and chlorogenic acid.

To characterize caffeic acid, chlorogenic acid, luteolin and quercetin, 25 ppm solutions were analyzed using the first dimension of the 2D-LC. 1.5  $\mu\text{L}$  aliquots of each standard were injected into the 2D-LC. The chromatograms of these four analytical standards are shown in Figure 3.1.2.2 with the retention times being 1.33, 1.65, 5.25, and 6.38 minutes for chlorogenic acid, caffeic acid, quercetin, and luteolin respectively.

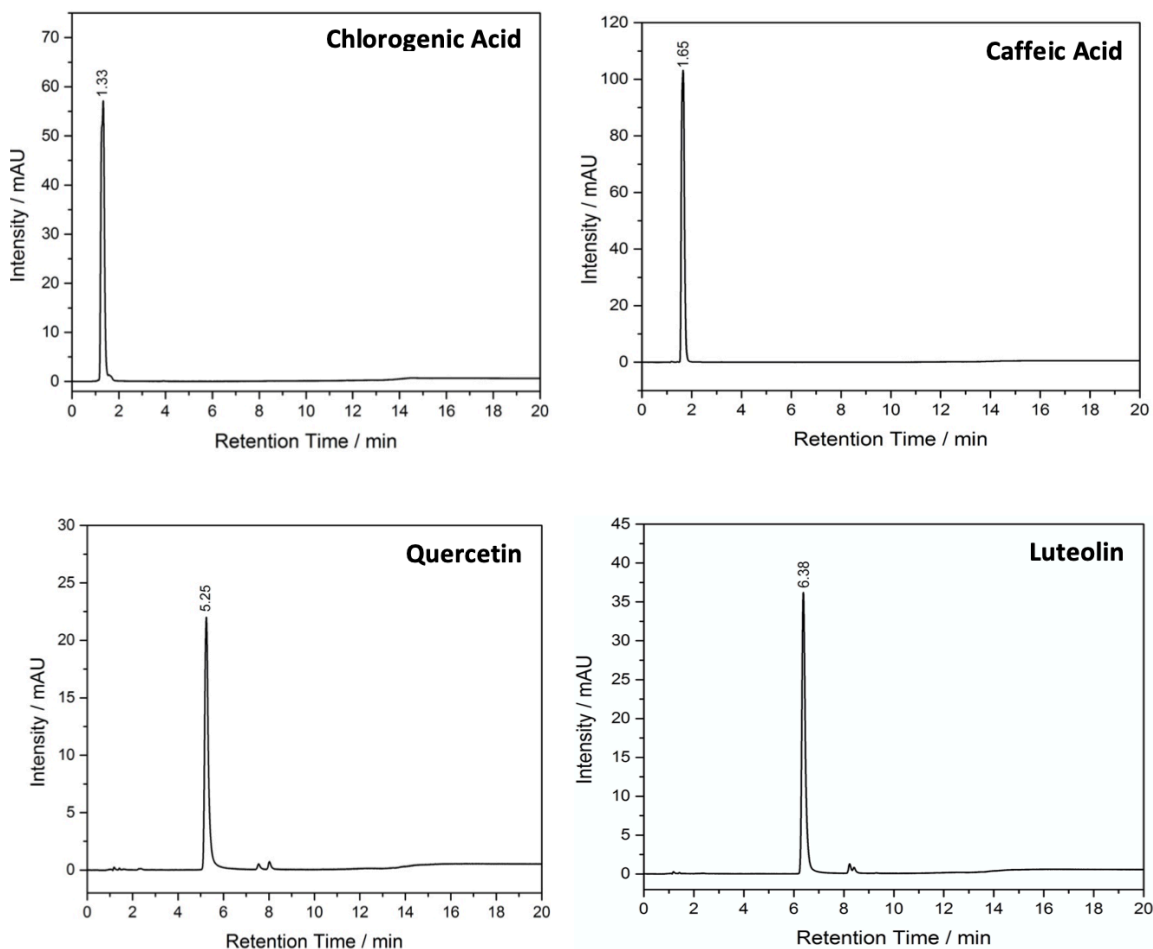


**Figure 3.1.2.2:** <sup>1</sup>D chromatograms for 25 ppm (5:95% (v/v) formic acid: methanol) solutions of chlorogenic acid, caffeic acid, quercetin and luteolin at 327 nm with retention times stated above each main peak.

To ensure each of these four standards could be separated out from a mixture with the same retention time, a 25 ppm mixture was prepared in 5:95% (v/v) formic acid/methanol solvent. A 1.5  $\mu$ L aliquot of the mixture was subsequently analysed in the first dimension of the 2D-LC. The <sup>1</sup>D chromatogram of the separated mixture can be seen in Figure 3.1.2.3 where the retention times are very much comparable with those of the pure standards. The retention times of 1.29, 1.61, 5.07 and 6.14 minutes relate to chlorogenic acid, caffeic acid, quercetin, and luteolin respectively.

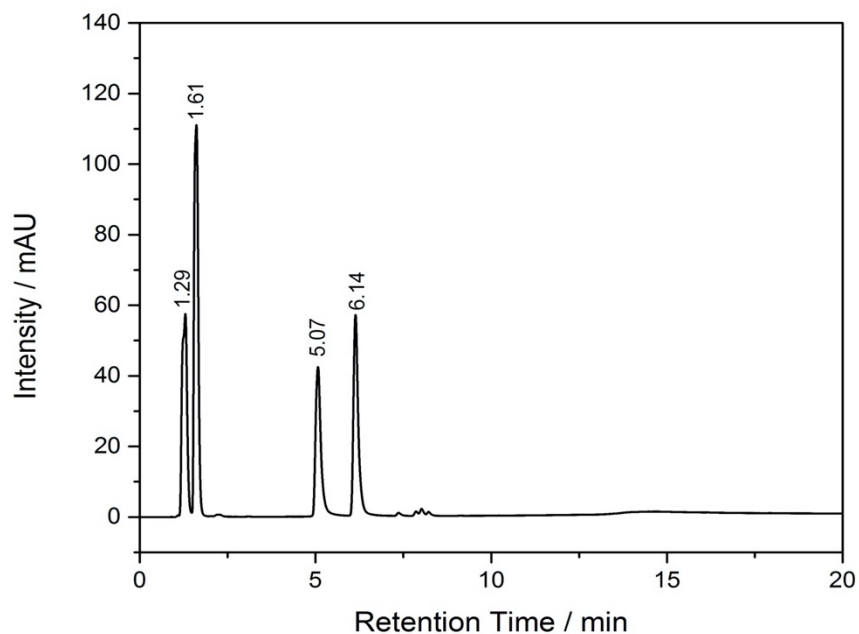


**Figure 3.1.2.3:** <sup>1</sup>D chromatogram for 25 ppm (5:95% (v/v) formic acid: methanol) mixture of chlorogenic acid, caffeic acid, quercetin and luteolin at 327 nm with retention times stated above each main peak.

Four additional standards (kaempferol, rhamnetin, apigenin and emodin) were prepared at varying concentrations and then analyzed using 2D-LC. The chromatograms of these four standards are shown in Figures 3.1.2.4 and 3.1.2.5 with the retention times being 7.21, 9.65, 8.29, and 14.24 minutes for kaempferol, rhamnetin, apigenin and emodin respectively.

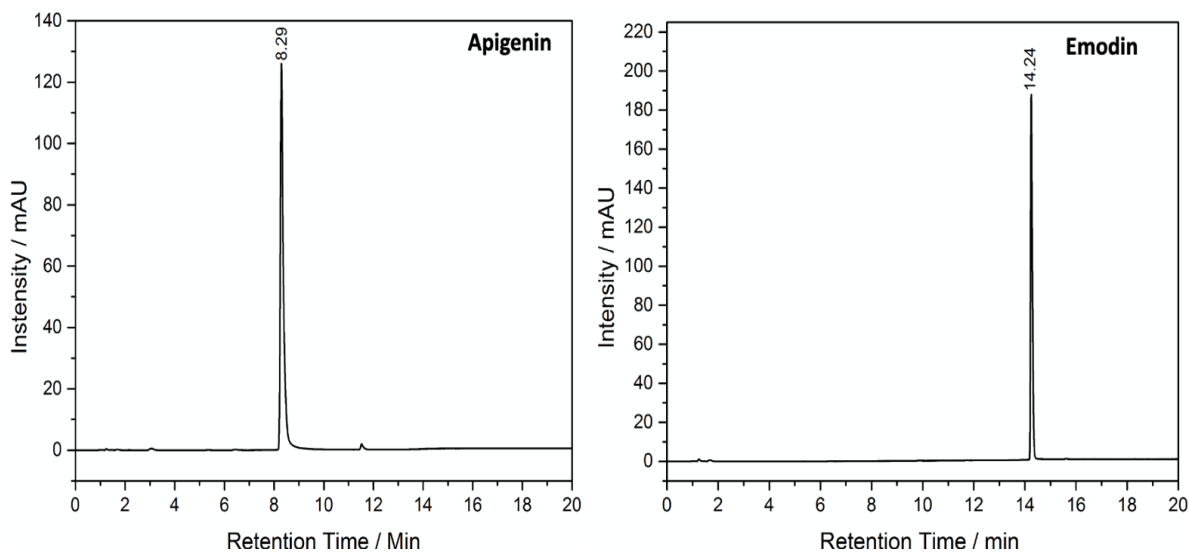


**Figure 3.1.2.4:**  $^1\text{D}$  chromatograms for 25 ppm (5:95% (v/v) formic acid: methanol) solutions of apigenin and emodin at 363 nm and 292nm with retention times stated above each main peak.

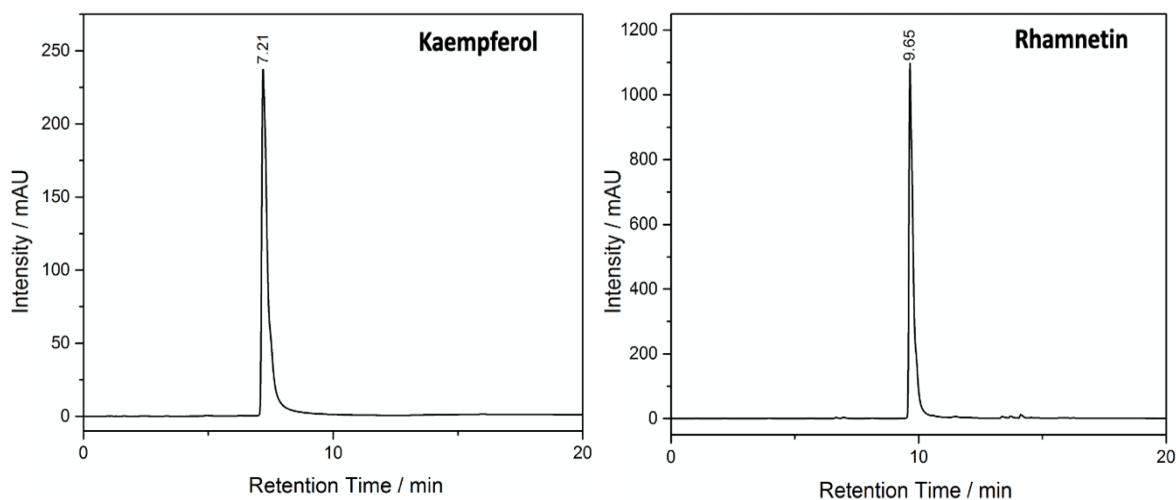


**Figure 3.1.2.5:**  $^1\text{D}$  chromatograms for 2000 ppm and 500 ppm (5:95% (v/v) formic acid: methanol) solutions of kaempferol and rhamnetin at 363 nm with retention times stated above each main peak.

To ensure each standard could be separated out from a mixture of eight polyphenol compounds, 250 ppm solutions of each of the eight standards were prepared in 5:95% (v/v) formic acid/methanol, then 250  $\mu\text{L}$  of each standard was put into one vial to obtain a total concentration of 31 ppm each. A 1.5  $\mu\text{L}$  aliquot the mixture was subsequently analysed in the first dimension of the 2D-LC. The  $^1\text{D}$  chromatogram of the separated mixture can be

seen in Figure 3.1.2.6 where the retention times were similar to those of the eight individual standards. The peaks of interest were all resolved, which was promising for further investigation using EC-SERS, as a fraction of each of these components from the second dimension separation are required for proof-of-concept work for this thesis. Comparison of retention times for the eight individual polyphenol standards run separately and the polyphenol mixture are summarized in Table 3.1.2.

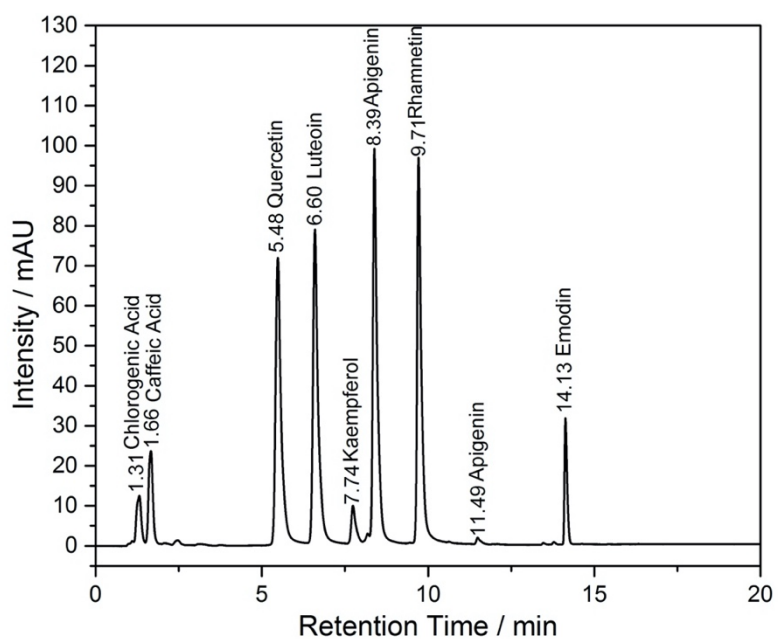


**Figure 3.1.2.6:** <sup>1</sup>D chromatogram (5:95% (v/v) formic acid: methanol) mixture of chlorogenic acid, caffeic acid, quercetin, luteolin, kaempferol, rhamnetin, apigenin and emodin (31 ppm each) at 363 nm with retention times and names of compounds stated above each main peak.

**Table 3.1.2.1:** Comparison of retention times of eight individual polyphenol standards analyzed separately and in a mixture.

<b>Polyphenol Standard</b>	<b>Individual Retention Time (min)</b>	<b>Polyphenol Standard Mixture Retention Time (min)</b>
<b>Chlorogenic Acid</b>	1.33	1.31
<b>Caffeic Acid</b>	1.65	1.66
<b>Quercetin</b>	5.25	5.48
<b>Luteolin</b>	6.38	6.60
<b>Kaempferol</b>	7.21	7.74
<b>Apigenin</b>	8.29	8.39
<b>Rhamnetin</b>	9.65	9.71
<b>Emodin</b>	14.24	14.13

Comparing the chromatogram of the Reseda Lake/buckthorn berry pigment to the chromatograms of the standards, there are peaks with comparable retention times present in both, thus these eight polyphenol compounds could be present in this yellow lake pigment. With this knowledge, Figure 3.1.1.7 is a relabelled chromatogram of Reseda Lake/buckthorn berry pigment with the eight polyphenol compounds indicated. Table 3.1.2.2 lists the retention times of the individual eight polyphenol standards, the polyphenol mixture and the retentions times that are comparable to the standards individually and in the mixture. While some components of the Reseda lake/buckthorn berry can likely be identified through retention time comparisons, it is clear that many other components are not identified in this sample, and in addition the primary component at 11.66 minutes is not one of these eight main polyphenol components.

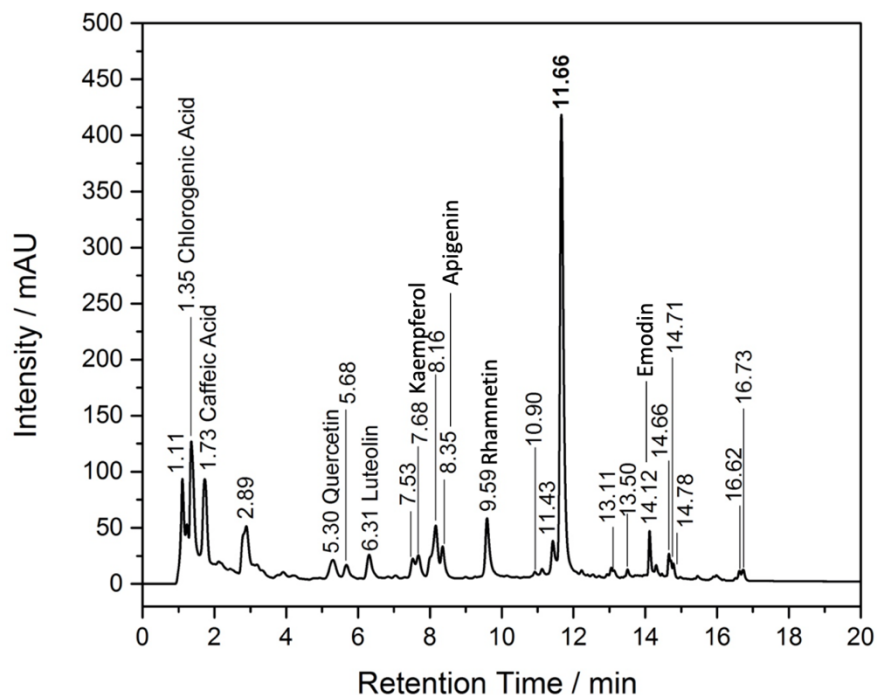


**Figure 3.1.2.7:** Relabelled  $^1\text{D}$  chromatogram of the Reseda Lake/buckthorn berry pigment (5:95% (v/v) formic acid/methanol) at 264 nm with retention times and polyphenol component stated above each main peak.

**Table 3.1.2.2:** Comparison of retention times of eight individual polyphenol standards, the polyphenol mixture and components in Reseda lake/buckthorn berry pigment with comparable retention times

Polyphenol Standard	Individual Standard Retention Time (min)	Standard Mixture Retention Time (min)	RL/BB Retention Time (min)
Chlorogenic Acid	1.33	1.31	1.35
Caffeic Acid	1.65	1.66	1.73
Quercetin	5.25	5.48	5.30
Luteolin	6.38	6.60	6.31
Kaempferol	7.21	7.74	7.68
Apigenin	8.29	8.39	8.35
Rhamnetin	9.65	9.71	9.71
Emodin	14.24	14.13	14.12

### 3.1.3 Reseda Lake/Buckthorn Berries Pigment Heart Cuts

The complexity of the Reseda lake/buckthorn berry pigment is evident and presents itself as an excellent candidate for multidimensional chromatography. Three peaks (1.11, 1.35, and 11.66 minutes) from the first dimension were selected to proceed into the second dimension of the 2D-LC through the multiple heartcutting mode. These peaks were chosen because they have the highest intensity, and thus contribute significantly to the potential degradation properties of the pigment. In addition, these three peaks would have a higher concentration to perform mass spectrometry on these peaks, which would help to validate the 2D-LC-EC-SERS method.

Figure 3.1.3.1 is the <sup>2</sup>D chromatogram of the first peak, 1.11 minutes, that went through the multiple heartcutting mode. It can be observed that there are two peaks that were separated in the second dimension that were not in the first dimension. Additionally, it can be seen that there are three peaks present in the chromatogram of the second dimension separation for the 1.35 minute peak taken from the first dimension in Figure 3.1.3.2. These three peaks the second dimension demonstrate that there is more than one component present in the 1.35 minute peak from the first dimension. However, they were co-eluting together in one peak, indication these components are very similar in structure. Therefore, the separation that occurred in Figures 3.1.3.1 and 3.1.3.2 represents the power of 2D-LC. It is clear from these figures that the yellow lake pigment is much more complex, and an instrument is needed with much more separating and resolving power than just the conventional 1D-LC to achieve full separation of the various components in this pigment. However, these peaks are not very well resolved (i.e. a resolution below 1.5); one way to solve this problem is to change the gradient of the mobile phase, which was not done in this thesis work, but should be explored in future experiments.

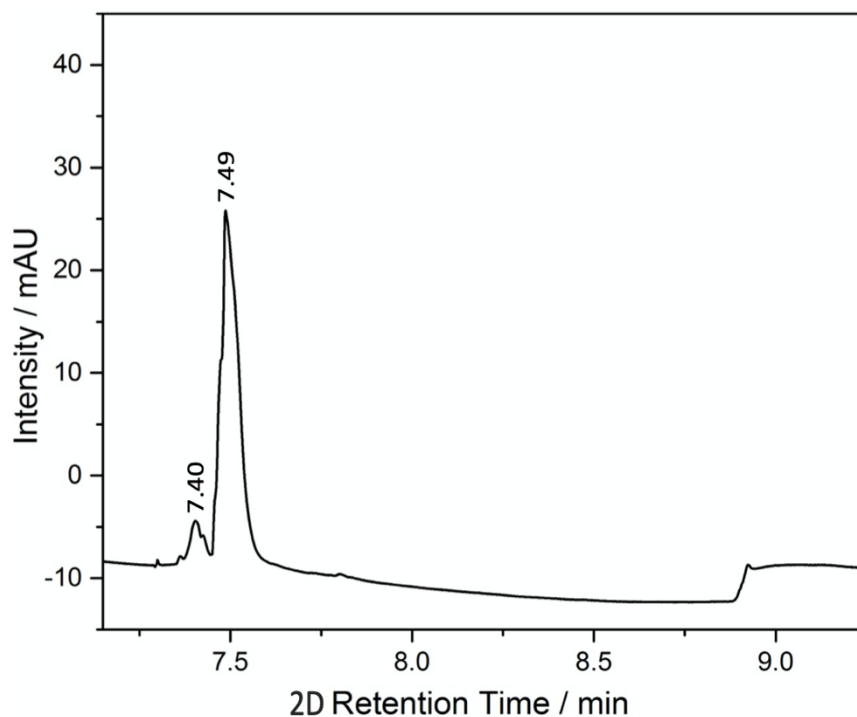


**Figure 3.1.3.1:** <sup>2</sup>D chromatogram 1.11 minute peak heart cut of the yellow lake pigment (5:95% (v/v) formic acid/methanol) chromatogram at 292 nm with retention times stated above each main peak.

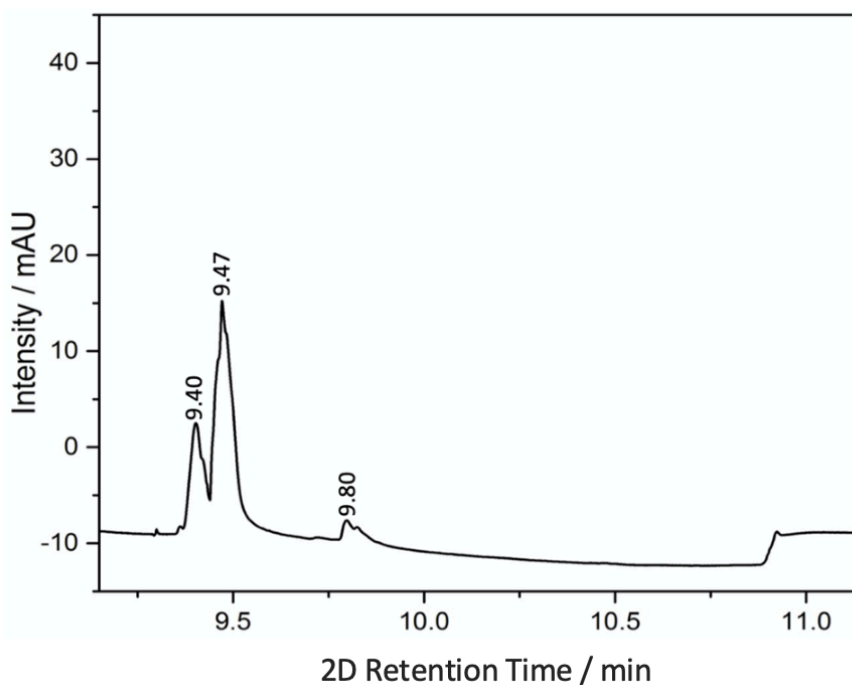


**Figure 3.1.3.2:** <sup>2</sup>D chromatogram of 1.35 minute peak heart cut of the yellow lake pigment (5:95% (v/v) formic acid/methanol) chromatogram at 292 nm with retention times stated above each main peak.

The 11.66 minute peak in the first dimension has four peaks present in the second dimension as shown in Figure 3.1.3.2 and, again, this is showcasing that there is more than one component present the 11.66 minute peak that was not separated in the first dimension.

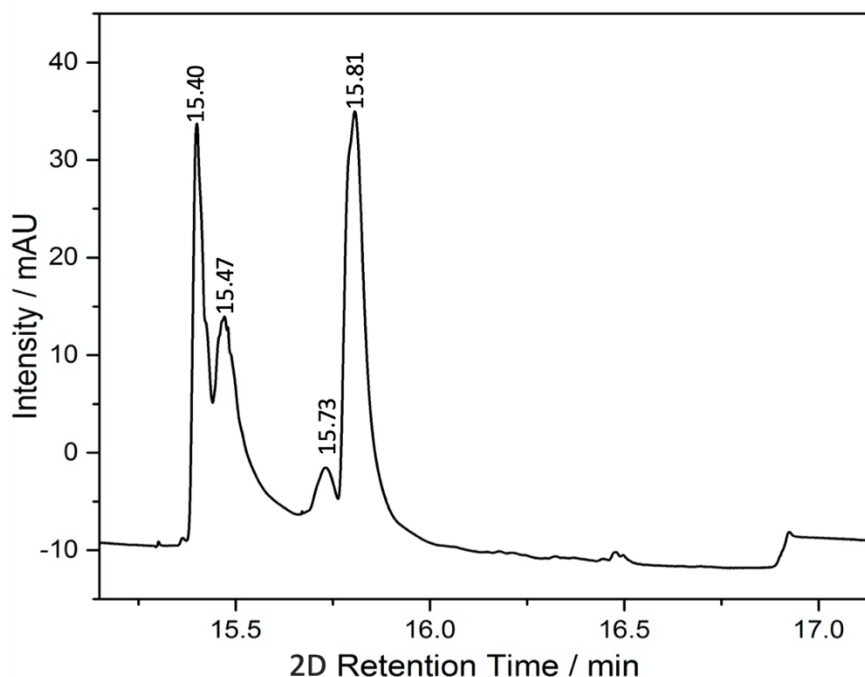


**Figure 3.1.3.3:** <sup>2</sup>D chromatogram of 11.66 minute peak heart cut of the yellow lake pigment (5:95% (v/v) formic acid/methanol) chromatogram at 292 nm with retention times stated above each main peak.

### 3.1.4 Comparison of Yellow Lake Pigments

In this thesis work, a pigment that is a mixture of Reseda lake and buckthorn berry was examined. In order to decouple the contribution of each dyestuff to the pigment, both buckthorn berry and Reseda lake were investigated individually to see how each of these components are represented in the mixture. The pictures of the individual Reseda lake and buckthorn berry pigments in the centrifuge tubes are shown in Figures 3.1.4.1 (B) and 3.1.4.2 (B), which can be seen to be quite different. It can be observed from the two pictures of these pigments that it seems like buckthorn berry is the main contributor of the colour to

the Reseda lake/buckthorn berry mixture because it is yellow in colour. The Reseda lake pigment is not yellow in colour, suggesting that it is not the main contributor to the colour of the yellow lake mixture. Figures 3.1.4.1 (A) and 3.1.4.2 (A) are the <sup>1</sup>D chromatograms of Reseda Lake and buckthorn berry, respectively, which again look to be quite different from one another. From the Reseda lake chromatogram in Figure 3.1.4.1, it is observed that luteolin and apigenin are indeed present in this pigment at 6.18 and 8.22 minutes, respectively, which is also consistent with the literature.<sup>7,12</sup> In Figure 3.1.4.2, the chromatogram of the buckthorn berries confirms what is found in the literature, since it is observed that indeed quercetin, kaempferol, and rhamnetin are present in this pigment at retention times: 5.18, 7.56 and 9.43 minutes respectively.<sup>7,12</sup> However, emodin, which is another polyphenol known to be extracted from buckthorn berries is not present or is present in a very low amount in this chromatogram at around 14 minutes. It is also observed that caffeic acid and chlorogenic acid are present in the Reseda lake pigment, with retention times close to those of the standards at 1.32 and 1.60 minutes in Figure 3.1.4.1.

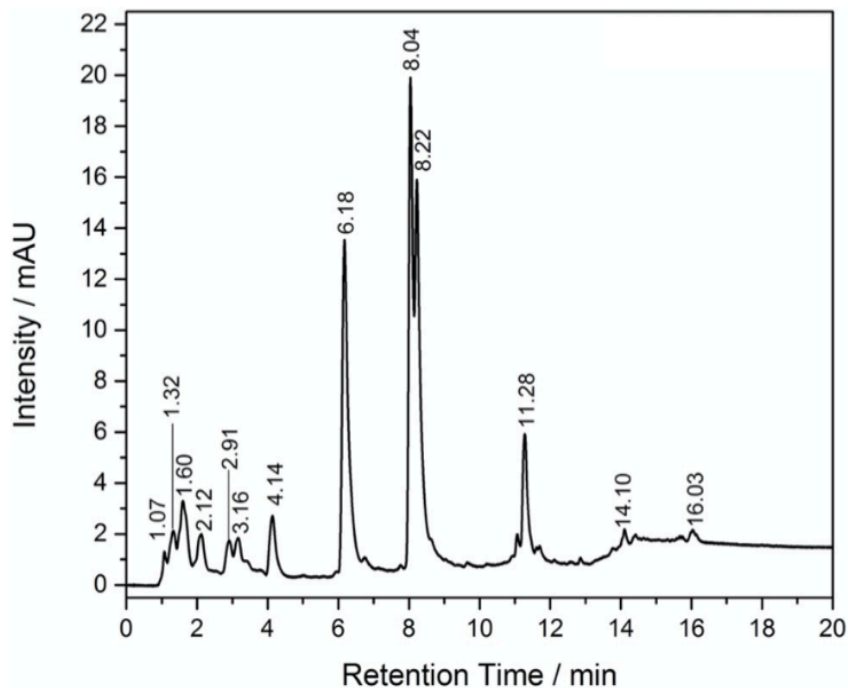


**Figure 3.1.4.1:**  $^1\text{D}$  chromatogram of Reseda lake pigment (5:95% (v/v) formic acid/methanol) at 327 nm (A) and a picture of the pigment in 5:95% (v/v) formic acid/methanol.

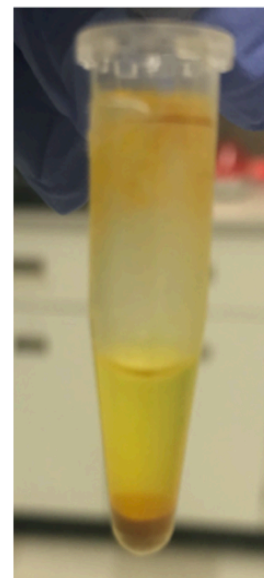
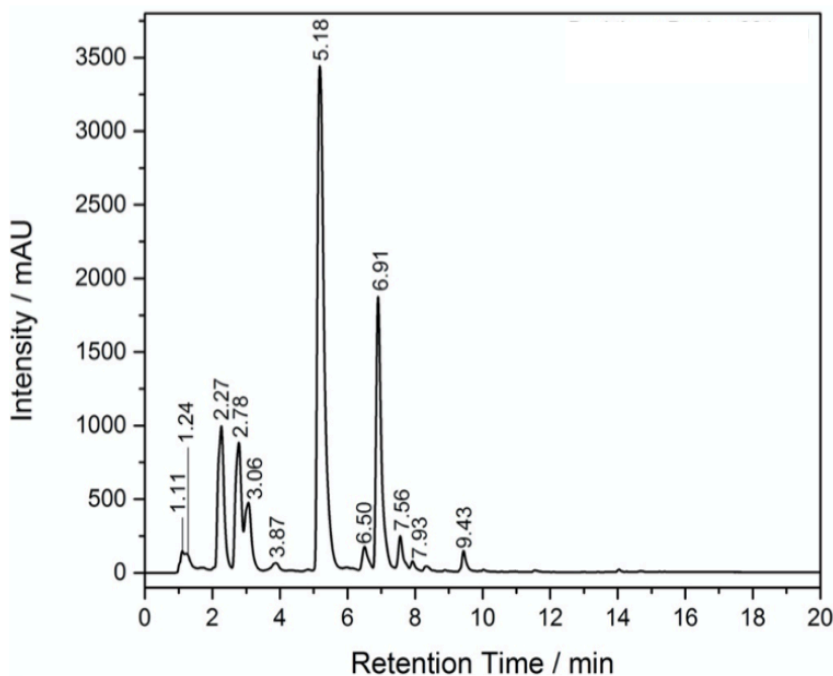


**Figure 3.1.4.2:**  $^1\text{D}$  chromatogram of buckthorn berry pigment (5:95% (v/v) formic acid/methanol) at 327 nm (A) and a picture of the pigment in 5:95% (v/v) formic acid/methanol.

Figure 3.1.4.3 is a comparison of the <sup>1</sup>D chromatograms of the Reseda lake, buckthorn berry and the mixture at both 264 nm (A) and 327 nm (B) wavelengths. It can be perceived from both wavelengths that neither buckthorn berries nor Reseda lake individually contribute to the large peak at around 12.00 minute. It was explained in section 3.1.1 that this was a very important peak to identify (however, it was 11.66 minute in Figure 3.1.1.1), meaning that this component might not be a dyestuff extracted from a weld or buckthorn berries. Therefore, this adds to the mystery of solving the identification of this component present in this peak. It is observed that there are peaks present in both the individual pigment chromatograms that are found to be in the mixture. For example, at between 5 to 6 minutes, there is a peak present in buckthorn berries and the mixture chromatograms. However, the peak present in the pigment mixture is a small amount in comparison and this peak is representing the quercetin component.

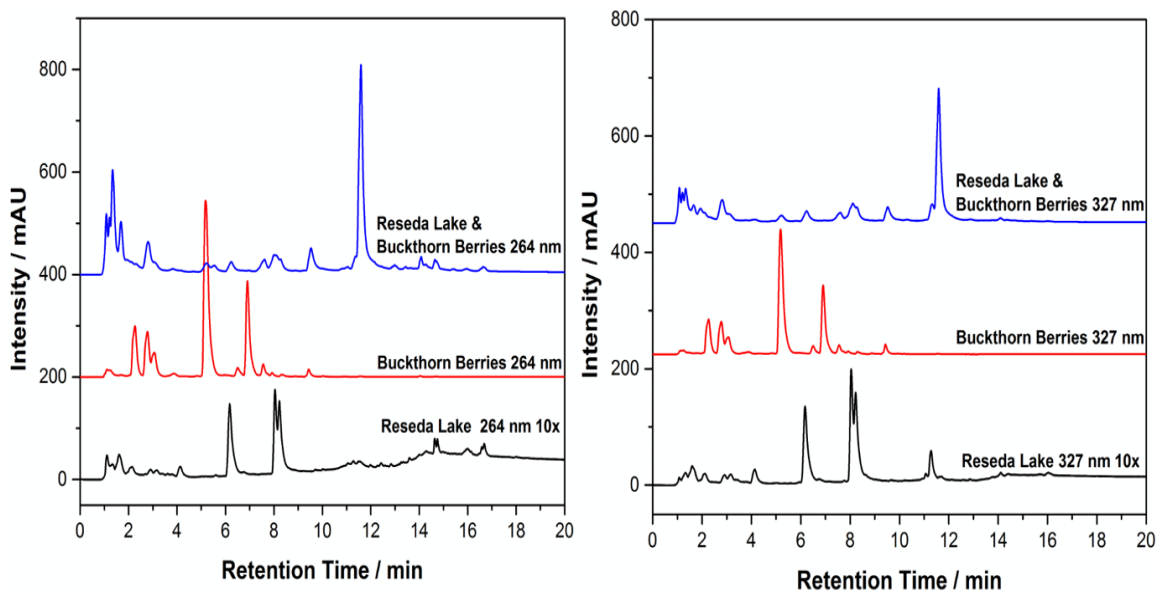


**Figure 3.1.4.3:** <sup>1</sup>D chromatogram overlays of the different yellow lake pigments (5:95% (v/v) formic acid/methanol) at 264 nm (A) and 327 nm (B).

### 3.1.5 Sunlight Effect on Reseda Lake and Buckthorn Berries Yellow Lake Reference Pigment Study

Photodegradation of natural yellow dyes is a significant issue in conservation, and an area of active scientific study. In this thesis work, photodegradation was explored for the Reseda lake and buckthorn berry yellow lake pigment. A vial of the yellow lake pigment suspended in 5:95 % (v/v) formic acid/methanol was placed on a windowsill in full sunlight, and after one week, the pigment lost its yellow colour, becoming a light peachy pink colour (Figure 3.1.5.1). The photodegraded yellow lake pigment solution was then analyzed in the first dimension of the 2D-LC using the same parameters noted previously, and the chromatogram was obtained (Figure 3.1.5.2). One major difference between the two chromatograms is that the 11.66 minute peak was no longer present after sunlight exposure for a week. Therefore, this component is greatly affected by the sunlight exposure and could be one of the reasons why this pigment loses its colour.

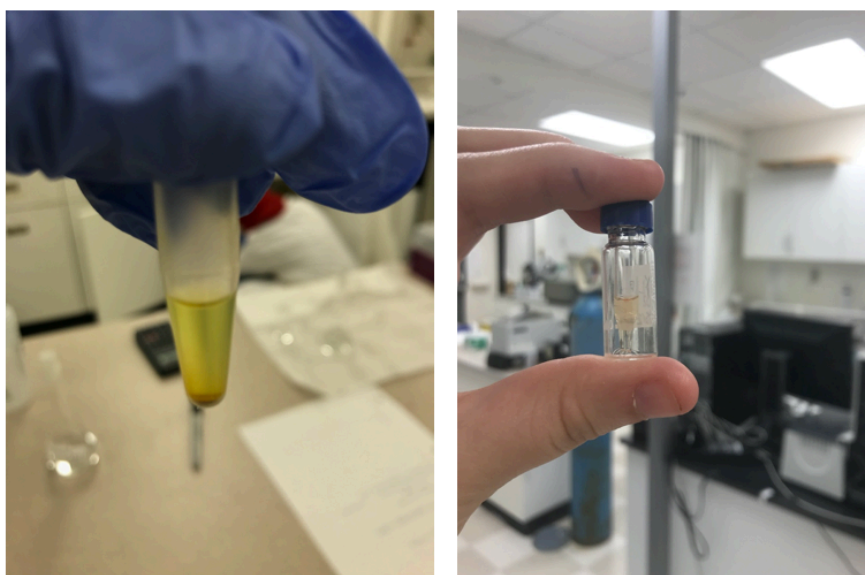


**Figure 3.1.5.1:** Pictures of before (left) and after (right) the yellow lake sample in 5:95% (v/v) formic acid/methanol was exposed to sunlight for 1 week.

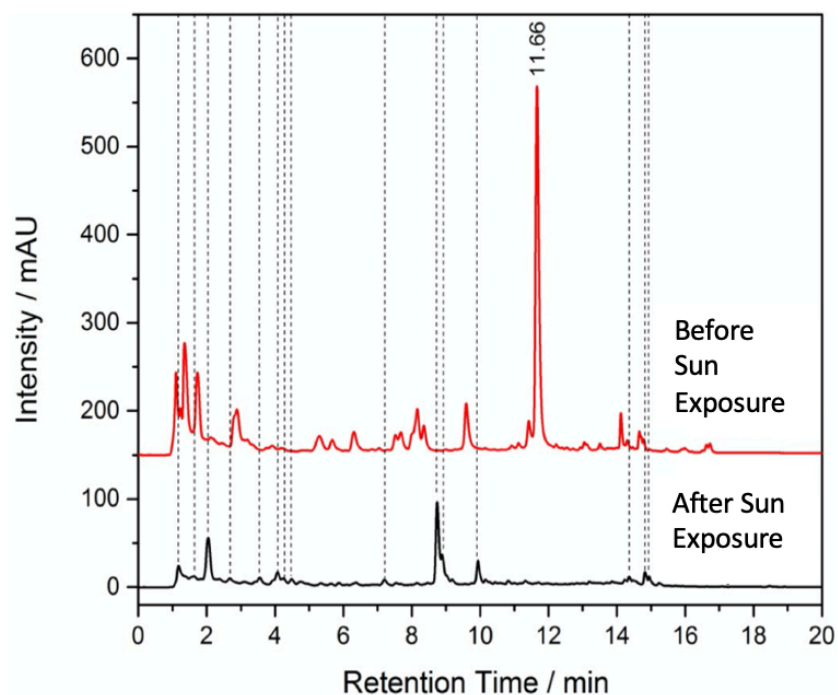


**Figure 3.1.5.2:** Overlay of chromatograms of yellow lake sample before and after having sun exposure for 1 week at 327 nm.

### 3.1.6 Reseda Lake and Buckthorn Berry Mixture Lake Pigment Heart Cut for EC-SERS Analysis

For the SERS studies, a new sample of the Reseda lake/buckthorn berry yellow lake pigment was obtained. To check that this new sample was the same as the previously studied sample, 1D-LC analysis was completed, and the resulting chromatogram is shown in Figure 3.1.6.1. It should be noted that the new chromatogram is quite similar to the first chromatogram of the mixture, with many of the peaks with similar retention times as before. However, there are more peaks in this separation that are not resolved such as the 8.09 minute peak. The main peak of interest at 11.59 minutes is present

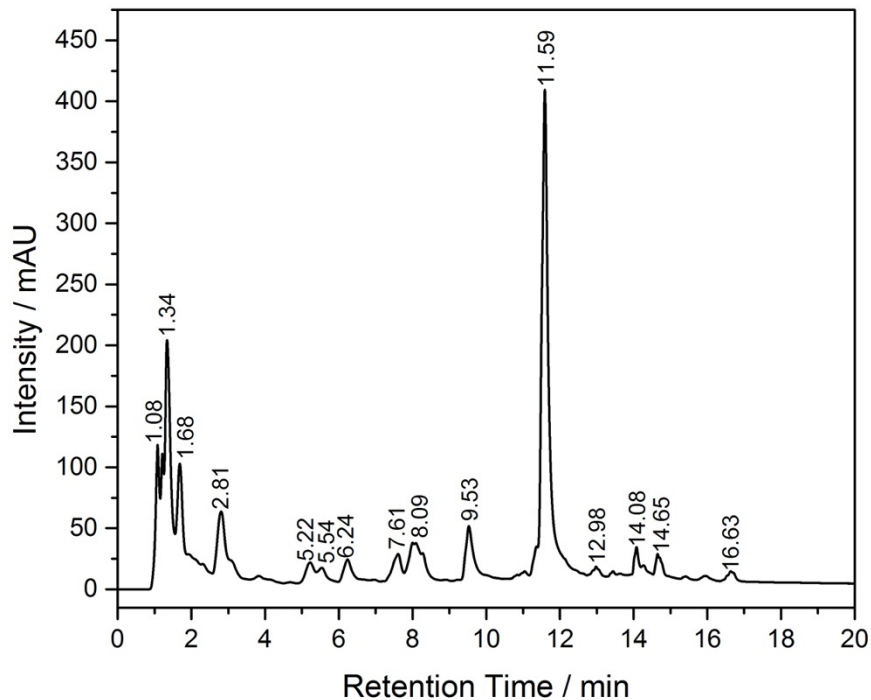


**Figure 3.1.6.1:** <sup>1</sup>D chromatogram of the Reseda Lake/buckthorn berry pigment (5:95% (v/v) formic acid/methanol) at 264 nm. Retention times are stated above each main peak.

Heart cuts were performed on peaks at 1.34, 1.54, 7.61, 8.09 and 11.59 minutes in the first dimension, and their <sup>2</sup>D chromatograms are shown below in Figures 3.1.6.2 to 3.1.6.6. In cut 2, there are many peaks present therefore showcasing the advantage of having an extra dimension of separation. In contrast, in the other cuts 3, 6 and 7 there are two distinct peaks that were separated in the second dimension, therefore implying that the peak is not as complex as cut 1 or, possibly, peaks are coeluting together.

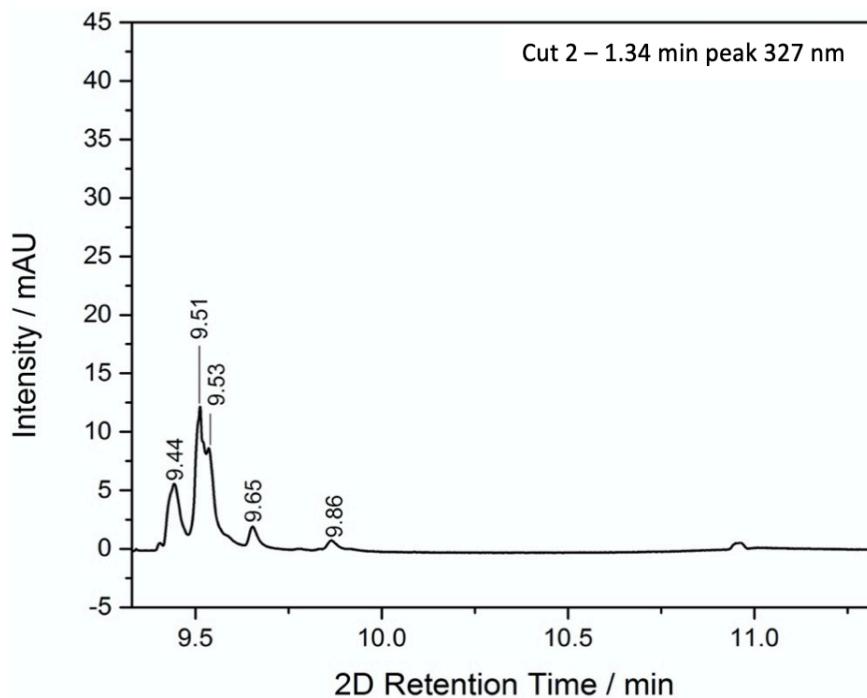


**Figure 3.1.6.2:** <sup>2</sup>D chromatogram of the cut 2 of Reseda Lake/buckthorn berry pigment (5:95% (v/v) formic acid/methanol) at 327 nm. Retention times are stated above each main peak.

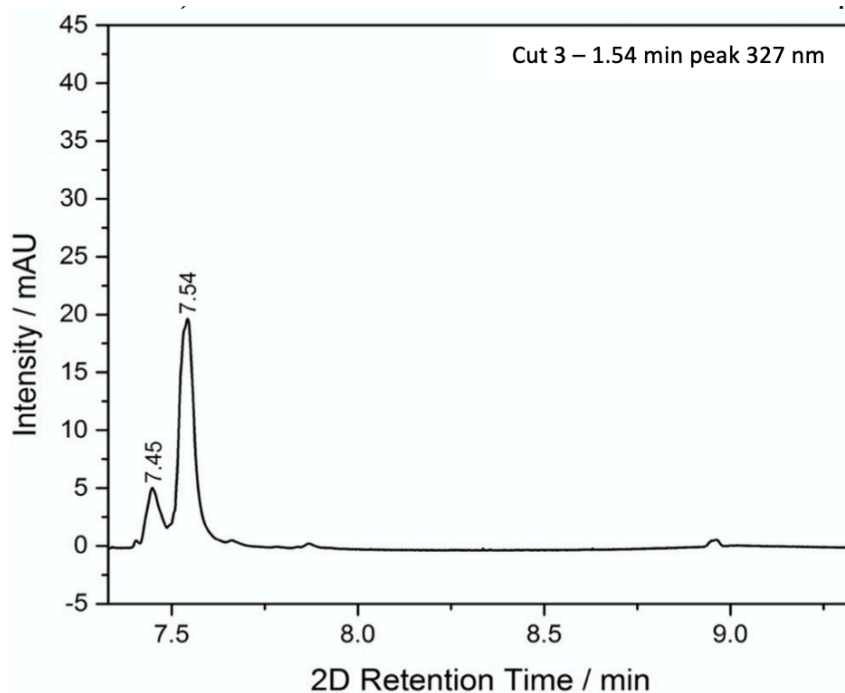


**Figure 3.1.6.3:** <sup>2</sup>D chromatogram of the cut 3 of Reseda Lake/buckthorn berry pigment (5:95% (v/v) formic acid/methanol) at 327 nm. Retention times are stated above each main peak.

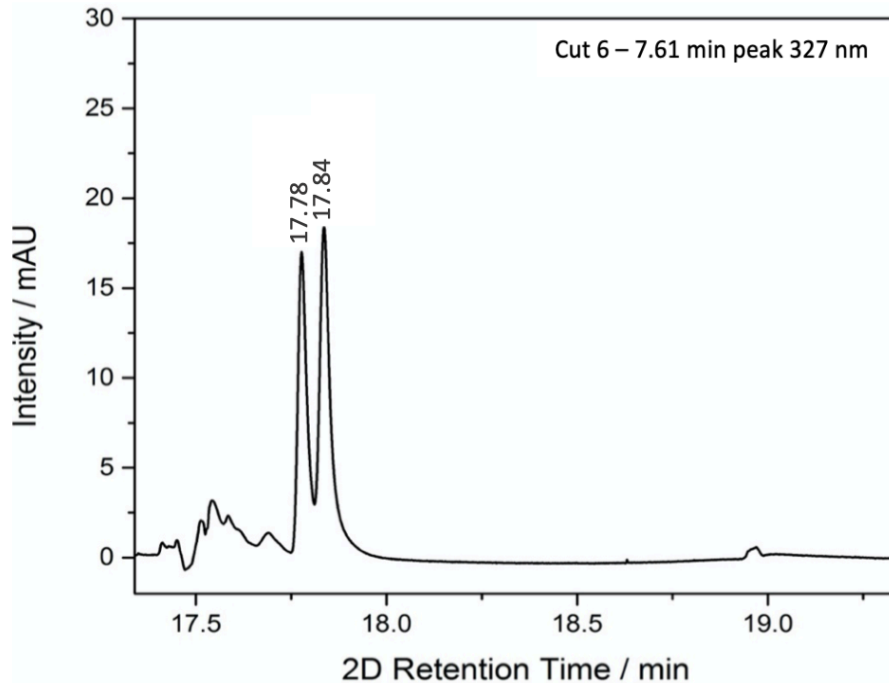


**Figure 3.1.6.4:** <sup>2</sup>D chromatogram of the cut 6 of Reseda Lake/buckthorn berry pigment (5:95% (v/v) formic acid/methanol) at 327 nm. Retention times are stated above each main peak.

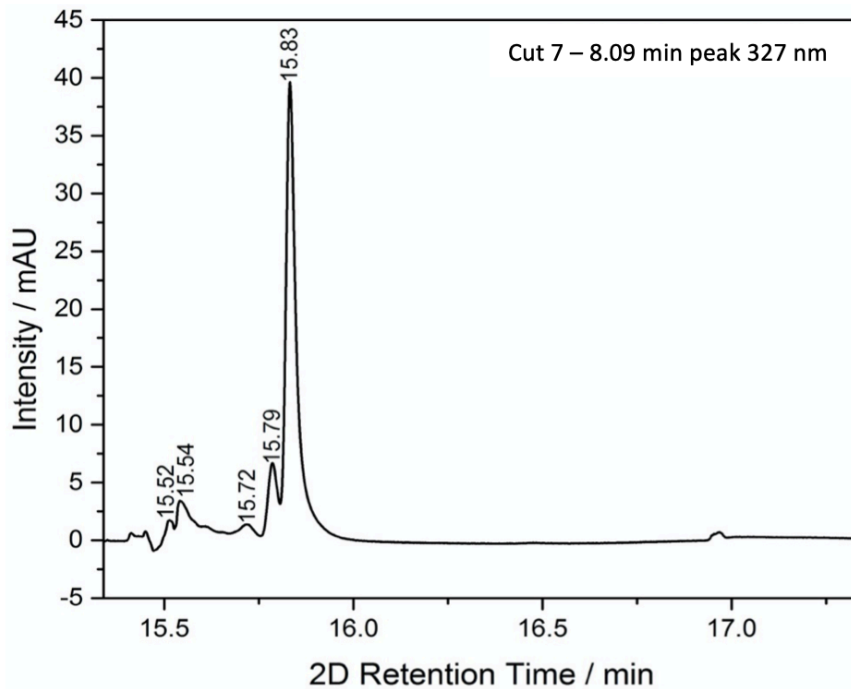


**Figure 3.1.6.5:** <sup>2</sup>D chromatogram of the cut 7 of Reseda Lake/buckthorn berry pigment (5:95% (v/v) formic acid/methanol) at 327 nm. Retention times are stated above each main peak.

The heart cut of the 11.59 minute showcases one main peak in the second dimension in Figure 3.1.6.6 and this is quite different compared to what was shown in Figure 3.1.3.3. There were 4 peaks present in that <sup>2</sup>D chromatogram in Figure 3.1.3.3 therefore this could be mean that now these peaks were co-eluting together as the 12.23 minute peak in the second dimension in Figure 3.1.6.6. There <sup>2</sup>D chromatograms should be relatively the same since the same peak was chosen from the first dimension of the same pigment mixture to be heart cut in the second dimension. In future work, changing the gradient in the second dimension should be explored to see if it is actually more than one peak that is in fact co-eluting as one peak.

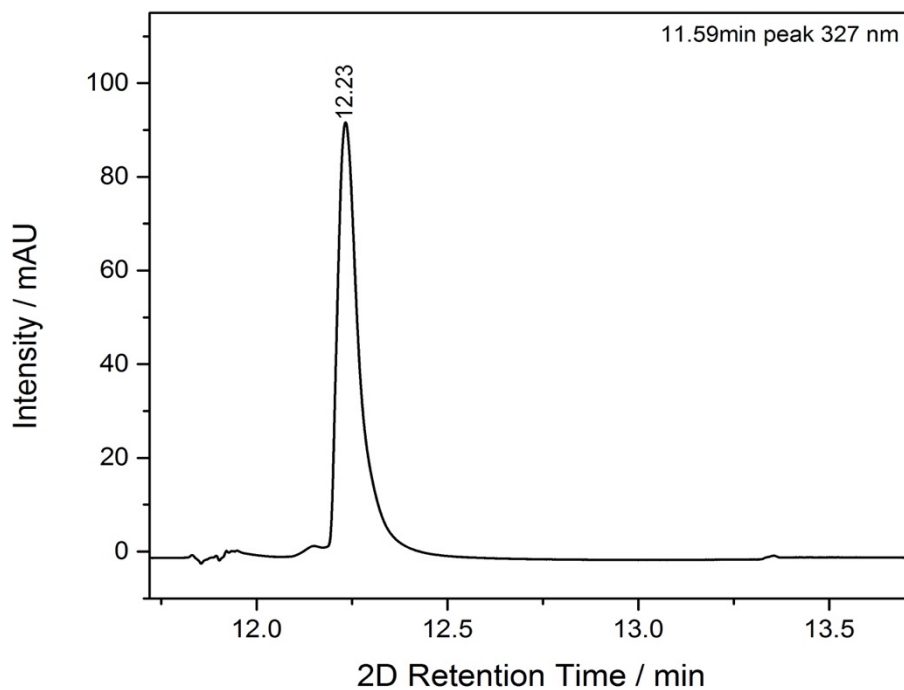


**Figure 3.1.6.6:** <sup>2</sup>D chromatogram of the 11.59 minute peak of Reseda Lake/buckthorn berry pigment (5:95% (v/v) formic acid/methanol) at 327 nm. Retention times are stated above each main peak.

## 3.2 EC-SERS Studies

### 3.2.1 Polyphenol Standards

The goal of this thesis work is to assess whether electrochemical SERS (EC-SERS) can be a useful offline detection modality for 2D-LC and will eventually require the collection of fractions from the second dimension and conducting EC-SERS on these fractions. Since the primary components of the yellow lake pigment are polyphenol compounds, this class of molecules will be used for the proof-of-concept work for this thesis. To start, EC-SERS was first conducted using the standard solutions for the eight polyphenol standards explored in this thesis and is an important first step, as it will allow for the determination of whether EC-SERS will be useful for the detection of polyphenols or not. As an example, Figure 3.2.1.1 shows the cathodic and anodic progression of caffeic acid on the AgNP modified SPE to demonstrate the effect of applied potential on the SERS spectrum. Figure 3.2.1.1 highlights how the spectral intensity and quality improves greatly with the application of potential. Next, in a typical experiment, the in air SERS signal is collected for reference. An electrolyte is then added (0.1 M NaF) and the SERS signal is again collected, but in the absence of any applied potential, termed the open circuit potential (OCP) spectrum. Since this OCP spectrum is collected prior to potential stepping it is termed the OCP cathodic spectrum. The potential is then stepped in 100 mV increments from 0.0 V to -1.0 V (cathodic progression) and the SERS signal is collected at each voltage. The potential is then stepped back in the anodic direction (anodic progression) from -1.0 V to 0.0 V and the signal is again collected at each potential. Finally, the OCP spectrum is collected again after the anodic progression (termed the OCP anodic spectrum).

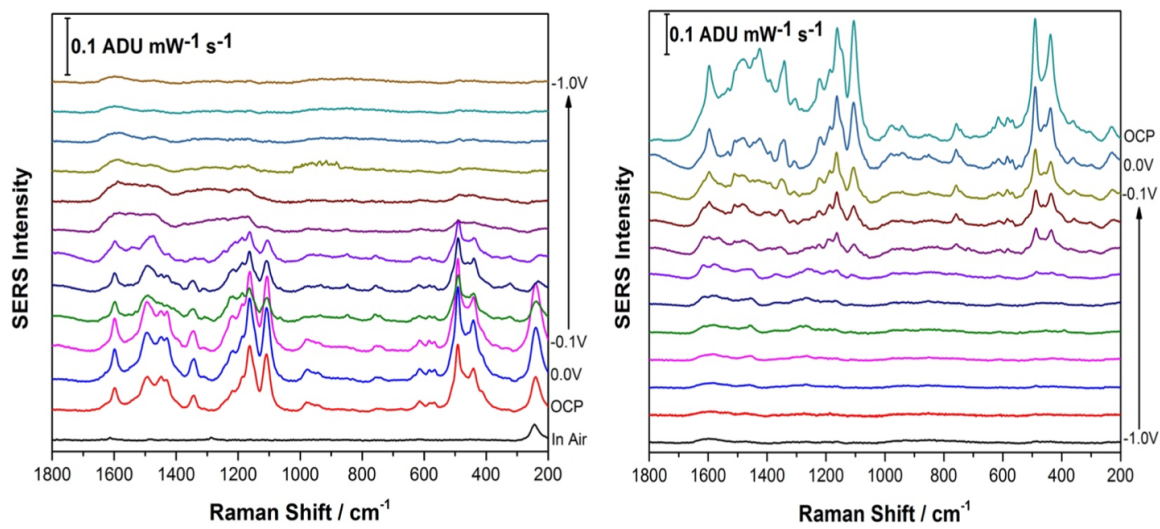


**Figure 3.2.1.1:** EC-SERS analysis of 2000 ppm caffeic acid on the surface of AgNP coated screen-printed electrode (Cathodic, 0.1V stepwise progression from 0V to -1.0V and Anodic, 0.1V step-wise progression from 0V to -1.0V) on the surface of AgNP coated screen-printed electrode using an excitation wavelength of 780 nm with a laser power of 80 mW and acquisition time of 30 seconds.

In Figure 3.2.1.1, the SERS signal collected in air is exceedingly weak. Once the electrolyte was added and the OCP spectrum was collected, the SERS signal was observed to be much stronger. This is likely due to the poor water solubility of the molecule, which allows for an enhanced interaction between the metal electrode surface and the molecule. After the cathodic progression, it can be noted that the signal at -1.0 V is lost. Once the voltage is then stepped back in the anodic direction, the SERS signal returns, and is actually maximum at OCP. It is clear that the EC-SERS spectrum at OCP in the anodic progression is a significant improvement over the in-air spectrum obtained initially, and this observation shows that EC-SERS has the potential to improve upon the normal SERS spectra of caffeic acid significantly. The great improvement of EC-SERS over normal SERS for the detection of polyphenol compounds can likely be attributed to a number of factors. In order to prepare the SERS electrodes for analysis, interfering citrate (the reducing agent and capping agent

in the nanoparticle synthesis) is first removed through displacement with chloride anion. As a consequence, the surface is covered in silver chloride, with the silver chloride stretching vibration being the most prominent feature in the spectrum. The silver chloride vibration at  $240\text{ cm}^{-1}$  disappears as the potential is stepped more negative, as it is desorbed from the surface of the electrode, which then likely allows the caffeic acid to have better access to the surface of the electrode through electrostatic interactions. With a potential of zero charge (PZC) of  $-0.95\text{ V}$ , the silver metal surface becomes less positively charged as the potential is stepped in the negative (cathodic) direction, causing the negatively charged chloride ions to desorb from the surface at approximately  $-0.2\text{ V}$ , after which the Ag-Cl peak then disappears. In addition, the peaks associated with caffeic acid disappear, as well, as the potential is stepped in the negative (cathodic) direction. The possible reason for this occurring is caffeic acid could be deprotonated, since the pKa of carboxylic acids are between 4-5, and therefore likely has an attraction to the positively charged surface of the electrode in the beginning of the analysis, similar to the chloride ions. However, as the potential is increased in the negative direction, the caffeic acid is desorbed from the surface of the electrode, since the negative surface of the electrode is now repelling the carboxylate present in caffeic acid. Clearly, however, the molecule is still within the double layer region, since when the potential is stepped back in the anodic direction, the signal for caffeic acid returns. The remaining eight polyphenol compounds present similar patterns depending on the structure of the compound. However, different patterns consist of the chloride ions interfering with the signal more for some compounds than others, such as emodin. EC-SERS analysis of remaining polyphenol compounds can be found in the appendix Figure A1 – A7

Table 3.2.1.1 lists the potentials where the best signal is produced for each of the eight polyphenol standards and these will be particularly useful when analyzing the yellow lake pigment through EC-SERS, because at different voltages it is hoped that different components adhere to the surface of the electrode to obtain a spectrum.

**Table 3.2.1.1:** Voltages that provide the best EC-SERS signal for each polyphenol standard

<b>Standard</b>	<b>Voltage</b>
<b>Caffeic Acid</b>	OCP Anodic
<b>Chlorogenic Acid</b>	-0.1 Anodic
<b>Apigenin</b>	0.0V Anodic
<b>Kaempferol</b>	-0.2V Anodic
<b>Quercetin</b>	0.0V Anodic
<b>Luteolin</b>	-0.3V Cathodic
<b>Rhamnetin</b>	-0.2V Cathodic
<b>Emodin</b>	-0.4V Cathodic

### 3.2.2 Polyphenol Standards Mixture

5  $\mu\text{L}$  of a mixture of the eight polyphenol standards was drop coated onto a silver coated electrode for EC-SERS. Figure 3.2.2.1 is a cathodic and anodic comparison of EC-SERS spectra of the polyphenol mixture. As shown by the spectra, the in air spectrum is producing a signal, but it is not as strong compared to the OCP spectrum. However, the voltage that produced the best signal was -0.1 V cathodic, which is then lost as an increase of negative potential is added to the electrode, and this could be indicating that the

components in the mixture are being repelled from the surface of the electrode from the buildup of negative charge present. As the potential and, consequently, the negative charge is then decreased, signal is again produced, but not as strong as seen before.

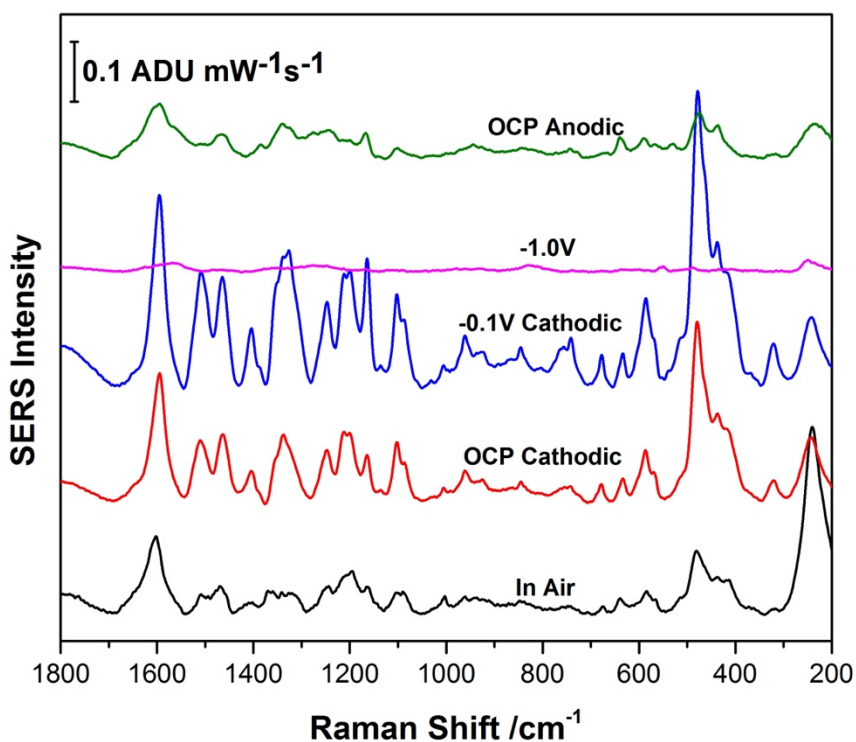


**Figure 3.2.2.1:** Comparison of EC-SERS spectra of a mixture of chlorogenic acid, caffeic acid, quercetin, luteolin, kaempferol, rhamnetin, apigenin and emodin (31 ppm each) on the surface of AgNP coated screen-printed electrode using an excitation wavelength of 780 nm with a laser power of 80 mW and acquisition time of 30 seconds.

Various spectra from different voltages of the polyphenol mixture were then compared to the corresponding voltage of the individual polyphenol standards and this was done to determine if different polyphenol compounds were adhering to the surface of the electrode at different voltages. As a result, these findings will be useful when analyzing the Reseda lake/buckthorn berry mixture, because some of the many components could adhere to the surface of the electrode at different voltages being applied to the electrode, which can then be identified by standard spectra. Figure 3.2.2.2 is a comparison of two polyphenol

standards (2000 ppm quercetin and 500 ppm rhamnetin) with the eight polyphenol standards mixture at -0.1V. It can be observed that these two standards are very similar to the polyphenol mixture at this voltage. However, it can also be observed (along with Figure 3.2.2.3) that the rhamnetin standard is much more similar to the polyphenol mixture at -0.1V than the quercetin standard. For example, the rhamnetin standard has the two peaks present at wavenumbers of 1100  $\text{cm}^{-1}$  to 1200  $\text{cm}^{-1}$ , while quercetin only has one peak present.

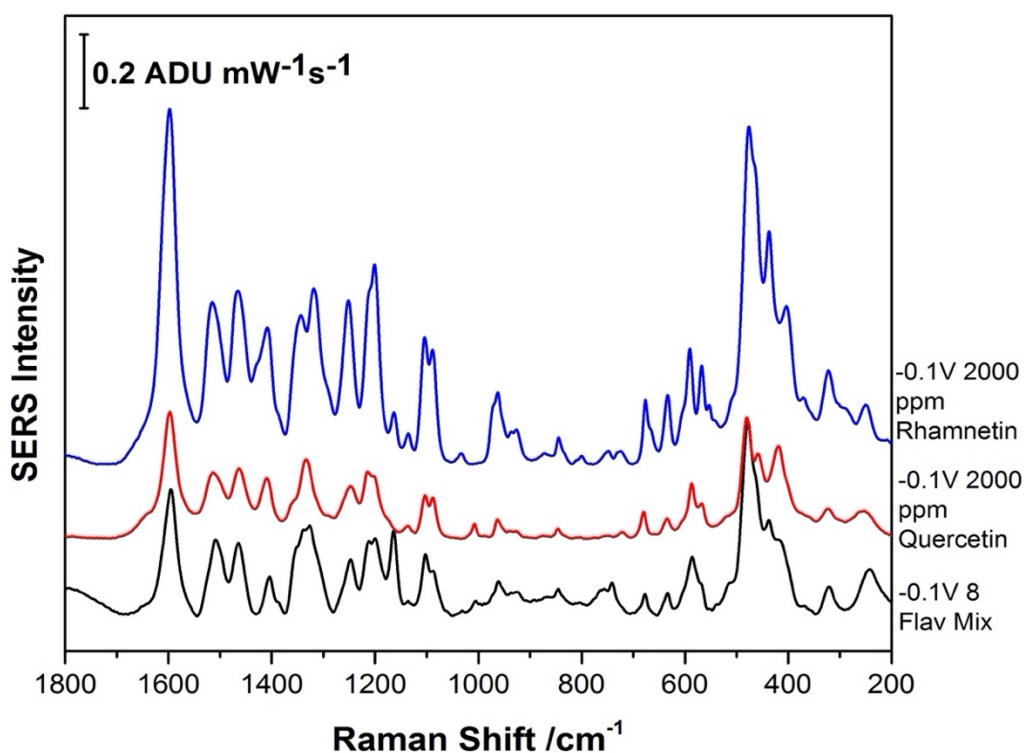


**Figure 3.2.2.2:** Comparison of EC-SERS spectra of eight polyphenol compounds in a mixture (8 Flav Mix), 2000 ppm quercetin standard and 500 ppm rhamnetin standard at -0.1V during the cathodic progression on the surface of AgNP coated screen-printed electrode using an excitation wavelength of 780 nm with a laser power of 80 mW and acquisition time of 30 seconds.

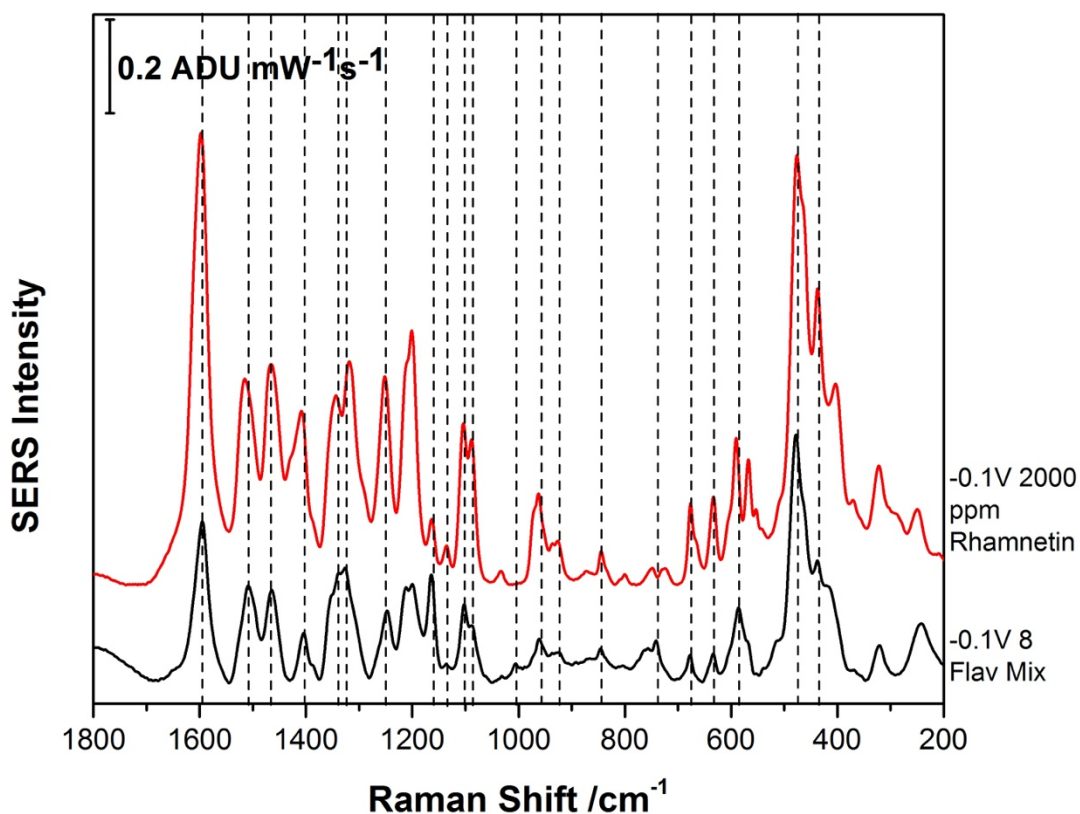


**Figure 3.2.2.3:** Comparison of EC-SERS spectra of eight polyphenol compounds in a mixture (8 flavonoid mixture) standard and 500 ppm rhamnetin standard at -0.1V during the cathodic progression on the surface of AgNP coated screen-printed electrode using an excitation wavelength of 780 nm with a laser power of 80 mW and acquisition time of 30 seconds.

Figure 3.2.2.4 is a comparison of OCP spectra after the anodic progression for 2000 ppm quercetin and the eight polyphenol compound mixture. Quercetin gave the best comparison to the mixture than the other standards because it is observed that the spectra of these two solutions are similar. Quercetin has five hydroxyl groups present in its chemical structure. There could be strong electrostatic interaction of the lone pairs of electrons from the oxygen in the hydroxyl groups with the surface of the electrode. Nevertheless, there are some peaks that do not match up. Therefore, it is observed that, possibly, when adding varying voltages to the electrode, different polyphenol compounds

adhere to the surface of the electrode as shown above between -0.1V during the cathodic progression and the OCP anodic progression.

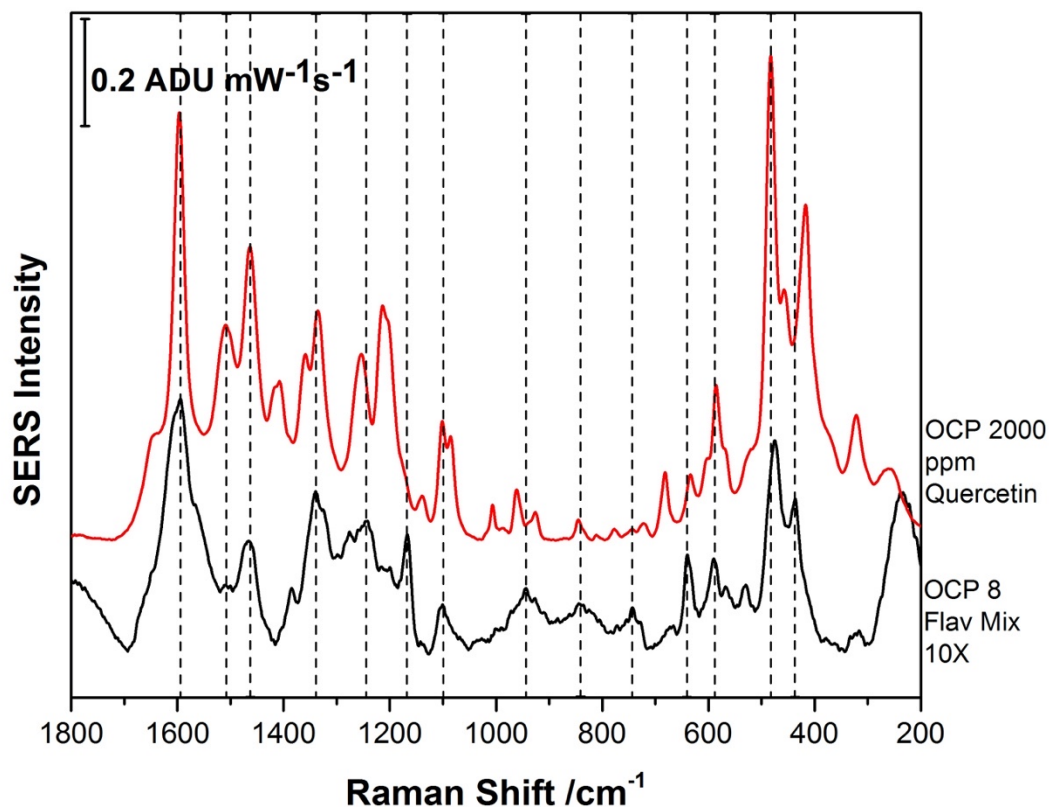


**Figure 3.2.2.4:** Comparison of EC-SERS spectra of eight polyphenol compounds in a mixture (8 Flav Mix) and 2000 ppm quercetin standard at OCP during the anodic progression on the surface of AgNP coated screen-printed electrode using an excitation wavelength of 780 nm with a laser power of 80 mW and acquisition time of 30 seconds.

### 3.2.3 Polyphenol Standards Mixture Fractions

Seven fractions were collected for the polyphenol mixture after the second dimension separation, one for each of the components, with the exception of kaempferol since the intensity for this component was too low to allow for adequate collection (Figure 3.1.2.6). Figure 3.2.3.1 (A) is a comparison of EC-SERS spectra of the caffeic acid fraction obtained from the polyphenol mixture. The in air spectrum produces a large signal, which then disappears when increasing the potential. It is believed that that signal produced in this

spectrum is actually from the  $^{2D}$  mobile phase, and not from caffeic acid from the fraction. Figure 3.2.3.1 (B) is the in air spectrum of the caffeic acid fraction compared to both the in air and OCP spectra of the caffeic acid standard. It is observed that there is not much of a comparison. Very strong Raman shifts between 1100 to 1200  $\text{cm}^{-1}$  present in the 2000 ppm caffeic acid are not present at all for the in air fraction spectrum. However, there is a sharp peak present at 1000  $\text{cm}^{-1}$  of the in air spectrum of the caffeic acid fraction from the polyphenol mixture that is not present in the 2000 ppm caffeic acid standard in air or the OCP cathodic spectra. It is known from recent work that after a sample has undergone 2D-LC analysis, the sample becomes very dilute, which is the most likely case for this. There are simply not enough components of interest within the fraction that is adhering to the electrode in order to be detected. The mobile phase is simply interfering with the signal from the components of interest, and this was also experienced with the other fractions obtained from the mixture. The EC-SERS spectra of the remaining fractions from the eight polyphenol mixture can be found in the appendix (A8-A13).

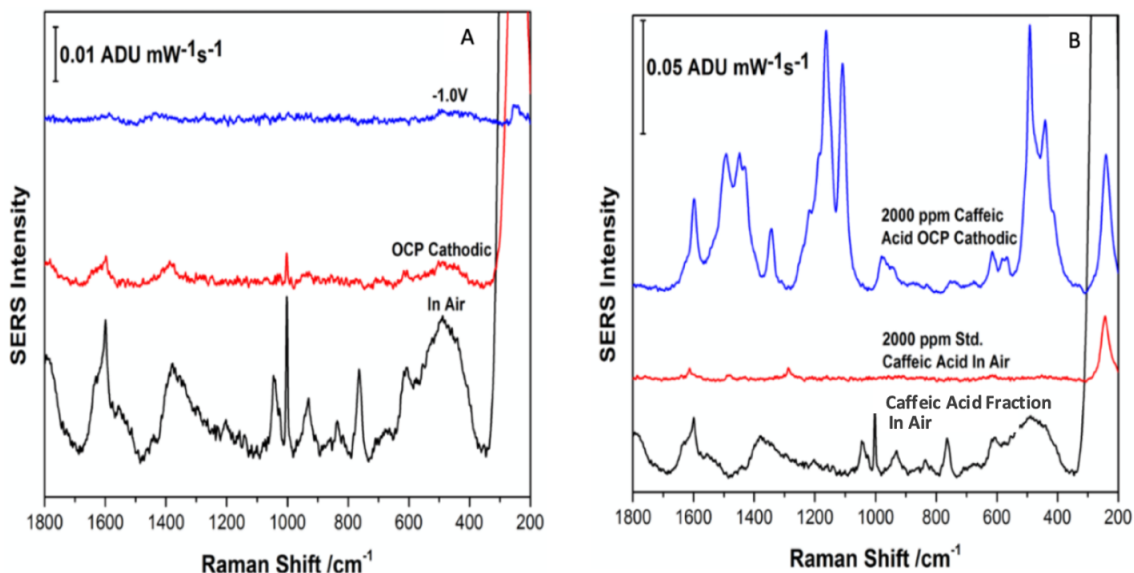


**Figure 3.2.3.1:** Comparison of EC-SERS spectra of caffeic acid from eight polyphenols in a mixture (A) and comparison with 2000 ppm caffeic acid standard EC-SERS spectra (B) with the in air spectrum 2D-LC fraction of caffeic acid from 8 polyphenol mixture on the surface of AgNP coated screen-printed electrode using an excitation wavelength of 780 nm with a laser power of 80 mW and acquisition time of 30 seconds.

Figure 3.2.3.2 (A) and (B) is a comparison of spectra of the 7 fractions of the polyphenol mixture to the <sup>2</sup>D mobile phase at in air and -1.0V respectively. It is observed that in Figure 3.2.3.2 (A) there is a common peak at a Raman shift of 1000 cm<sup>-1</sup> throughout all in air spectra except for the mobile phase spectrum. However, in Figure 3.2.3.2 (B), the rhamnetin fraction and the mobile phase are very much comparable indicating that the components in the mobile phase are being detected rather than the rhamnetin molecules in the fraction. Again, in Figure 3.2.3.2 (B), the 1000 cm<sup>-1</sup> peak is present expect for cuts 1, 2, 3, and 4. When obtaining the fractions from the 2D-LC the gradient of the second dimension mobile phase is at 95 % of 0.1% formic acid in acetonitrile. What could be occurring is the formic acid or acetonitrile molecules could be adhering to the surface of the electrode, since there are more of these molecules present than rhamnetin molecules. It is known that, when a sample undergoes 2D-LC analysis, the sample often undergoes

extreme dilution, therefore meaning there could in fact be more mobile phase molecules, such as formic acid, than actual components of the Reseda lake/buckthorn berry mixture after 2D-LC analysis.<sup>3</sup>

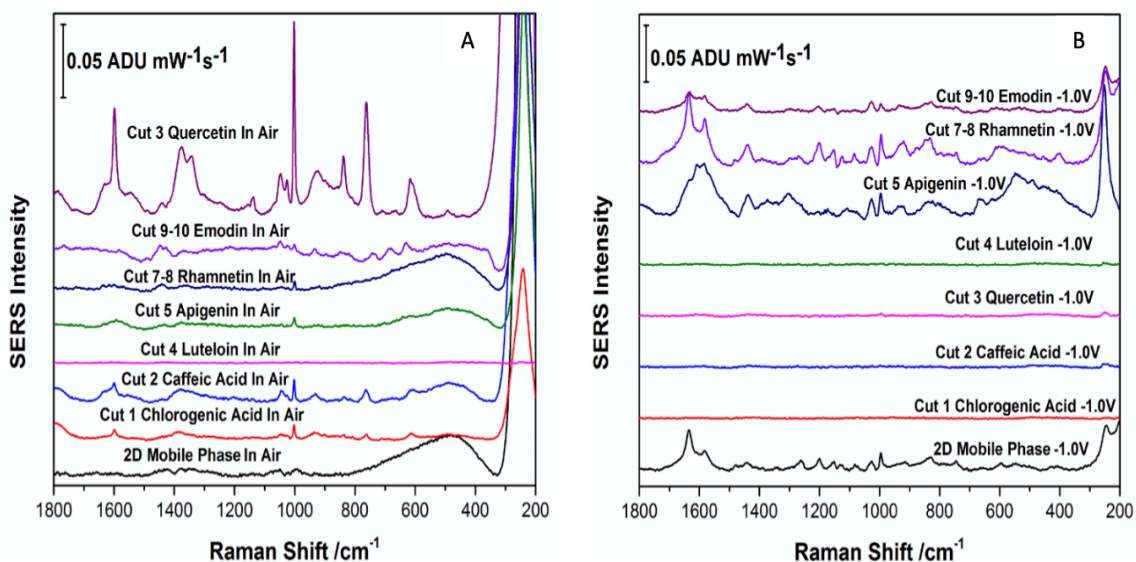


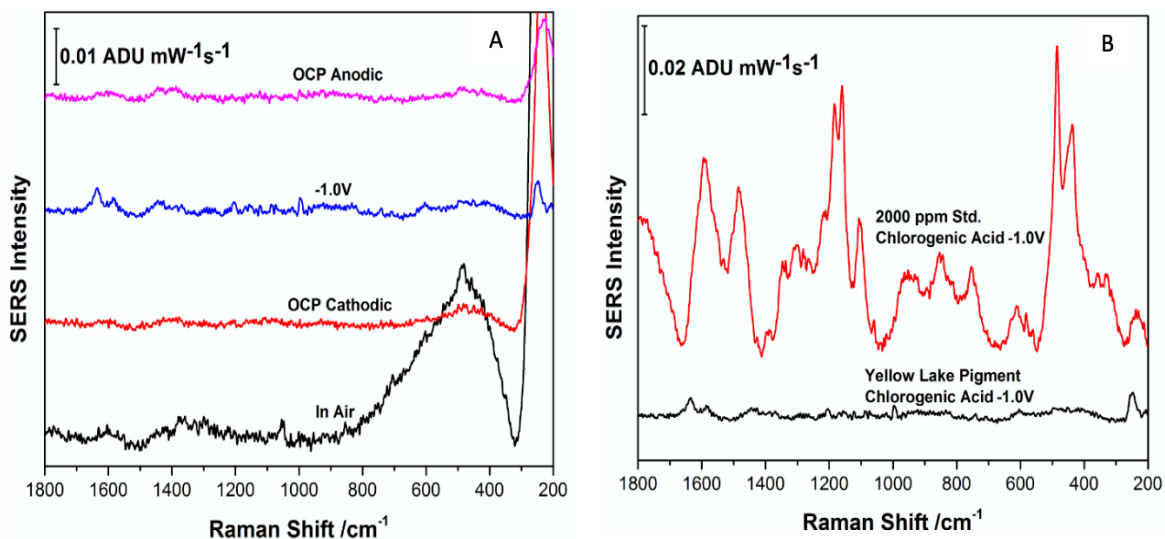
**Figure 3.2.3.2:** Comparison of in air (A) and -1.0V (B) EC-SERS spectra of 8 polyphenol mix 2D-LC fractions and the <sup>2</sup>D mobile phase on the surface of AgNP coated screen-printed electrode using an excitation wavelength of 780 nm with a laser power of 80 mW and acquisition time of 30 seconds.

### 3.2.4 Reseda Lake and Buckthorn Berries Pigment Fractions

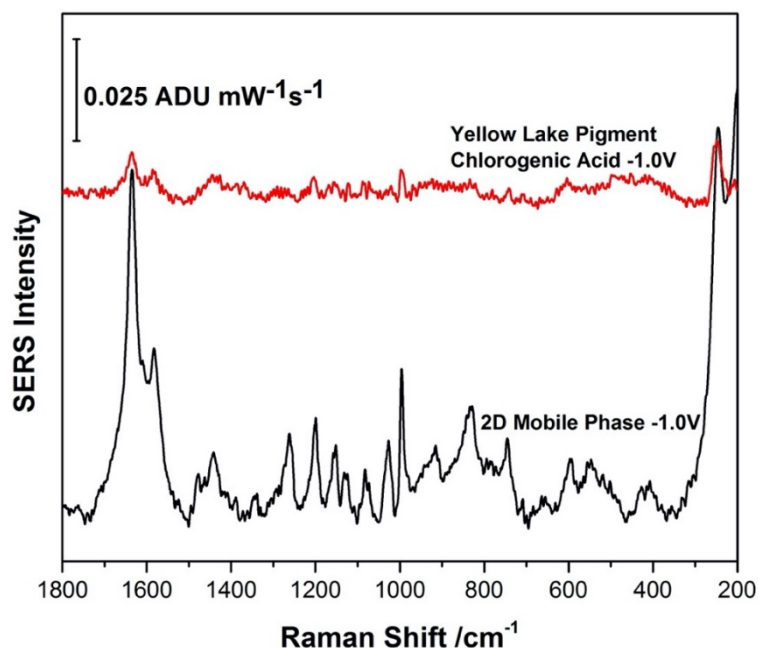
When collecting fractions from the Reseda lake/buckthorn berry mixture, it was hard to obtain fractions of certain peaks because the intensities of these peaks were too low (meaning there was not enough of those components to be collected). Therefore, only five fractions were collected: chlorogenic acid at 1.34 minutes, caffeic acid at 1.64 minutes, kaempferol at 7.61 minutes, apigenin at 8.09 minutes and the 11.59 minute peak.

Figure 3.2.4.1 (A) is a comparison of EC-SERS spectra of the fractions of chlorogenic acid taken from the yellow lake pigment and it can be observed that not much signal is present throughout these spectra, but the spectra at -1.0V provides the best signal. At the -1.0V spectrum, the peaks of interest that will be mentioned again later on in other

sections of this thesis are at Raman shifts between 1700 to 1500  $\text{cm}^{-1}$  and at around 1000  $\text{cm}^{-1}$ . The peak at 1000  $\text{cm}^{-1}$  has been present in other spectra of other fractions, discussed earlier in section 3.2.3. Figure 3.2.4.1 (B) is a comparison of EC-SERS spectra between the chlorogenic acid fraction and its standard. The comparison between these two spectra at -1.0V is not similar, although it is known that the fraction is much more dilute than the standard. It can be seen by Figure 3.2.4.2 that at a voltage of -1.0V, that the chlorogenic acid fraction spectrum is similar to the spectrum of the  $^{2D}$  mobile phase, but not as strong, reconfirming the theory that the components from the yellow lake pigment are unfortunately not being detected, but instead showing the components of the  $^{2D}$  mobile phase, since the sample is now much more dilute than what it was originally.



**Figure 3.2.4.1:** Comparison of EC-SERS spectra of chlorogenic acid fraction of Reseda lake/buckthorn berry pigment (A) and with 2D-LC fraction of 2000 ppm chlorogenic acid standard (B) on the surface of AgNP coated screen-printed electrode using an excitation wavelength of 780 nm with a laser power of 80 mW and acquisition time of 30 seconds.



**Figure 3.2.4.2:** Comparison between EC-SERS spectra of 2D mobile phase and chlorogenic acid fraction from Reseda lake/buckthorn berry pigment on the surface of AgNP coated screen-printed electrode using an excitation wavelength of 780 nm with a laser power of 80 mW and acquisition time of 30 seconds.

Figure 3.2.4.3 (A) is an overlay of various EC-SERS spectra of the 11.59 minute peak. It is noted that there are not many peaks present in these spectra, but the largest peak is present at around  $1000\text{ cm}^{-1}$ . Throughout all the spectra after the in air spectrum in this Figure, the intensity of this peak decreases, indicating the molecules in the fraction are not adhering to the electrode surface as well anymore when electrolyte and voltage is added to the electrochemical cell. Figure 3.2.4.3 (B) is a comparison of EC-SERS spectra of the 11.59 minute fraction to the  $^2\text{D}$  mobile phase. The EC-SERS spectra between these two fractions are not as similar as shown with other fractions previously. The largest peak present in the 11.59 minute fraction spectrum is not quite at a Raman shift of  $1000\text{ cm}^{-1}$  which is where one of the biggest peaks in the  $^2\text{D}$  mobile phase spectrum is between  $1000$  and  $1100\text{ cm}^{-1}$ . Consequently, the component being detected might not be part of the mobile phase, but actually part of the of the yellow lake pigment mixture. The rest of the spectra

for the fractions, which experience similar patterns as the chlorogenic acid fraction, are present in the appendix (A14-A19).

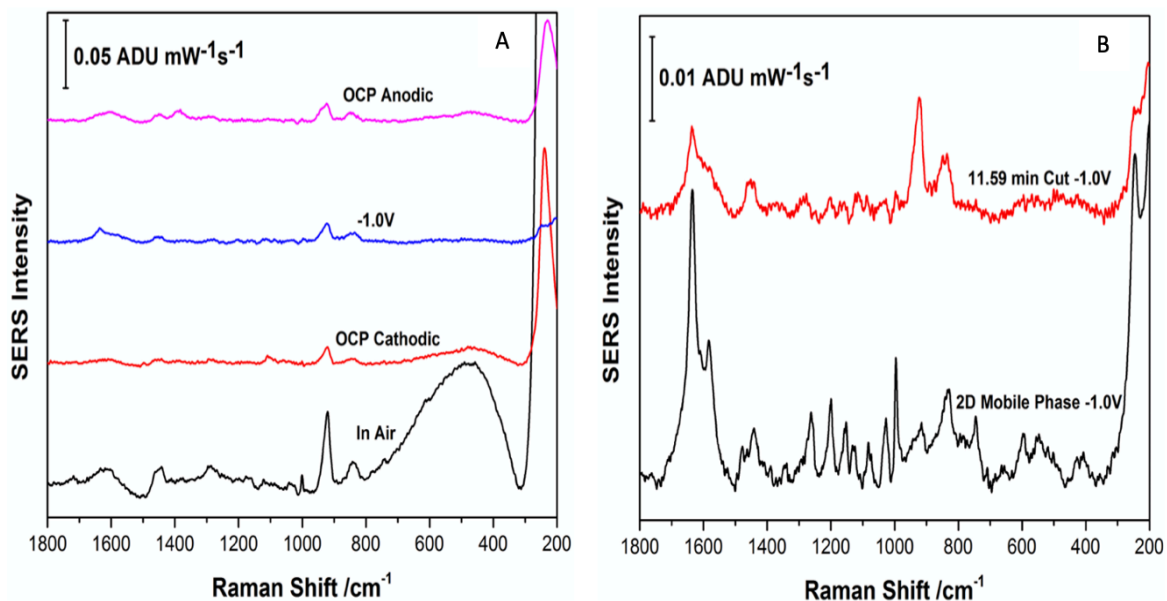


**Figure 3.2.4.3:** Comparison of EC-SERS spectra of 11.59 minute peak fraction of Reseda lake/buckthorn berry pigment (A) and with <sup>2</sup>D mobile phase (B) on the surface of AgNP coated screen-printed electrode using an excitation wavelength of 780 nm with a laser power of 80 mW and acquisition time of 30 seconds.

### 3.2.5 <sup>2</sup>D Mobile Phase Eluate (95:5% (v/v) 0.1% Formic Acid in Acetonitrile / 0.1% Formic Acid in Water)

Figure 3.2.5.1 is a comparison of EC-SERS spectra of the <sup>2</sup>D mobile phase 95/5 0.1% formic acid in acetonitrile/0.1% formic acid in water. It was found that at -1.0V the best EC-SERS signal was obtained. It is crucial to find out what is being adsorbed to the surface of the electrode that is producing this signal, since it could be interfering with the compounds of interest present in the fractions from the 2D-LC.

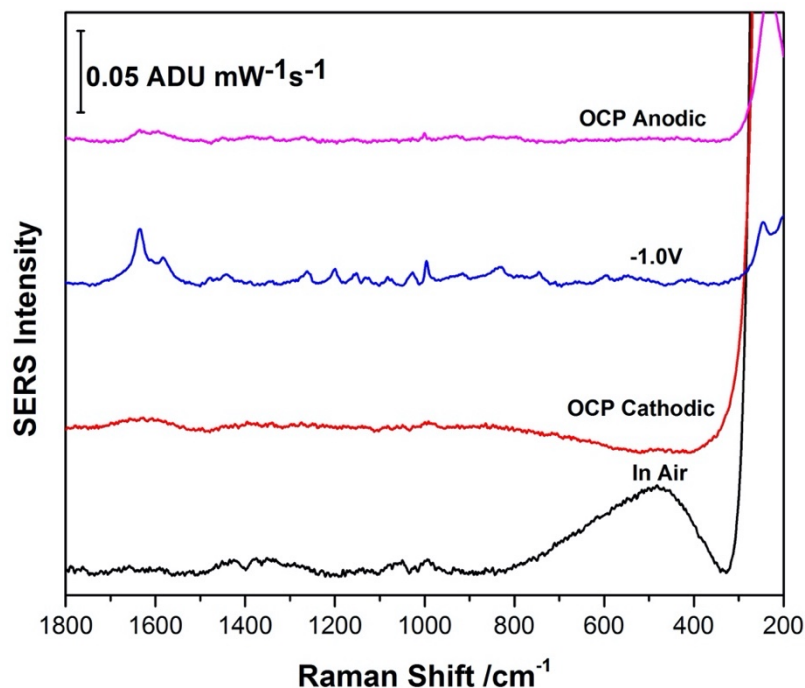
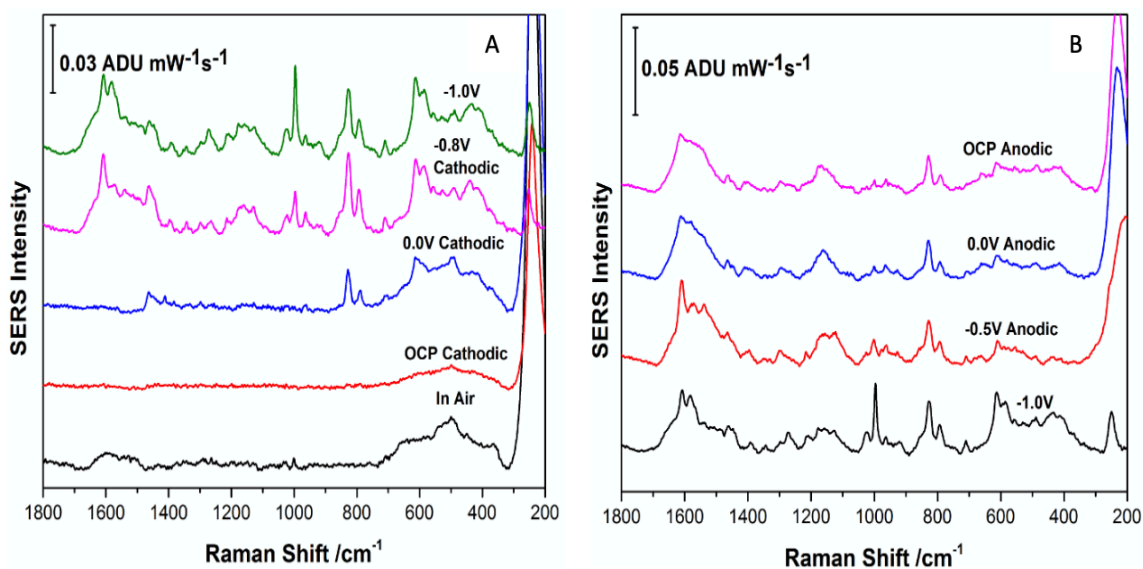


**Figure 3.2.5.1:** Comparison of EC-SERS spectra of the <sup>2</sup>D mobile phase (95:5% (v/v) 0.1% formic acid in acetonitrile/ 0.1% formic acid in water) on the surface of AgNP coated screen-printed electrode using an excitation wavelength of 780 nm with a laser power of 80 mW and acquisition time of 30 seconds.

### 3.2.6 Identification of <sup>2</sup>D Mobile Phase Eluate

As mentioned in sections, 3.2.3, 3.2.4 and 3.2.5, it was believed that the <sup>2</sup>D mobile phase is interfering with the components from the Reseda lake/ buckthorn berry mixture in the fractions from adhering to the electrode in order to obtain a spectrum. Therefore, a study was conducted to find out if the compounds used in <sup>2</sup>D mobile phase are what is being seen in the spectra of the fractions. Figure 3.2.6.1 shows the EC-SERS spectra of prepared solution of 95:5% (v/v) of 0.1% formic acid in acetonitrile/ 0.1% formic acid in water. It can be seen from the Figure 3.2.6.1. (A) that, from the in air spectrum, there is a little peak present at around 1000 cm<sup>-1</sup>, which was also observed in the EC-SERS spectra of fractions collected from the 2D-LC from previous sections in Chapter 3. This peak then disappeared in the OCP spectrum; however, this peak then grew in intensity when 0.0V, -0.8V and -

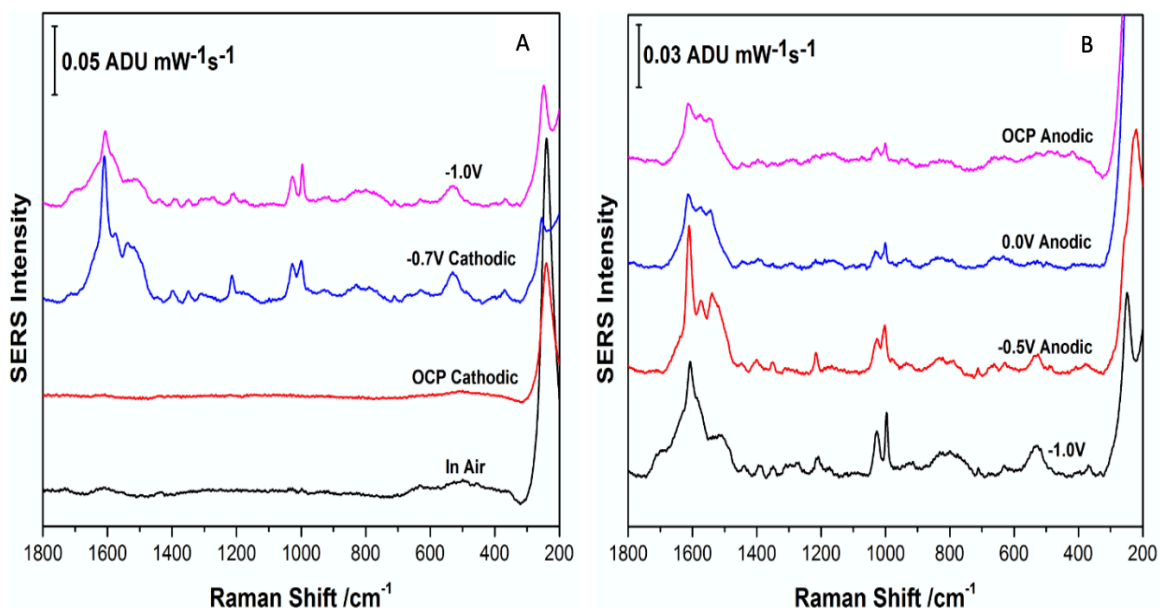
1.0V was applied to the electrode. In Figure 3.2.6.1 (B), when the voltage was decreased, the peak again decreased in intensity. In addition, it can be seen that when there is voltage applied to the electrode there are many more peaks present in the spectra than when there is not, such as at 0.0V and OCP, and the peaks present between 1500 to 1600  $\text{cm}^{-1}$  become less resolved.



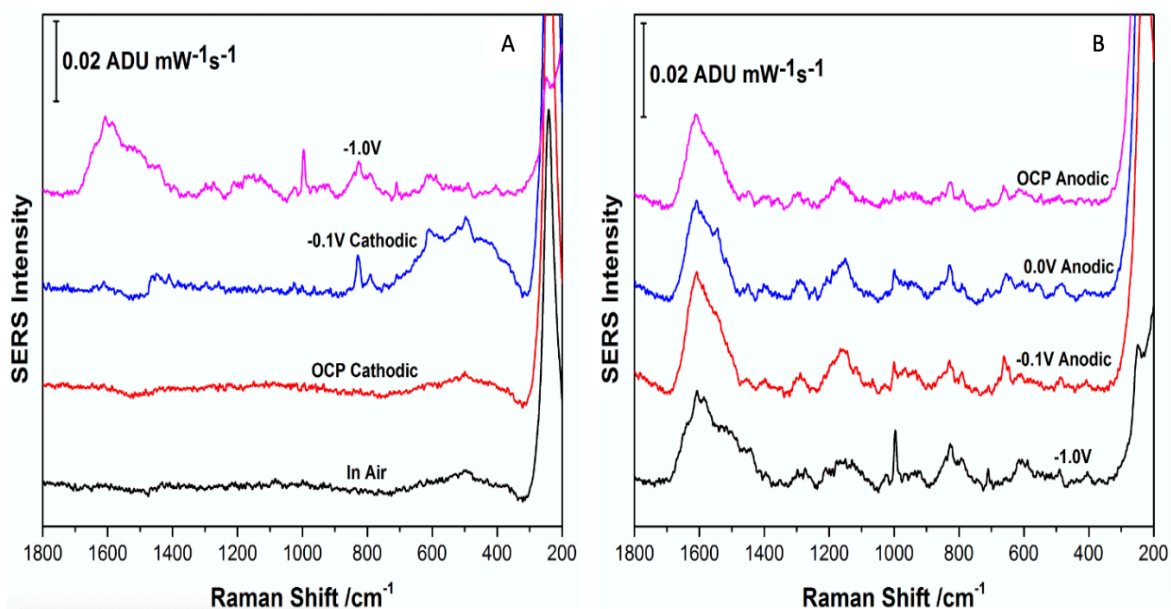
**Figure 3.2.6.1:** Comparison of cathodic EC-SERS spectra (A) and comparison of anodic EC-SERS spectra (B) of prepared solution of 95:5% (v/v) 0.1% formic acid in acetonitrile/ 0.1% formic acid in water on the surface of AgNP coated screen-printed electrode using an excitation wavelength of 780 nm with a laser power of 80 mW and acquisition time of 30 seconds.

Figure 3.2.6.2 (A) and (B) are EC-SERS spectra of prepared solution of 0.1% formic acid in acetonitrile. These spectra followed a similar pattern to what was seen with Figure 3.2.6.1, but for the in air spectrum in Figure 3.2.6.2 there was no peak present at 1000  $\text{cm}^{-1}$  like there was for the in air spectrum in Figure 3.2.6.1. Another noticeable difference is that there are not as many peaks present in Figure 3.2.6.2 (A) and (B) as there was in Figure 3.2.6.1. However, there are peaks present at Raman shifts at between 1600 and 1500  $\text{cm}^{-1}$  in many of the spectra in Figure 3.2.6.2, as observed in spectra of fractions seen in earlier

sections. Figure 3.2.6.3 is showing EC-SERS spectra of formic acid solution. Again, the in air and OCP spectra in Figure 3.2.6.3 (A) demonstrates little to no peaks being present, but when high voltage is added to the electrode (-0.7V and -1.0V), many more peaks are present as observed in earlier cases. However, these peaks then tend to decrease in intensity and are less resolved at -1.0V in Figure 3.2.6.3 (A), but these peaks decrease more in intensity in Figure 3.2.6.3 (B) when the voltage is decreased.



**Figure 3.2.6.2:** Comparison of cathodic EC-SERS spectra (A) and comparison of anodic EC-SERS spectra (B) of prepared solution of 0.1% formic acid in acetonitrile on the surface of AgNP coated screen-printed electrode using an excitation wavelength of 780 nm with a laser power of 80 mW and acquisition time of 30 seconds.



**Figure 3.2.6.3:** Comparison of cathodic EC-SERS spectra (A) and comparison of anodic EC-SERS spectra (B) of formic acid solution on the surface of AgNP coated screen-printed electrode using an excitation wavelength of 780 nm with a laser power of 80 mW and acquisition time of 30 seconds.

**Table 3.2.6.1:** Peak Assignments of Formic Acid.<sup>54</sup>

Raman Shift (cm <sup>-1</sup> )	Assignment
1600 – 1750	C=O stretch
1398	C-H bend
1333	$\delta(\text{OHO}) + \text{C-O stretch}$
1208	C-O stretch
650 - 725	OCO bend
~210	OH•••H out of plane bend
1060	C-H bend

Dr. Bartholomew did Raman spectral studies of solutions of formic acid and methyl formate, and the peak assignments of formic acid were mentioned in his PhD thesis.<sup>54</sup> These peaks assignments are presented in Table 3.2.6.1.<sup>54</sup> From comparing the Raman shifts from

Table 3.2.6.1 to the peaks present in Figure 3.2.6.3 of formic acid, it is observed that the carbonyl stretch, C-H bend, and C-O stretch are present at around  $1600\text{ cm}^{-1}$ ,  $1398\text{ cm}^{-1}$  and  $1060\text{ cm}^{-1}$ , and  $1208\text{ cm}^{-1}$  in Figure 3.2.6.3 respectively.

Comparing spectra at a  $-1.0$  voltage of the prepared  $^2\text{D}$  mobile phase solution, the formic acid and the  $^2\text{D}$  mobile phase eluate in Figure 3.2.6.4, it is pretty remarkable the comparison between these four different solutions. It can be noticed that the  $1000\text{ cm}^{-1}$  peak from the C-H bend and  $1600 - 1750\text{ cm}^{-1}$  peaks are present in all spectra at different intensities. It is therefore very possible from this study that formic acid is the leading compound that is being identified when performing EC-SERS on the fractions of the reference yellow lake pigment. This result is very important, as it indicates that future work in the development of 2D-LC-EC-SERS should focus on the removal of formic acid as a mobile phase additive if at all possible, as this molecule is readily detected using EC-SERS.

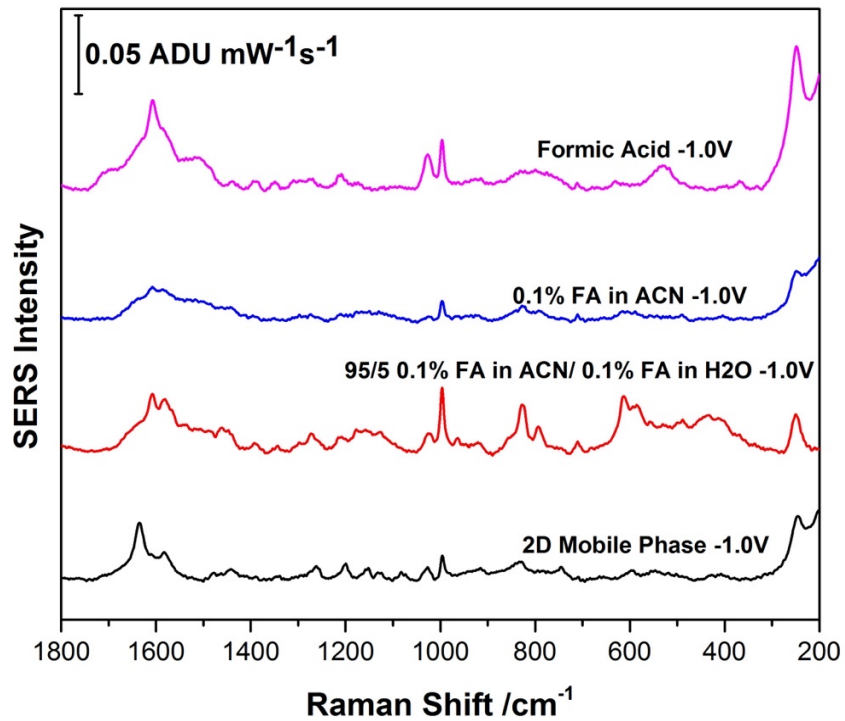


**Figure 3.2.6.4:** Comparison between EC-SERS spectra of <sup>2</sup>D mobile phase eluate and various prepared solutions of the <sup>2</sup>D mobile phase on the surface of AgNP coated screen-printed electrode using an excitation wavelength of 780 nm with a laser power of 80 mW and acquisition time of 30 seconds.

### **3.3 SEM – EDX Analysis on Reseda Lake and Buckthorn Berries Reference Pigment**

It is known that yellow lake pigments contain a mordant such as calcium sulphate or alum ( $\text{KAl}(\text{SO}_4)_2 \cdot (12\text{H}_2\text{O})$ ) or alumina ( $\text{Al}_2\text{O}_3$ ).<sup>6,10,14,28</sup> Therefore, it was important to determine what the nature of the mordant was in the Reseda lake/buckthorn berry mixture and this was determined by using scanning electron microscopy - energy-dispersive X-ray spectroscopy (SEM-EDX) analysis. In the first study, a small amount of the yellow lake pigment extract was placed on top of carbon tape for the SEM-EDX analysis. Figure 3.3.1 is an SEM image of the pigment extract solution (the solution observed in the centrifuge tube of Figure 3.1.5.1) under 50  $\mu\text{m}$  magnification and Figure 3.3.2 is the corresponding EDX spectrum of the extract solution, respectively. The EDX spectrum displays a high amount of sodium and chlorine present, which was not expected. The sodium and chlorine could be from the plant when extracting the dyestuff to create the pigment. Plants contain variable amounts of chlorides, and plant extracts can reach high concentrations of NaCl depending on the salinity of the soil where the plants grew.<sup>55</sup>

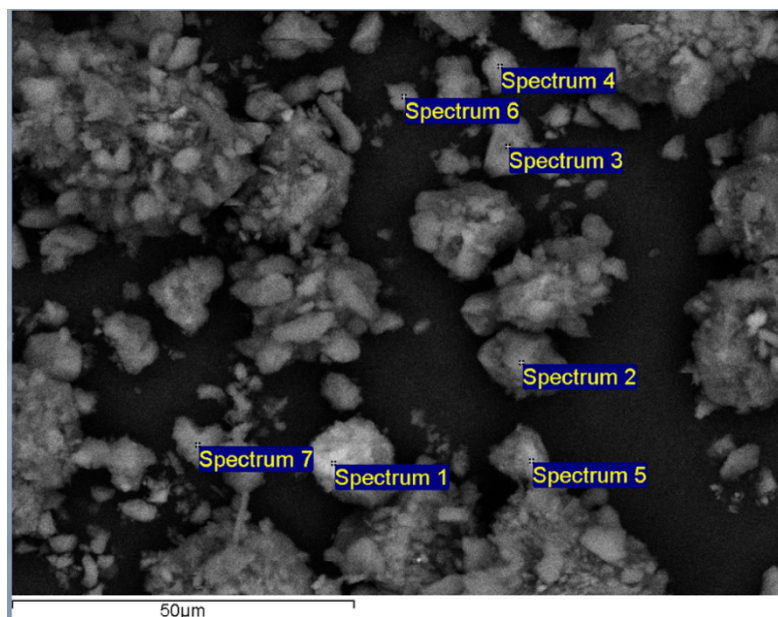


**Figure 3.3.1:** SEM image showing the particles present in Reseda lake/buckthorn berry pigment extract solution under 50  $\mu\text{m}$  magnification (voltage: 20 keV, Det: SE, Tescan MIRA3 LMU Field Emission SEM).

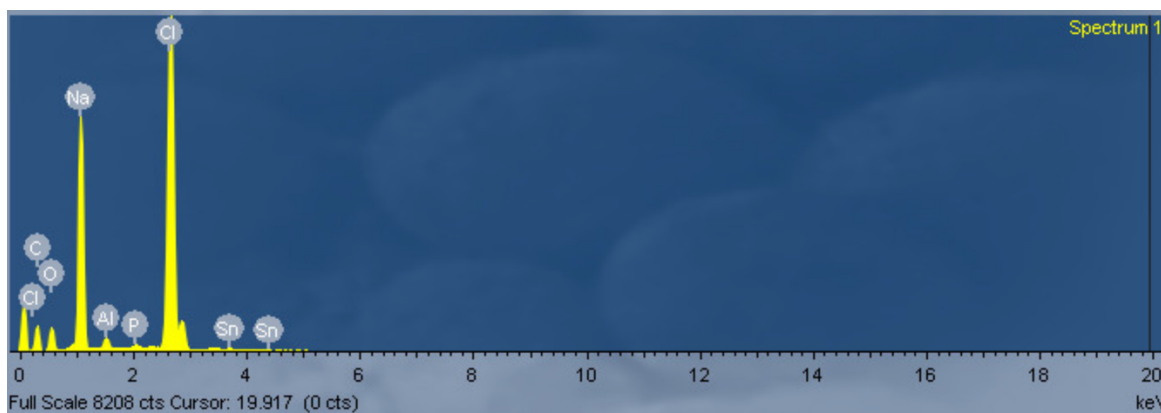


**Figure 3.3.2:** EDX spectrum of Reseda lake/buckthorn berry pigment extract solution present in Figure 3.3.1 (voltage: 20 keV, Det: SE, Tescan MIRA3 LMU Field Emission SEM)

Another SEM-EDX analysis was carried out only on the Reseda lake/buckthorn berry mixture to see if other elements would be present besides sodium and chlorine, as shown from the pigment extract solution. Figure 3.3.3 is the SEM image of Reseda lake/buckthorn berry mixture under 20  $\mu\text{m}$  magnification and Figure 3.3.4 is the corresponding EDX spectrum of the lake pigment. It can be observed that this EDX spectrum is different than

the previously obtained one from Figure 3.3.2. Figure 3.3.4 shows the presence of moderate levels of calcium and potassium, and a higher amount of sulfur. In addition, there is again a small amount of aluminum present in the spectrum, like previously in Figure 3.3.2. Figure 3.3.4 is different from Figure 3.3.2 because chlorine is no longer present and there is now a smaller amount of sodium in the spectrum. The calcium could be in combination with the sulfur and oxygen as calcium sulphate ( $\text{CaSO}_4$ ).<sup>56</sup> Figure 3.3.4 could be indicating that what is being observed is an alum or calcium sulphate mordant used to make the Reseda lake/buckthorn berry mixture.

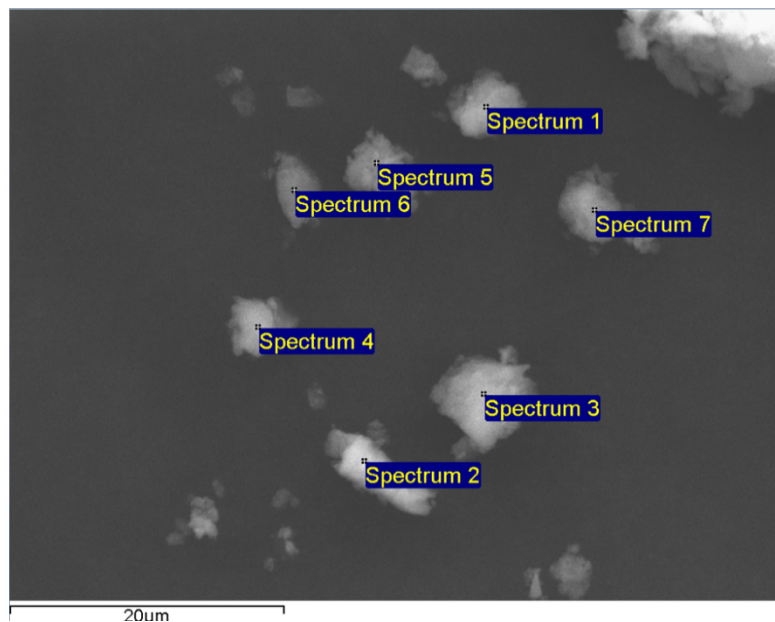


**Figure 3.3.3:** SEM image of Reseda lake/buckthorn berry pigment under 20  $\mu\text{m}$  magnification (voltage: 20 keV, Det: SE, Tescan MIRA3 LMU Field Emission SEM)

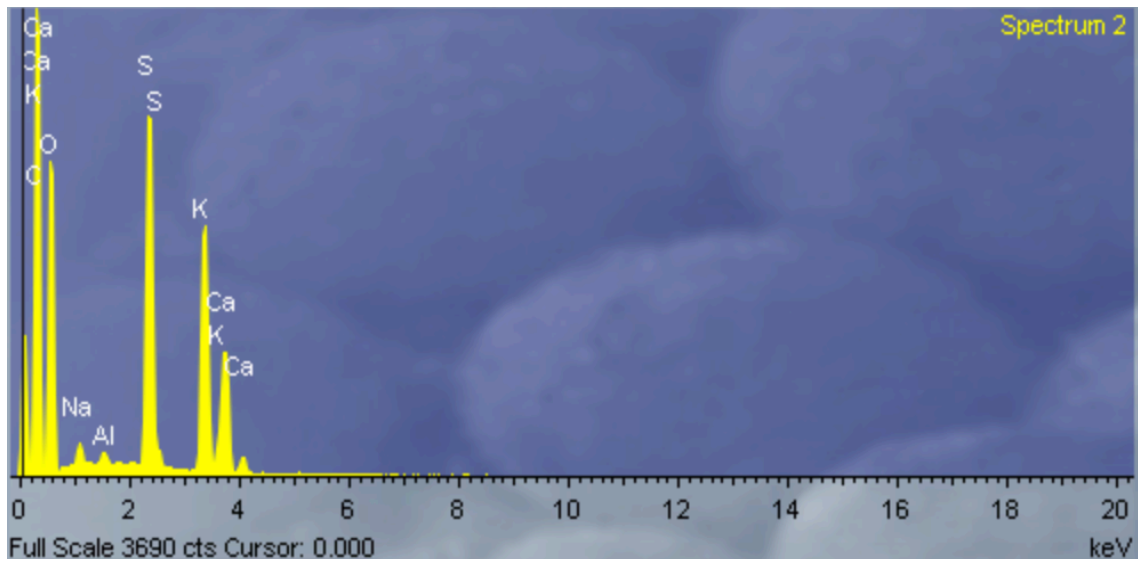


**Figure 3.3.4:** EDX spectrum of Reseda lake/buckthorn berry pigment in Figure 3.3.3. (voltage: 20 keV, Det: SE, Tescan MIRA3 LMU Field Emission SEM)

### 3.4 QTOF MS Analysis Results of 11.59 minute peak

Since the 11.59 minute peak still remains a mystery after performing chromatographic and spectroscopic analysis, quadrupole time of flight analysis mass spectrometry (QTOF MS) was performed on the collected fraction in an effort to try and identify it. It was anticipated that with this technique more information, such as molar mass, would be acquired to identify this component of the yellow lake pigment. Figure 3.4.1 represents the negative mode spectra of the  $^2\text{D}$  mobile phase (A) and the 11.59 minute peak from the Reseda lake/buckthorn berry pigment (B). Between the two spectra, the peaks present in both are quite the same, indicating that in the negative mode all that is being detected is the  $^2\text{D}$  mobile phase.

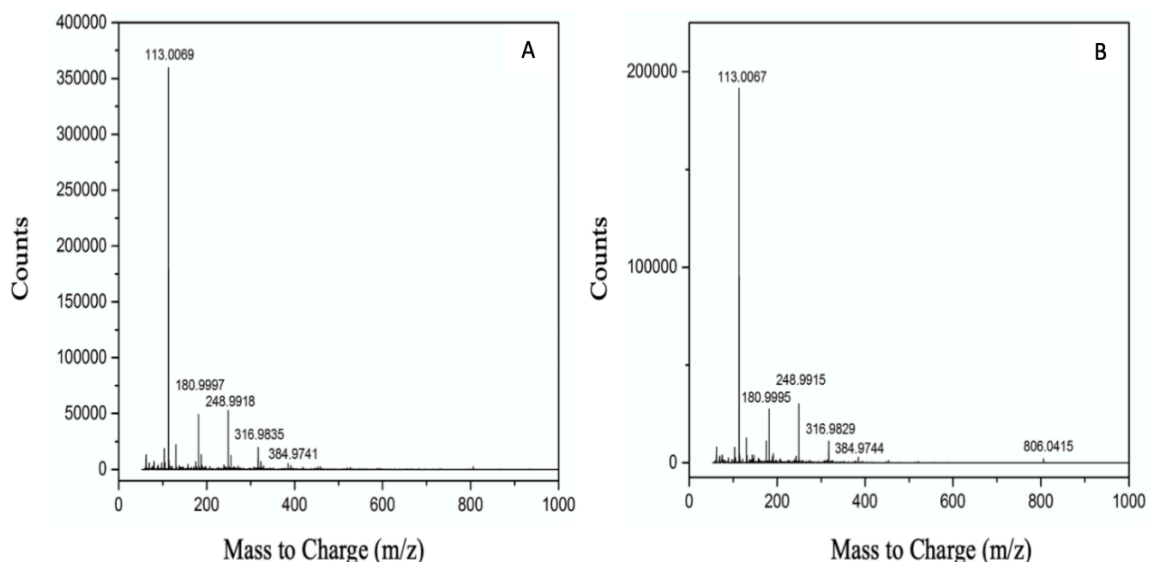


**Figure 3.4.1:** Negative mode of  $^2\text{D}$  mobile phase (95/5 0.1% formic acid in acetonitrile/0.1% formic acid in water (A) and Reseda Lake/buckthorn berry pigment (B).

Figure 3.4.2 is the positive mode spectra of the  $^2\text{D}$  mobile phase (A) and the 11.59 minute peak from the Reseda lake/buckthorn berry pigment (B). The results produced in the spectrum for the lake pigment was quite different in the positive mode than in the

negative mode. There are many more peaks present that are coming from the 11.59 minute peak. However, from the spectrum, there might be more than one component present in the 11.59 minute peak fraction, such as the dyestuff and possibly some peptides. There are large mass-to-charge ratios present in the spectrum such as 437.1972 m/z, 537.3988 m/z and 659.2915 m/z, which are typical mass-to charge ratios for proteins. It is known that some dyes are dispersed or diluted in a medium such as a protein binder which could have been the case in this instance.<sup>6</sup> The range of molar mass of the polyphenol compounds studied in this thesis work is 180.16 g/mol (caffeic acid) and 354.31 (chlorogenic acid). Therefore, the mass to charge ratios present in the spectrum that could be of interest of solving the mystery of what compound is present in the 11.59 minute peak would be 90.9788 m/z, 158.9665 m/z and 226.9543 m/z since the mass-to charge ratios fall in that range. However, there was some trouble identifying the dyestuff or components present with the libraries present at SMU because there was no way in picking just the mass-to-charge ratios of interest (i.e. 90.9788 m/z, 158.9665 m/z and 226.9543 m/z) in the library. Another trouble in this identification process was since QTOF MS analysis was just used, not LC-QTOF MS, and this was done by injecting the fraction into the QTOF MS part of the instrument. Therefore, this causes problems in another library used because there needed to be retention times in order to perform the analysis. In conclusion, the 11.59 minute peak was not able to determine because of these troubles with the library and no further investigation of the mass-to-charge ratios was not able to be conducted due to unforeseen circumstances due to COVID-19, therefore the component present in the 11.59 minute peak remains a unsolved mystery.

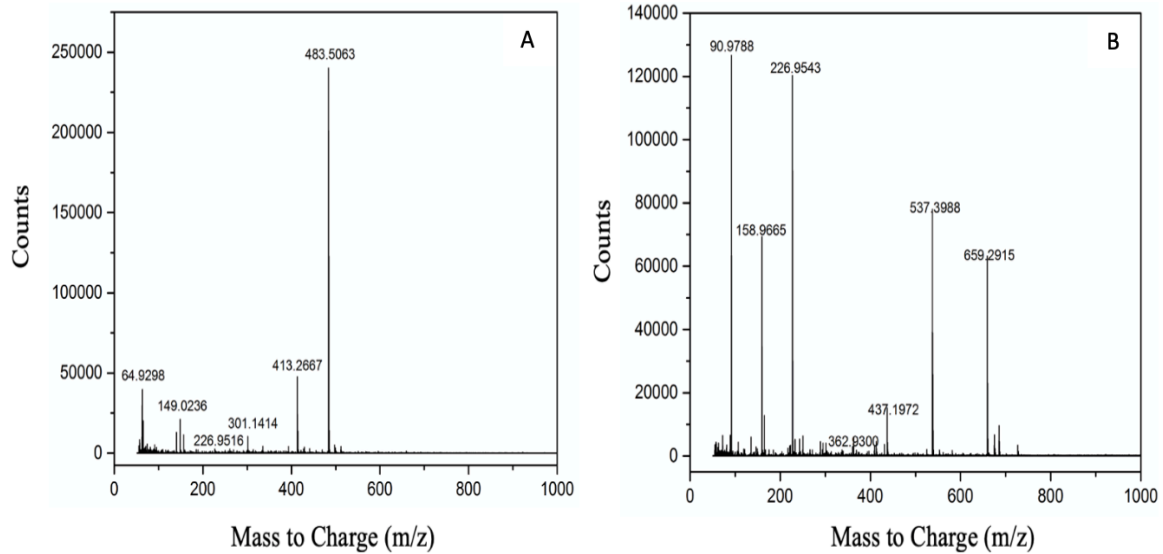


**Figure 3.4.2:** Positive mode of <sup>2</sup>D mobile phase (95/5 0.1% formic acid in acetonitrile/0.1% formic acid in water (A) and Reseda Lake/buckthorn berry pigment (B).

## **Chapter 4: Conclusion**

This thesis work explored 2D-LC-EC-SERS as a method for separating, detecting and identifying the many compounds present in a complex sample, in this case a yellow lake pigment composed of Reseda lake and buckthorn berry. It is a significant challenge to characterize natural pigments by a single method because they are complex and comprised of many components varying in similar chemical structure and properties. Eight polyphenol compounds that are known to be present in yellow lake pigments were used to try to identify the various compounds in a Reseda lake/buckthorn berry mixture. The eight polyphenol compounds used in this thesis work were caffeic acid, chlorogenic acid, luteolin, quercetin, apigenin, emodin, kaempferol and rhamnetin. These eight compounds were analyzed through a combination of 2D-LC and EC-SERS, exploring 2D-LC-EC-SERS as a potential new analytical method, and this was done by collecting the fractions of the components with retention times that were similar between the polyphenol standards. Subsequently, these fractions were drop coated onto a silver nanoparticle electrode for EC-SERS analysis. The results from the 2D-LC studies showed that the peak with the largest intensity, which was the 11.66 minute peak, was not identified as being one of the eight polyphenol compounds used. Additionally, this peak has proven to be important by the sunlight effect study since this peak was no longer present afterward sunlight exposure. Therefore, the absence of that compound could be a major contributor as to why the lake pigment has faded over time. However, there were eight compounds identified in the Reseda lake/buckthorn berry mixture through the conventional one dimensional chromatography, and by using multidimensional chromatography it was observed that further separation occurs, demonstrating the complexity of these yellow lake pigments. The results of the EC-

SERS studies of the eight polyphenol standards showed that the SERS spectrum could be greatly improved by a means of applied voltage, and when analyzing a mix of the eight polyphenol standard mixture that different compounds in the mix adhere to the surface of the electrode. Furthermore, when analyzing the fractions of the polyphenol compound mix and the Reseda lake and buckthorn berry pigment mixture, it was determined that what was being detected through EC-SERS was the formic acid additive from the second dimension mobile phase and not the polyphenol compounds. This thesis work explored the combination of two-dimensional liquid chromatography with electrochemical surface enhanced Raman spectroscopy for the first time to characterize a yellow lake pigment. Multidimensional chromatography has demonstrated it significantly enhances the separation of the components present in a yellow lake pigment sample. Electrochemical surface enhanced Raman spectroscopy demonstrated it was able to detect molecules present in the mobile phase used in the second dimension from the collected 2D-LC fractions, although no identifiable SERS signal was able to be obtained of the polyphenol compounds present in the yellow lake pigment. However, future work shows promise for future endeavours into this novel coupling of chromatographic and spectroscopic techniques.

## **Chapter 5: Future Work**

For future work, it is very important to determine the 11.59 minute peak present in the first dimension chromatogram of the Reseda Lake lake/buckthorn berry pigment mixture, since it has proven to be a significant component in this yellow lake pigment, and possibly a major contributor to the photodegradation of this pigment. There should be an effort in trying different gradients in the second dimension to improve the separation of the heart cuts of the yellow lake pigment. Additionally, to determine a way to increase the concentrations of the polyphenol compounds present in the fractions collected from the 2D-LC from 8 polyphenols in a mixture both the polyphenol mixture and the yellow lake pigment. This is very important in order to detect these polyphenol compounds in these fractions through EC-SERS instead of just detecting formic acid from the second dimension mobile phase. That way a spectroscopic library can be created to identify the many compounds in the yellow lake pigments by comparing them to the standards. Another area that should be explored is to try a LC separation without the addition of formic acid present in the mobile phase in order to avoid detecting formic acid through EC-SERS analysis. A key future goal for this project is to be able to apply this separation and detection method to real world samples such as samples taken from artworks. Another future goal is to be able to elucidate the pigment degradation pathways for yellow lake pigments since fading of these pigments is a very common problem for artworks.

## **Chapter 6: References:**

1. Zaffino, C.; Bedini, G. D.; Mazzola, G.; Guglielmi, V.; Bruni, S. Online coupling of high-performance liquid chromatography with surface-enhanced Raman spectroscopy for the identification of historical dyes. *J. Raman Spectrosc.* **2016**, *47*, 607-615.
2. Brosseau, C. L.; Gambardella, A.; Casadio, F.; Grzywacz, C. M.; Wouters, J.; Van Duyne, R. P. Ad-hoc surface-enhanced Raman spectroscopy methodologies for the detection of artist dyestuffs: thin layer chromatography-surface enhanced Raman spectroscopy and in situ on the fiber analysis. *Anal. Chem.* **2009**, *81*, 3056-3062.
3. Pirok, B. W.; den Uijl, M. J.; Moro, G.; Berbers, S. V.; Croes, C. J.; van Bommel, M. R.; Schoenmakers, P. J. Characterization of Dye Extracts from Historical Cultural-Heritage Objects Using State-of-the-Art Comprehensive Two-Dimensional Liquid Chromatography and Mass Spectrometry with Active Modulation and Optimized Shifting Gradients. *Anal. Chem.* **2019**, *91*, 3062-3069.
4. Pozzi, F.; Cesaratto, A.; Leona, M. Recent advances on the analysis of polychrome works of art: SERS of synthetic colorants and their mixtures with natural dyes. *Front. Chem.* **2019**, *7*, 105.
5. Fading of yellow and red lake pigments. The National Gallery. <https://www.nationalgallery.org.uk/research/about-research/the-meaning-of-making-vermeer-and-technique/fading-of-yellow-and-red-lake-pigments> (accessed November 14, 2019).
6. Casadio, F.; Leona, M.; Lombardi, J. R.; Van Duyne, R. Identification of organic colorants in fibers, paints, and glazes by surface enhanced Raman spectroscopy. *Acc. Chem. Res.* **2010**, *43*, 782-791.
7. Mayhew, H. E.; Fabian, D. M.; Svoboda, S. A.; Wustholz, K. L. Surface-enhanced Raman spectroscopy studies of yellow organic dyestuffs and lake pigments in oil paint. *Analyst.* **2013**, *138*, 4493-4499.
8. Madariaga, J. M. Analytical chemistry in the field of cultural heritage. *Anal. Methods*, **2015**, *7*, 4848-4876.
9. Brosseau, C. L.; Rayner, K. S.; Casadio, F.; Grzywacz, C. M.; Van Duyne, R. P. Surface-enhanced Raman spectroscopy: a direct method to identify colorants in various artist media. *Anal. Chem.* **2009**, *81*, 7443-7447.
10. Pauk, V.; Barták, P.; Lemr, K. Characterization of natural organic colorants in historical and art objects by high-performance liquid chromatography. *J. Sep. Sci.* **2014**, *37*, 3393-3410.

11. Wouters, J.; Verhecken, A. The coccid insect dyes: HPLC and computerized diode-array analysis of dyed yarns. *Stud. Conserv.* **1989**, *34*, 189-200.
12. Cristea, D.; Bareau, I.; Vilarem, G. Identification and quantitative HPLC analysis of the main flavonoids present in weld (*Reseda luteola* L.). *Dyes. Pigments.* **2003**, *57*, 267-272.
13. Deveoğlu, O.; Torgan, E.; Karadağ, R. High-performance liquid chromatography of some natural dyes: analysis of plant extracts and dyed textiles. *Color. Technol.* **2012**, *128*, 133-138.
14. Leona, M.; Stenger, J.; Ferloni, E. Application of surface-enhanced Raman scattering techniques to the ultrasensitive identification of natural dyes in works of art. *J. Raman Spectrosc.* **2006**, *37*, 981-992.
15. Brosseau, C. L.; Casadio, F.; Van Duyne, R. P. Revealing the invisible: using surface-enhanced Raman spectroscopy to identify minute remnants of color in Winslow Homer's colorless skies. *J. Raman Spectrosc.* **2011**, *42*, 1305-1310.
16. Jurasekova, Z.; Domingo, C.; Garcia-Ramos, J. V.; Sanchez-Cortes, S. In situ detection of flavonoids in weld-dyed wool and silk textiles by surface-enhanced Raman scattering. *J. Raman. Spectrosc.* **2008**, *39*, 1309-1312.
17. Stoll, D.R.; Carr, P.W. Two-Dimensional Liquid Chromatography: A State of the Art Tutorial. *Anal. Chem.* **2017**, *89*(1), 519-531.
18. Pirok, B. W.; Stoll, D. R.; Schoenmakers, P. J. Recent developments in two-dimensional liquid chromatography: Fundamental improvements for practical applications. *Anal. Chem.* **2018**, *91*, 240-263
19. Carr, P. W.; Stoll, D, R. Two- Dimensional Liquid Chromatography Principles, practical implementation and applications. *Agil. Tech. Note.* **2015**, 1-163.
20. Robinson, A. M.; Harroun, S. G.; Bergman, J.; Brosseau C. L. Portable Electrochemical Surface-Enhanced Raman Spectroscopy System for Routine Spectroelectrochemical Analysis. *Anal. Chem.* **2012**, *84*, 1760-1764.
21. Greene, B.; Alhatab, D. S.; Pye, C. C.; Brosseau, C. L. Electrochemical-Surface Enhanced Raman Spectroscopic (EC-SERS) Study of 6-Thiouric Acid: A Metabolite of the Chemotherapy Drug Azathioprine. *J. Phys. Chem. C.* **2017**, *121*, 8084-8090.
22. Turrell, G.; Corset, J. *Raman Microscopy: Developments and Applications*, 1<sup>st</sup> ed.; Academic Press, Inc.: San Diego, CA., 1996.

23. Rycenga, M.; Cogley, C. M.; Zeng, J.; Li, W.; Moran, C. H.; Zhang, Q.; Qin, D.; Xia, Y. Controlling the Synthesis and Assembly of Silver Nanostructures for Plasmonic Applications. *Chem. Rev.* **2011**, *111*, 3669-3712.
24. Stoll, D. R. In *Handbook of Advanced Chromatography/Mass Spectrometry Techniques*; Holcapek, M., Byrdwell, W. C., Eds.; Academic Press and AOCS Press: London, 2017; pp 227–286.
25. Wei, A. In *Nanoparticles: Building Blocks for Nanotechnology*; Rotello, V., Ed.; Kluwer Academic/ Plenum Publishers: New York, 2011; pp 173–200.
26. Sharma, B.; Frontiera, R. R.; Henry, A. I.; Ringe, E.; Van Duyne, R. P. SERS: Materials, applications, and the future. *Mater. Today.* **2012**, *15*, 16-25.
27. Jurasekova, Z.; Domingo, C.; Garcia-Ramos, J. V.; Sanchez-Cortes, S. In situ detection of flavonoids in weld-dyed wool and silk textiles by surface-enhanced Raman scattering. *J. Raman. Spectrosc.* **2008**, *39*, 1309-1312.
28. Bechtold, T.; Mussak, R. *Handbook of Natural Colorants*; John Wiley & Sons Ltd.: Chichester, UK, 2009.
29. Kiel, E. G.; Heertjes, P. M. Metal Complexes of Alizarin I—The Structure of the Calcium–Aluminium Lake of Alizarin. *J. Soc. Dyers. Colour.* **1963**, *79*, 21-27.
30. Bell, I. M.; Clark, R. J.; Gibbs, P. J. Raman spectroscopic library of natural and synthetic pigments (pre-~ 1850 AD). *Spectrochim. Acta. A.* **1997**, *53*, 2159-2179.
31. Burgio, L.; Clark, R. J. Library of FT-Raman spectra of pigments, minerals, pigment media and varnishes, and supplement to existing library of Raman spectra of pigments with visible excitation. *Spectrochim. Acta. A.* **2001**, *57*, 1491-1521.
32. Marucci, G.; Beeby, A.; Parker, A. W.; Nicholson, C. E. Raman spectroscopic library of medieval pigments collected with five different wavelengths for investigation of illuminated manuscripts. *Anal. methods-UK.* **2018**, *10*, 1219-1236.
33. Oakley, L. H.; Fabian, D. M.; Mayhew, H. E.; Svoboda, S. A.; Wustholz, K. L. Pre-treatment strategies for SERS analysis of Indigo and Prussian blue in aged painted surfaces. *Anal. Chem.* **2012**, *84*, 8006-8012.
34. Zhang, X.; Laursen, R. A. Development of mild extraction methods for the analysis of natural dyes in textiles of historical interest using LC-diode array detector-MS. *Anal. Chem.* **2005**, *77*, 2022-2025.
35. Perry, J. J.; Brown, L.; Jurneczko, E.; Ludkin, E.; Singer, B. W. Identify the Plant Origin of Artists' Yellow Lake Pigments by Electrospray Mass Spectrometry. *Archaeometry.* **2011**, *53*, 164-177.

36. Campanella, B.; Botti, J.; Cavaleri, T.; Cicogna, F.; Legnaioli, S.; Pagnotta, S.; Poggialini, F.; Poli, T.; Scalarone, D.; Palleschi, V. The shining brightness of daylight fluorescent pigments: Raman and SERS study of a modern class of painting materials. *Microchem. J.* **2020**, *152*, 104292
37. Meyer, V. R. *Practical High-Performance Liquid Chromatography*, 4th ed.; John Wiley & Sons, Inc.: Hoboken, New Jersey, 2004.
38. Dołowy, M.; Pyka, A. Application of TLC, HPLC and GC methods to the study of amino acid and peptide enantiomers: a review. *Biomed. Chromatogr.* **2014**, *28(1)*, 84-101.
39. Beni, Á; Lajtha, K.; Kozma, J.; Fekete, I. Application of a Stir Bar Sorptive Extraction sample preparation method with HPLC for soil fungal biomass determination in soils from a detrital manipulation study. *J. Microbiol. Methods.* **2017**, *136*, 1-5.
40. Hattori, H.; Ito, K.; Iwai, M.; Arinobu, T.; Mizutani, Y.; Kumazawa, T.; Ishii, A.; Suzuki, O.; Seno, H. Rapid analysis of sertraline, fluvoxamine, and paroxetine in serum specimens by LC-MS-MS using a new polymer column. *Forensic. Toxicol.* **2007**, *25*, 100-103.
41. Nováková, L.; Matysová, L.; Solich, P. Advantages of application of UPLC in pharmaceutical analysis. *Talanta.* **2006**, *68*, 908-918.
42. Hafpenny, A.P; Brown, P.R. Application of HPLC to the Separation of Metabolites of Nucleic Acids in Physiological Fluids. In *Practice of High-Performance Liquid Chromatography*; Engelhardt, H., Ed.; Springer, Berlin, Heidelberg: Berlin, 1986, pp 323-342.
43. Manz, A.; Dittrich, P. S.; Pamme, N.; Iossifidis, D. *Bioanalytical Chemistry*, 2<sup>nd</sup> ed.; Imperial College Press, 2015.
44. The Theory of HPLC Chromatographic Parameters. [https://www.chromacademy.com/lms/sco2/Theory\\_Of\\_HPLC\\_Chromatographic\\_Parameters.pdf](https://www.chromacademy.com/lms/sco2/Theory_Of_HPLC_Chromatographic_Parameters.pdf) (accessed February 15<sup>th</sup>, 2020)
45. Skoog, D. A.; West, D. M.; Holler, F. J.; Crouch, S. R. *Fundamentals of analytical chemistry*, 8<sup>th</sup> ed.; Brook/Cole: Belmont, CA., 2004.
46. Cavaliere, C.; Capriotti, A. L.; La Barbera, G.; Montone, C. M.; Piovesana, S.; Laganà, A. Liquid chromatographic strategies for separation of bioactive compounds in food matrices. *Molecules.* **2018**, *23*, 3091.
47. Brandão, P. F.; Duarte, A. C.; Duarte, R. M. Comprehensive multidimensional liquid chromatography for advancing environmental and natural products research. *Trac-Trend. Anal. Chem.* **2019**, *116*, 186-197.

48. Ferraro, J. R.; Nakamoto, K. *Introductory Raman Spectroscopy*, 1<sup>st</sup> ed.; Academic Press, Inc.: San Diego, CA., 1994.
49. Bumrah, G. S.; Sharma, R. M. Raman spectroscopy – Basic principle, instrumentation and selected applications for the characterization of drugs and abuse. *Egypt. J. Forensic Sci.* **2016**, *6*, 209-215.
50. Haynes, C. L.; McFarland, A. D.; Van Duyne, R. P. Surface-Enhanced Raman Spectroscopy. *Anal. Chem.* **2005**, *77*, 338A-346A.
51. Wu, D. Y; Li, J. F; Ren, B; Tian, Z, Q. Electrochemical surface-enhanced Raman spectroscopy of nanostructures. *Chem. Soc. Rev.* **2008**, *37*, 1025-1041.
52. Wang, J. *Analytical Electrochemistry*, 2<sup>nd</sup> ed.: Wiley-VCH: New York, 2000; pp 1-3, 100-103.
53. The Electrical Double Layer. <https://www.ceb.cam.ac.uk/research/groups/rg-eme/Edu/the-electrical-double-layer>. (accessed February 12<sup>th</sup>, 2020)
54. Bartholomew, R. J. Raman spectral studies of solutions of formic acid and methyl formate. Ph.D. Dissertation, University of Waterloo, Ontario, CA, **1996**.
55. Giménez, J.; Espriu-Gascon, A.; Bastos-Arrieta, J.; de Pablo, J. Effect of NaCl on the fabrication of the Egyptian blue pigment. *J. Archaeol. Sci.* **2017**, *14*, 174-180.
56. Kirby, J.; Spring, M.; Higgitt, C. National Gallery Technical Bulletin. In *the Technology of Red Lake Pigment Manufacture: Study of the Dyestuff Substrate*; Roy. A., Ed.; National Gallery Company Limited: Great Britain, 2005; pp 71-77.

## Appendix:

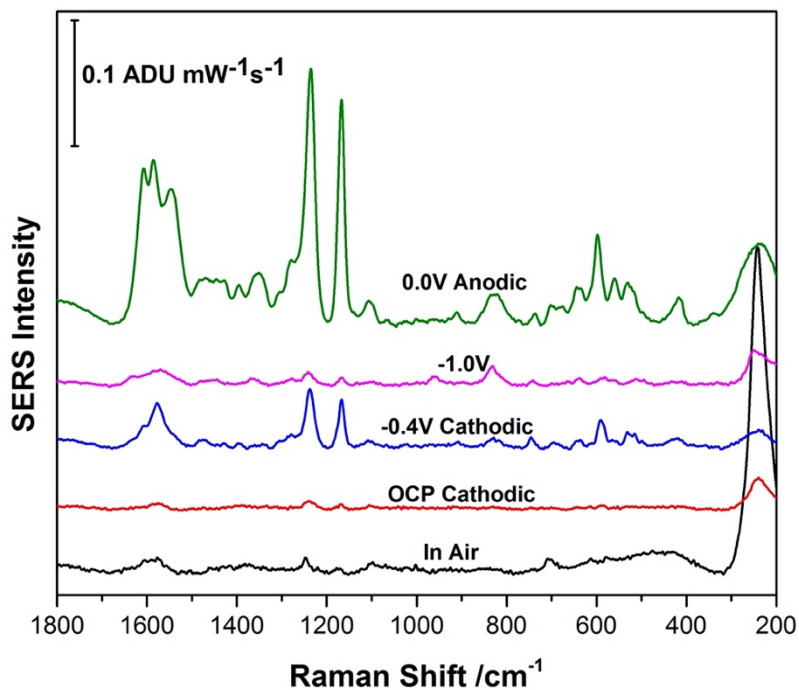


**Figure A1:** Comparison of EC-SERS spectra 250 ppm apigenin on the surface of AgNP coated screen-printed electrode using an excitation wavelength of 780 nm with a laser power of 80 mW and acquisition time of 30 seconds.

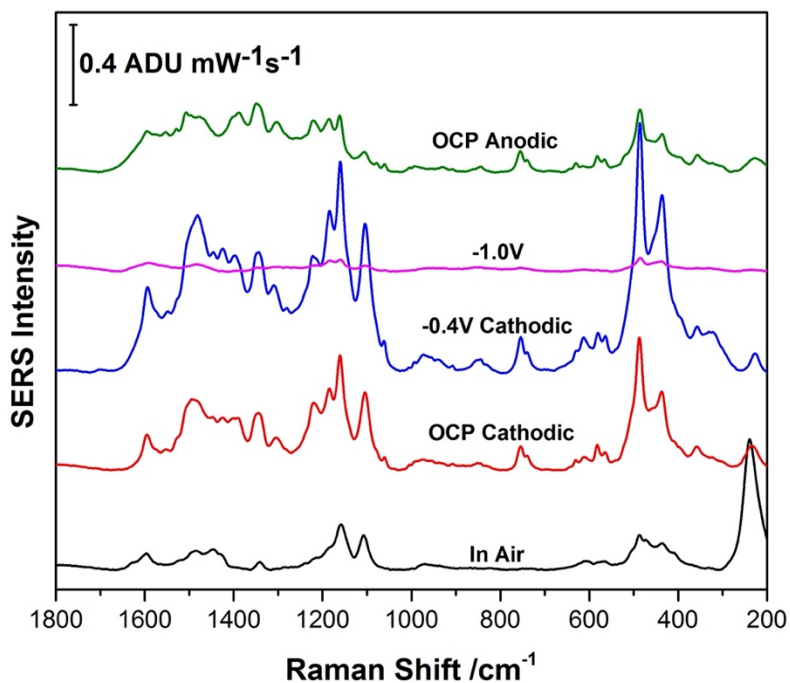


**Figure A2:** Comparison of EC-SERS spectra of 2000 ppm chlorogenic acid on the surface of AgNP coated screen-printed electrode using an excitation wavelength of 780 nm with a laser power of 80 mW and acquisition time of 30 seconds.

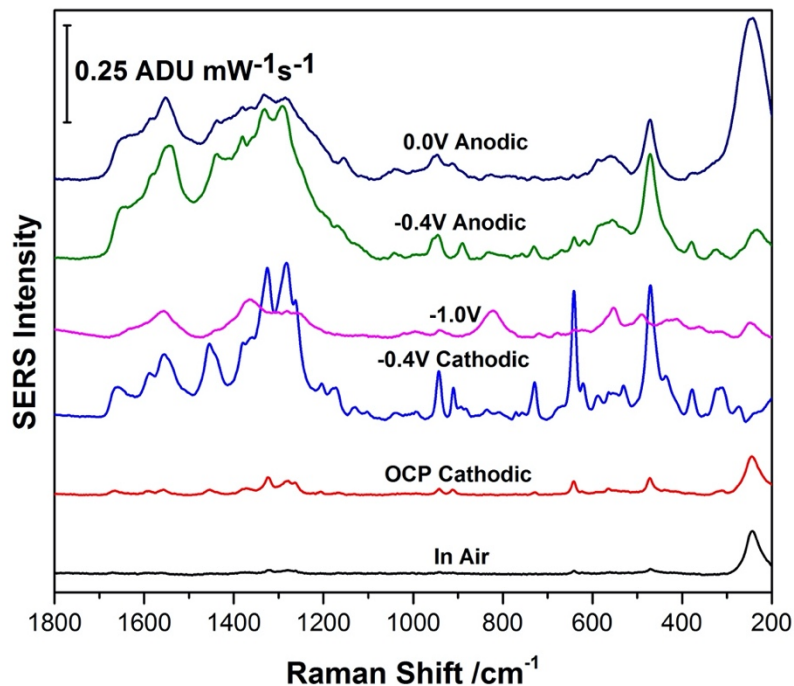


**Figure A3:** Comparison of EC-SERS spectra of 250 ppm emodin on the surface of AgNP coated screen-printed electrode using an excitation wavelength of 780 nm with a laser power of 80 mW and acquisition time of 30 seconds.

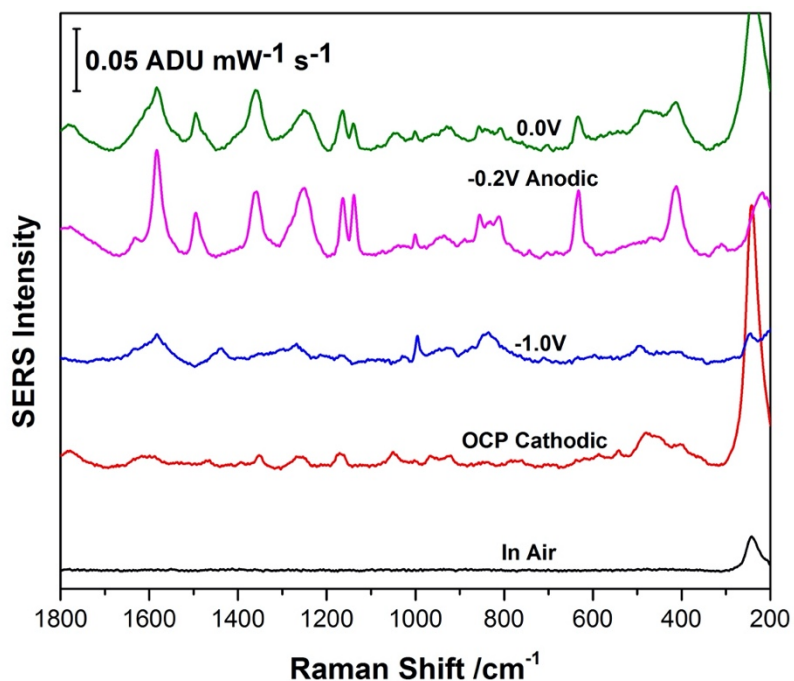


**Figure A4:** Comparison of EC-SERS spectra of 2000 ppm kaempferol on the surface of AgNP coated screen-printed electrode using an excitation wavelength of 780 nm with a laser power of 80 mW and acquisition time of 30 seconds.

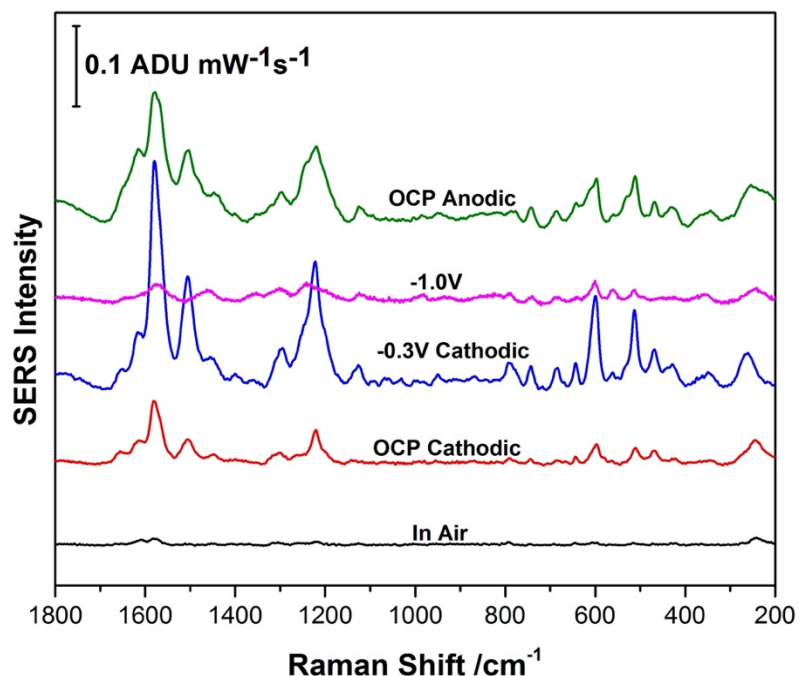


**Figure A5:** Comparison of EC-SERS spectra of 2000 ppm luteolin on the surface of AgNP coated screen-printed electrode using an excitation wavelength of 780 nm with a laser power of 80 mW and acquisition time of 30 seconds.

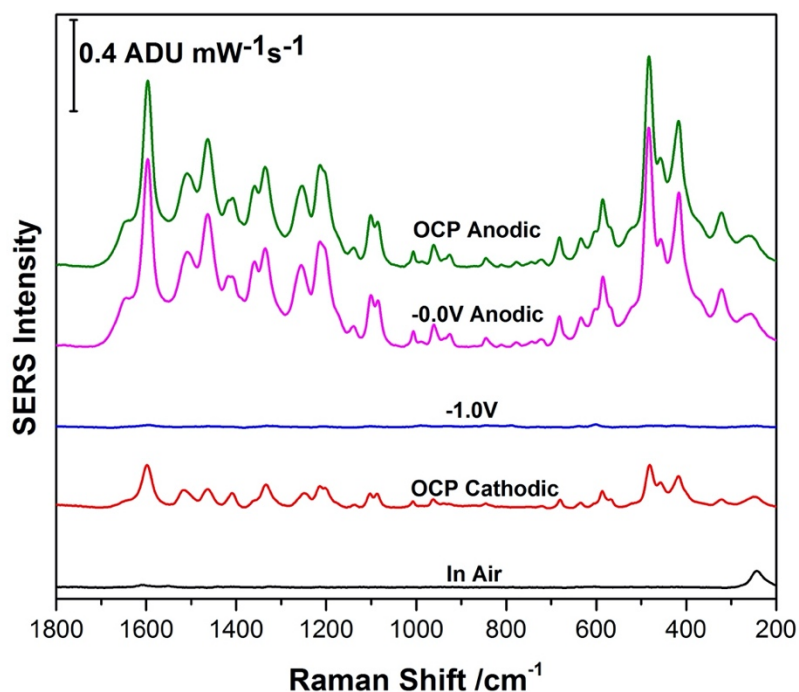


**Figure A6:** Comparison of EC-SERS spectra of 2000 ppm quercetin on the surface of AgNP coated screen-printed electrode using an excitation wavelength of 780 nm with a laser power of 80 mW and acquisition time of 30 seconds.

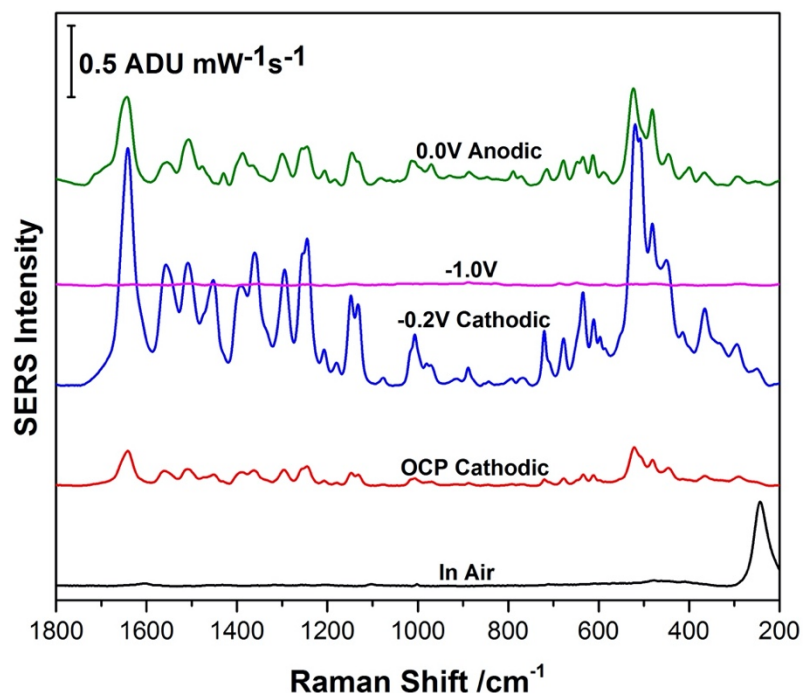


**Figure A7:** Comparison of EC-SERS spectra of 500 ppm rhamnetin on the surface of AgNP coated screen-printed electrode using an excitation wavelength of 780 nm with a laser power of 80 mW and acquisition time of 30 seconds.

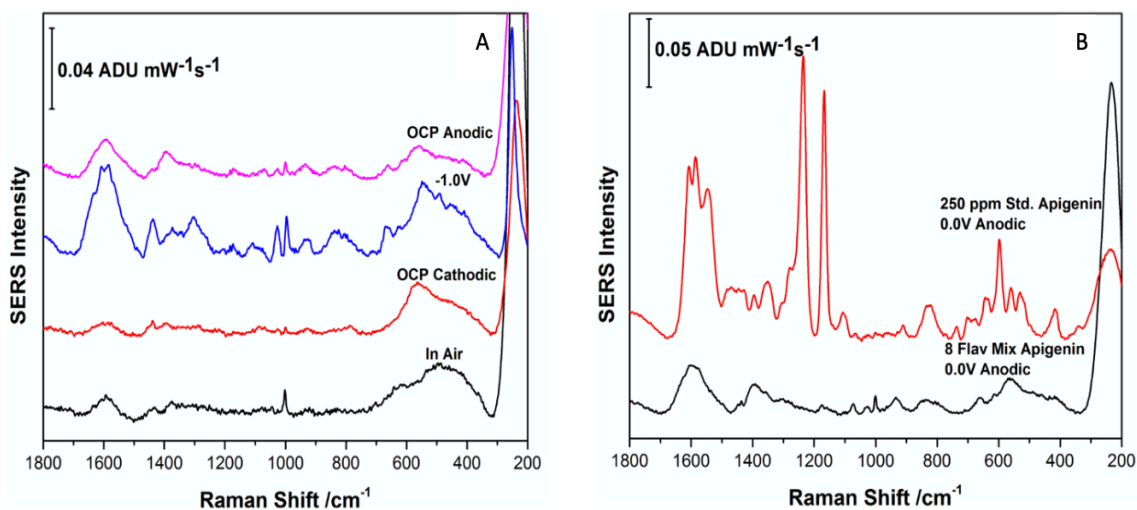


**Figure A8:** Comparison of EC-SERS spectra of apigenin 2D-LC fraction from 8 polyphenol mix (A) and comparison with 250 ppm apigenin standard EC-SERS spectrum with 0.0V anodic spectrum of apigenin 2D-LC fraction from 8 polyphenol mix (B) on the surface of AgNP coated screen-printed electrode using an excitation wavelength of 780 nm with a laser power of 80 mW and acquisition time of 30 seconds.

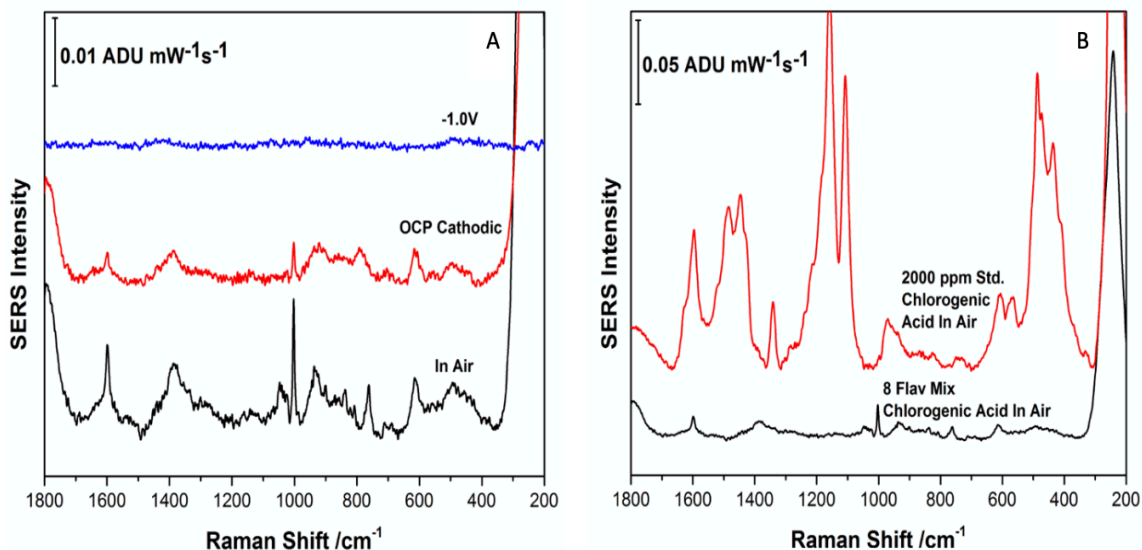


**Figure A9:** Comparison of EC-SERS spectra of chlorogenic acid 2D-LC fraction from 8 polyphenol mix (A) and comparison with 2000 ppm chlorogenic acid standard EC-SERS spectrum with in air spectrum of chlorogenic acid 2D-LC fraction from 8 polyphenol mix (B) on the surface of AgNP coated screen-printed electrode using an excitation wavelength of 780 nm with a laser power of 80 mW and acquisition time of 30 seconds.

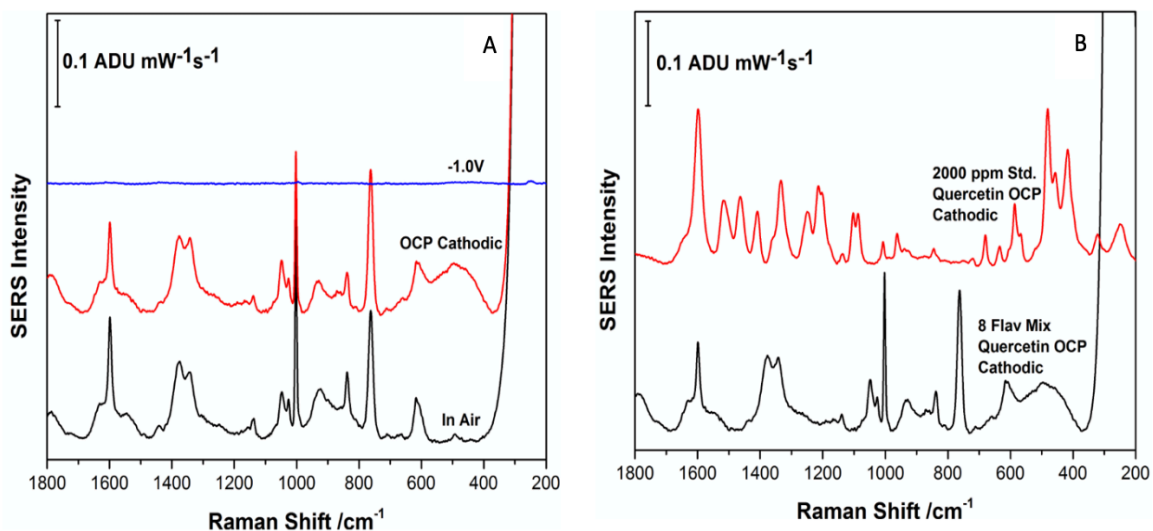


**Figure A10:** Comparison of EC-SERS spectra of quercetin 2D-LC fraction from 8 polyphenol mix (A) and comparison with 2000 ppm quercetin standard EC-SERS spectrum with OCP cathodic spectrum of quercetin 2D-LC fraction from 8 polyphenol mix (B) on the surface of AgNP coated screen-printed electrode using an excitation wavelength of 780 nm with a laser power of 80 mW and acquisition time of 30 seconds.

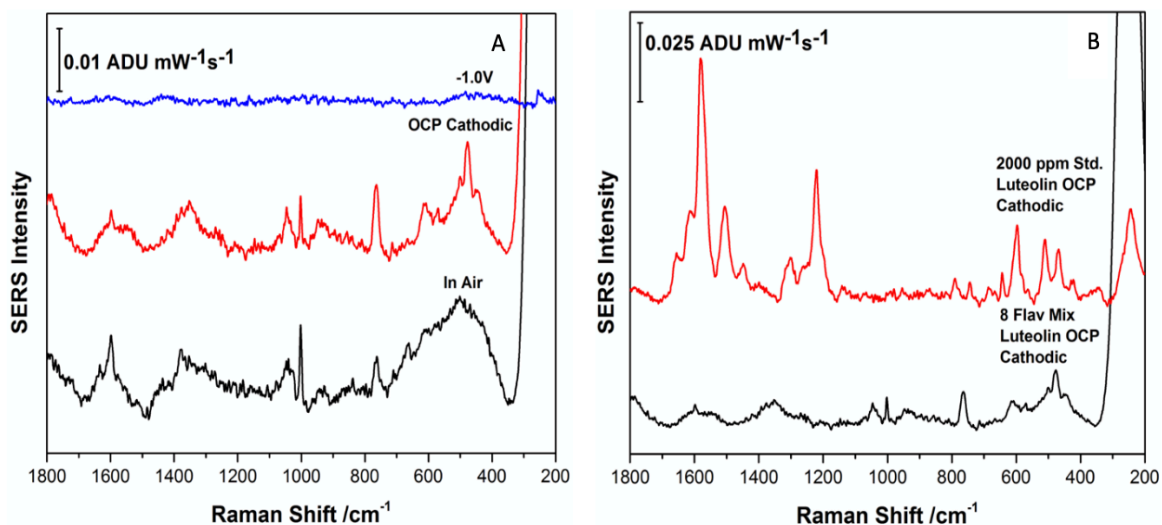


**Figure A11:** Comparison of EC-SERS spectra of luteolin 2D-LC fraction from 8 polyphenol mix (A) and comparison with 2000 ppm luteolin standard EC-SERS spectrum with OCP cathodic spectrum of luteolin 2D-LC fraction from 8 polyphenol mix (B) on the surface of AgNP coated screen-printed electrode using an excitation wavelength of 780 nm with a laser power of 80 mW and acquisition time of 30 seconds.

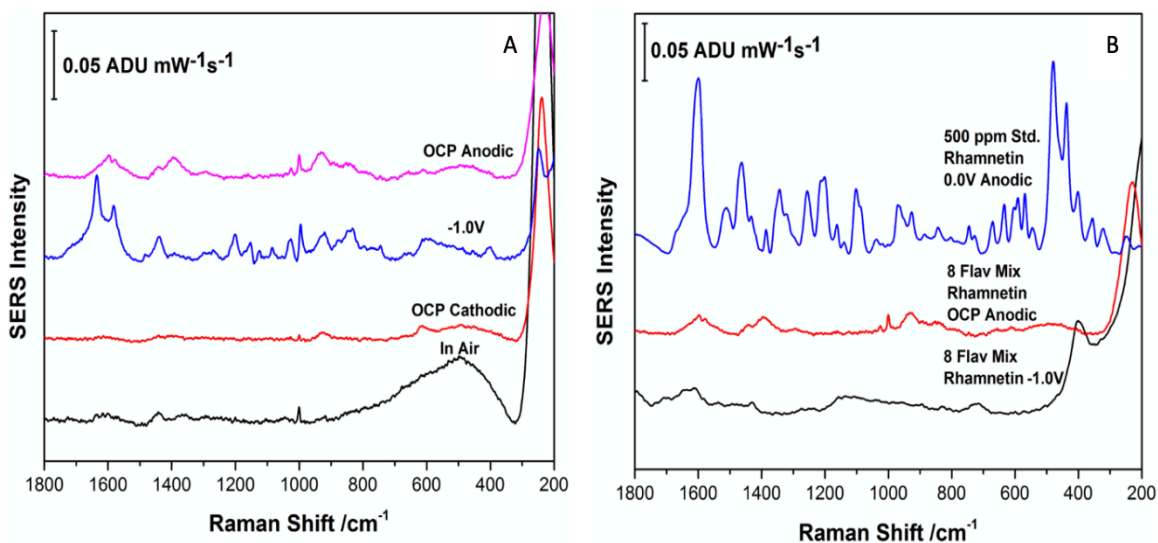


**Figure A12:** Comparison of EC-SERS spectra of rhamnetin 2D-LC fraction from 8 polyphenol mix (A) and comparison with 500 ppm rhamnetin standard EC-SERS spectra with -1.0V spectrum of rhamnetin 2D-LC fraction from 8 polyphenol mix on the surface of AgNP coated screen-printed electrode using an excitation wavelength of 780 nm with a laser power of 80 mW and acquisition time of 30 seconds.

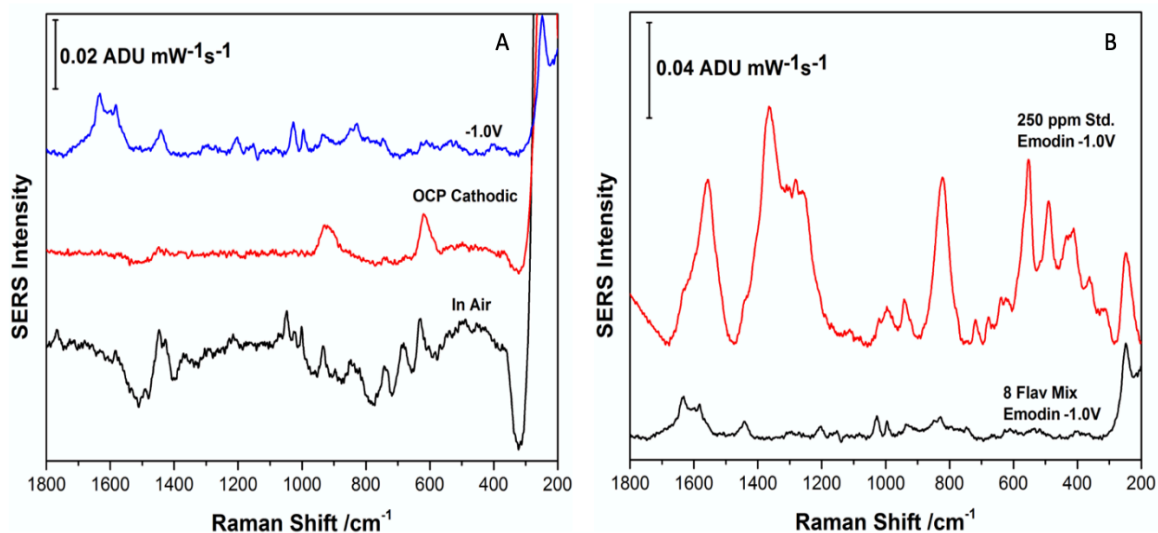


**Figure A13:** Comparison of EC-SERS spectra of emodin 2D-LC fraction from 8 polyphenol mix (A) and comparison with 250 ppm emodin standard EC-SERS spectrum with -1.0V spectrum of emodin 2D-LC fraction from 8 polyphenol mix (B) on the surface of AgNP coated screen-printed electrode using an excitation wavelength of 780 nm with a laser power of 80 mW and acquisition time of 30 seconds.

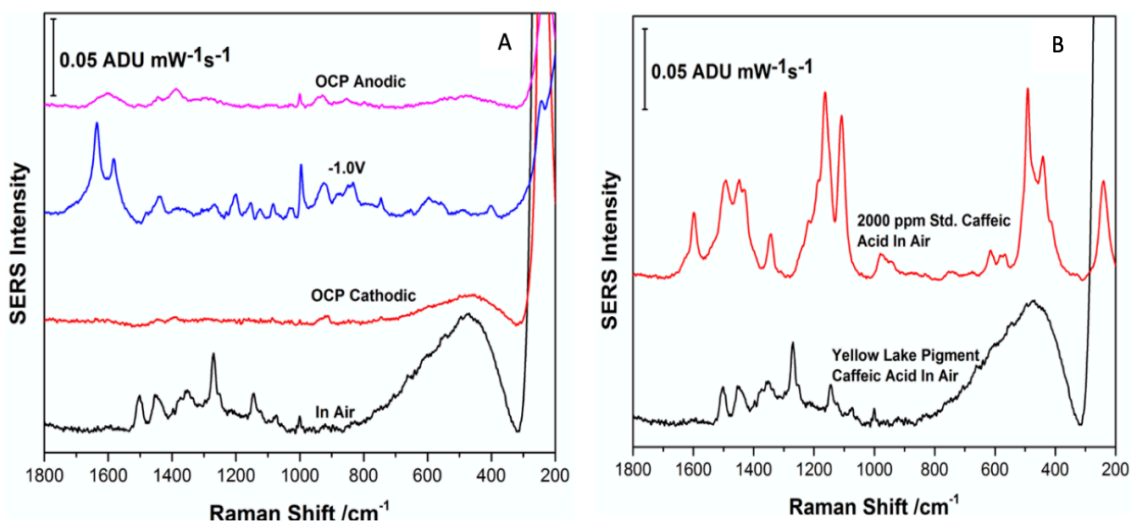


**Figure A14:** Comparison of EC-SERS spectra of caffeic acid fraction of Reseda lake/buckthorn berry pigment (A) and with 2D-LC fraction of 2000 ppm caffeic acid standard (B) on the surface of AgNP coated screen-printed electrode using an excitation wavelength of 780 nm with a laser power of 80 mW and acquisition time of 30 seconds.

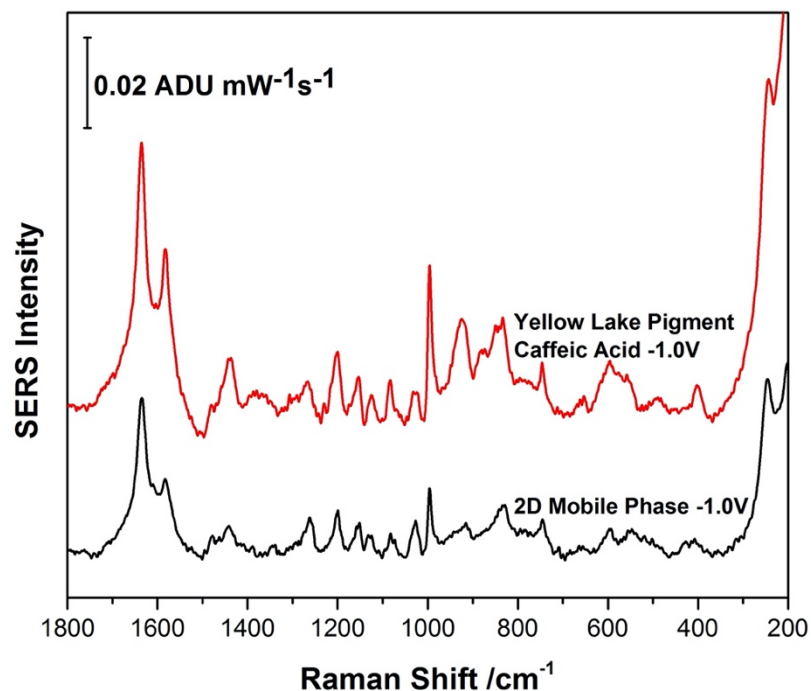


**Figure A15:** Comparison between EC-SERS spectra of <sup>2</sup>D mobile phase and caffeic acid fraction from Reseda lake/buckthorn berry pigment at -1.0V on the surface of AgNP coated screen-printed electrode using an excitation wavelength of 780 nm with a laser power of 80 mW and acquisition time of 30 seconds.

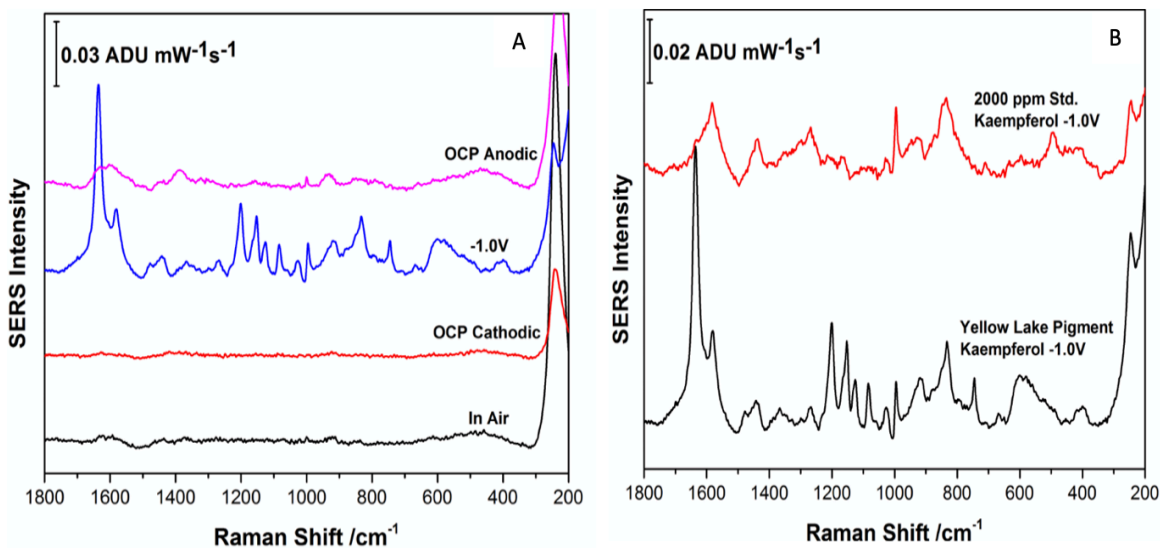


**Figure A16:** Comparison of EC-SERS spectra of kaempferol fraction of Reseda lake/buckthorn berry pigment (A) and with 2D-LC fraction of 2000 ppm kaempferol standard (B) on the surface of AgNP coated screen-printed electrode using an excitation wavelength of 780 nm with a laser power of 80 mW and acquisition time of 30 seconds.

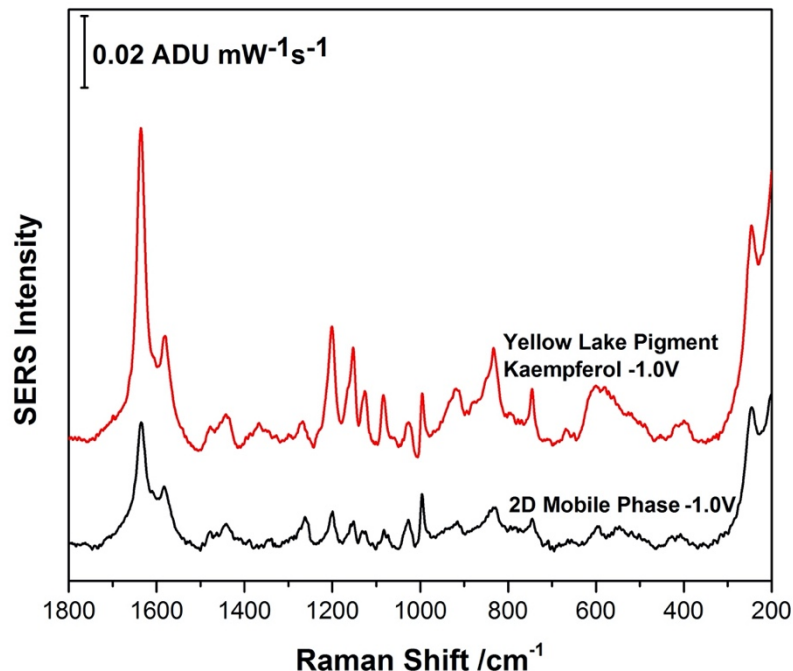


**Figure A17:** Comparison between EC-SERS spectra of <sup>2</sup>D mobile phase and kaempferol fraction from Reseda lake/buckthorn berry pigment at -1.0V on the surface of AgNP coated screen-printed electrode using an excitation wavelength of 780 nm with a laser power of 80 mW and acquisition time of 30 seconds.

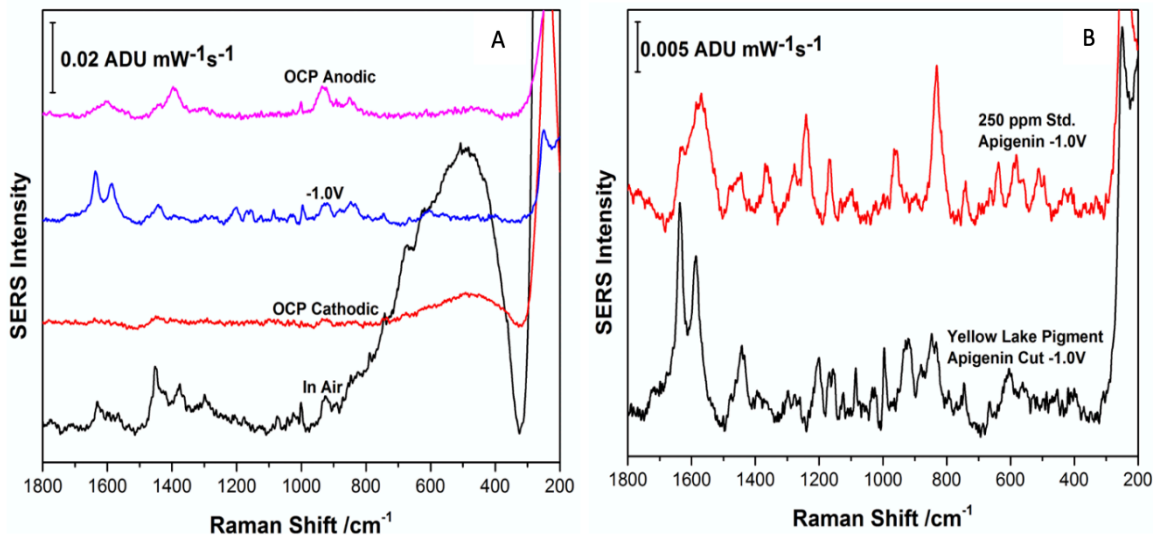


**Figure A18:** Comparison of EC-SERS spectra of apigenin fraction of Reseda lake/buckthorn berry pigment (A) and with 2D-LC fraction of 250 ppm apigenin standard (B) on the surface of AgNP coated screen-printed electrode using an excitation wavelength of 780 nm with a laser power of 80 mW and acquisition time of 30 seconds.

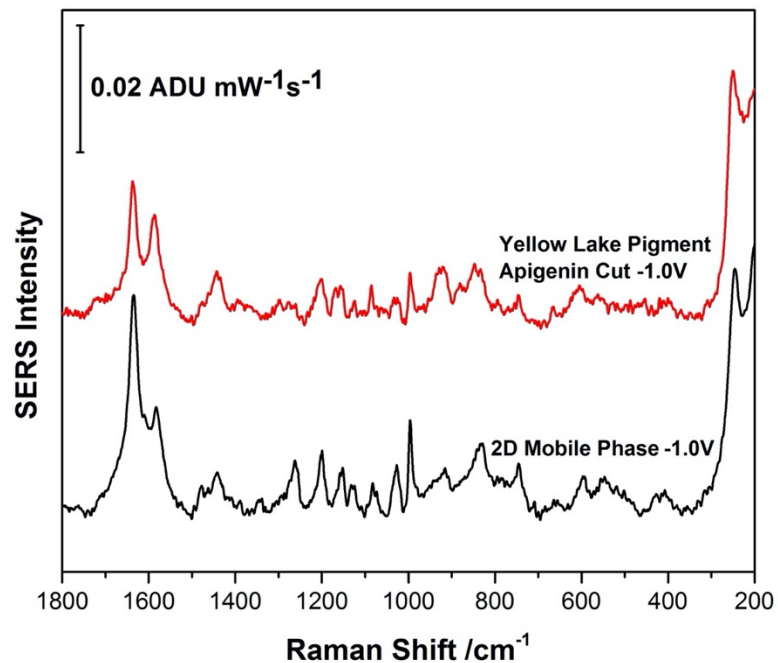


**Figure A19:** Comparison between EC-SERS spectra of <sup>2</sup>D mobile phase and apigenin fraction from Reseda lake/buckthorn berry pigment at -1.0V on the surface of AgNP coated screen-printed electrode using an excitation wavelength of 780 nm with a laser power of 80 mW and acquisition time of 30 seconds.